International Committee for Future Accelerators

Sponsored by the Particles and Fields Commission of IUPAP

Beam Dynamics Newsletter

No. 40

Issue Editor:
J. Wang

Editor in Chief:
W. Chou

August 2006

Contents

4

6

1   Foreword

1.1   From the Chairman

Weiren Chou, Fermilab
mail to: chou@fnal.gov

An ICFA meeting was held in Moscow on July 30th during the XXXIII International Conference on High Energy Physics (ICHEP'06). Reports were received from the ILCSC (including a revised ILCSC mandate), FALC (now standing for *Funding Agencies for Large Colliders*), the CERN Council Strategy Group and EPP2010. ICFA discussed the road map for particle physics and planned to launch a global coordination of neutrino studies. Prof. Albrecht Wagner, Chair of ICFA, reported the status of the ICFA's proposal to merge the three regional particle accelerator conferences – PAC, EPAC and APAC – into a yearly International Particle Accelerator Conference (IPAC), rotating around the world. There was no agreement yet because of some region's objections and more discussions are underway. The meeting also approved a new member of the Beam Dynamics Panel, Dr. A. D. Ghodke from RRCAT of Indore, India. India has a well-established accelerator community and plays an important role in this field. On behalf of the panel, I welcome Dr. Ghodke on board and look forward to working with him in the coming years.

Prior to the ICFA meeting, there was an ILCSC meeting. Both meetings heard a report on *The International Accelerator School for Linear Colliders*, which was held in Sokendai (The Graduate University for Advanced Studies), Hayama, Japan from May 19 to 27, 2006 (http://www.linearcollider.org/school/). The school was a great success (see the report in Section 2). Based on the huge interest and demand, there will be a second school in 2007 or 2008, in either the U.S. or Europe and it will collaborate with a regional particle accelerator school, as the first school did with the KEK Accelerator School (KAS).

We received an unexpected gift from Prof. Wolther von Drachenfels of the University of Bonn, Germany. He had a copy of the first issue of the ICFA BD Newsletter, which we have been searching for a long time. He kindly scanned it and sent us an electronic copy. Dr. Yuhong Zhang, the newsletter archivist from Jlab, U.S.A., added it to the archive (http://icfa-usa.jlab.org/archive/newsletter.shtml). So now we have a complete collection of all the issues from no. 1 through no. 40 (the current issue). They are valuable documents for our community.

The editor of this issue is Dr. Jiuqing Wang, a panel member and Deputy Director of the Institute for High Energy Physics (IHEP) in Beijing, China. He collected a number of well-written articles, in particular those from Asian countries, where the accelerator community is growing rapidly following the remarkable economic growth in this area. I'd like to express my gratitude to Jiuqing for this well-organized and high quality Newsletter.

1.2   From the Editor

Jiuqing Wang

IHEP, P.O. Box 918, Beijing 100049, China

mail to: wangjq@ihep.ac.cn

To choose the theme of this issue, I consulted with Weiren Chou. We decided to focus on accelerators in Asia, since interest there is high and progress is rapid. Thanks to the enthusiasm of the contact persons, I received 9 papers from countries including Australia, China, India, Japan, Korea and Singapore. They are arranged in sequence: e^+e^- high luminosity factories, light sources, proton and heavy ion accelerators. I had expected more articles in this theme issue, but some of the potential authors were too busy and may submit papers to future issues. And also I noticed that some new projects in this area have already been reported in recent BD newsletter issues. However, I hope that papers collected here can be representative and somewhat reflect the flourishing activities on accelerator based scientific research in Asia.

This issue contains a section dedicated to the International Linear Collider (ILC). This includes an article from Barry Barish, Director of the GDE, a report on the international accelerator school for linear colliders held 19-27 May in Hayama, Japan, and a report on ILC accelerator related R&D activities in IHEP, Beijing.

I have received three workshop and conference reports: one about the 37th ICFA Beam Dynamics Workshop on Future Light Sources, one about the mini-workshop on CSNS (Chinese Spallation Neutron Source) accelerator Engineering Design and one about the OCPA (Overseas Chinese Physics Association) accelerator school.

I appreciate very much the high quality of the papers from all the contributors. Finally, I want to thank Ms. Shan Liu, secretary of the accelerator division of IHEP, for her professional editing of the whole issue.

2   International Linear Collider

2.1   The Baseline Configuration for the ILC

Barry C. Barish, Director of the GDE

mail to: barish@ligo.caltech.edu

2.1.1   Introduction

I wrote about the formation of the GDE and my plans for creating a baseline design in the April 2005 issue of Beam Dynamics Newsletter. I outlined what I called a few key elements in how we are going to approach the design. I stated that the GDE would be a distributed effort, so that we could fully involve the key persons who have been developing the technologies and designs for a linear collider over the previous decade or so. This approach was modelled after large particle experiments, where there is a

tradition of developing a design for complex and difficult projects with a dispersed collaboration.

The GDE members have remained in their home laboratories and many continue non-GDE work. Our guideline is that GDE members are expected to spend at least half their time on the ILC design. To guide the efforts of the accelerator design group, I appointed three accelerator leaders (Tor Raubenheimer, Nick Walker and Kaoru Yokoya) one from each region, who serve in the GDE top management as members of our Executive Committee. In addition to these core GDE members, there are three "Regional Directors" who also serve on the Executive Committee. Since the resources are regional this assures that the programs (especially the R&D programs) in those regions are well aligned with the goals and priorities of the GDE.

The other very important appointments to the top management of the GDE were three senior engineering-cost persons, one from each region, who have developed the costing methodology and are now leading an effort to apply value engineering, trade studies and more generally give us the ability to optimize cost to performance in our reference design.

Let me briefly outline our schedule and milestones. Our first goal was to develop a complete consensus baseline configuration by the end of 2005 that was meant to serve as starting point for a reference design to be completed by the end of 2006. This reference design is meant to include the whole scope of the project, including our understanding of siting issues and site dependence, the detector scope and the performance and a reliable costing of the baseline concept. This reference design should set the stage for embarking on a detailed engineering design over the coming 2-3 years.

Below I outline the main feature of the baseline configuration we have created and documented in our Baseline Configuration Document (BCD). This is truly a living baseline, as we have instituted a process by which the design can be evolved through proposals to a Change Control Board (chaired by Nobu Toge), and as of this writing we have made 14 changes to the baseline we created in December. Very recently we have obtained cost information on the various subsystems and technical systems and we are now focussing on re-examining various choices in the baseline to optimize cost to performance. As a result, the description below of the baseline design will, by design, become outdated. I indicate some of these considerations or choices in the narrative descriptions, anticipating some possible design changes.

2.1.2 Machine Parameters

The international high energy physics community, through an ICFA subcommittee, has studied the range of physics goals for the linear collider. An ICFA subcommittee report [1] was released in 2003 that lays out the main requirements for an electron-positron collider that will be capable of addressing the physics goals.

Some of the main parameters include:

- Ecm adjustable from 200 – 500 GeV
- Luminosity → ∫Ldt = 500 fb-1 in 4 years
- Ability to scan between 200 and 500 GeV
- Energy stability and precision below 0.1%
- Electron polarization of at least 80%

and

- The machine must be upgradeable to 1 TeV

For designing the ILC this parameters report serves to give us effectively a set of top level requirements for the machine and we are basically designing the machine to flow down from those requirements. Of course, we must take into account technical risk, costs, schedule, etc, so that in the end we will play off the ICFA machine parameters and the other factors to optimize the cost to performance for the machine we will propose to build.

2.1.3   The Technology Choice

Last August 2004, a crucial milestone was reached in making the choice of which technology to pursue for linear collider. The International Technology Recommendation Panel (ITRP), which I chaired, submitted its recommendation [2] to the International Linear Collider Steering Committee (ILCSC) chaired by Maury Tigner and to its parent body, ICFA, chaired by Jonathan Dorfan.

Figure 1: Niobium 9 cell 1 meter long TESLA cavity

The recommendation read:

"We recommend that the linear collider be based on superconducting rf technology. This recommendation is made with the understanding that we are recommending a technology, not a design. We expect the final design to be developed by a team drawn from the combined warm and cold linear collider communities, taking full advantage of the experience and expertise of both." (From the ITRP Report Executive Summary)

2.1.4   The ILC Baseline Configuration

The Baseline Configuration Document [3] defines the machine parameters for a 500 billion-electron-volt (GeV) energy level, and allows for an upgrade to 1 trillion-electron-volts (TeV) during the second stage of the project.
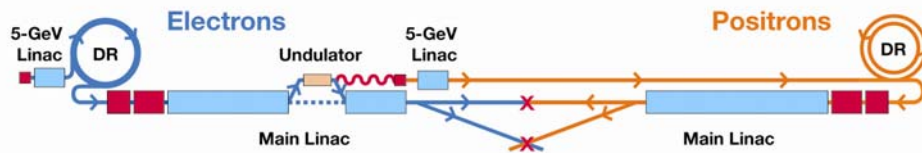
Figure 2: The Initial ILC Baeline Configuration (December 2005).

The baseline configuration has been document in a tiered electronic document [3]. Some of the key features are discussed briefly below.

2.1.4.1   *The Main Linac*

The cavity shape affects the performance and several factors must be compared:

- The ratio of the peak magnetic field to the accelerating gradient (H_{pk}/E_{acc}).
- The ratio of the peak electric field to the accelerating gradient (E_{pk}/E_{acc}).
- The product of the geometry factor G and R/Q ($G \times R/Q$).
- The cell-to-cell coupling factor (k_c).
- The loss factors of longitudinal (k_l) and transverse (k_t) wakefields.
- The Lorentz detuning factor (K_L).

The choice determines the cavity performance, beam quality, beam stability and manufacturability. The TESLA shape has a favourable low E_{pk}/E_{acc}, acceptable cell-to-cell coupling and wakefield loss factors.

Although our baseline is the TESLA shape, we are doing R&D on two newer shapes, the Cornell re-entrant shape and the DESY/KEK low-loss shape. Both new shapes have a lower H_{pk}/E_{acc} and a higher $G \times R/Q$. They have a higher ultimate gradient reach since H_{pk} is the fundamental limit, and they have lower cryogenic losses. However, both shapes carry higher risk of field emission and dark current, since E_{pk}/E_{acc} is 20% higher than the TESLA shape. The iris aperture have different apertures, with the DESY/KEK low-loss shape having a smaller iris aperture by about 15%, whereas the Cornell re-entrant shape has the same aperture as that of the TESLA shape.

The baseline gradient we are assuming for the TESLA cavities is that they will be qualified to operate at a gradient of at least 35 MV/m with a Q > 0.8 $\times 10^{10}$ in CW tests (cavities not meeting these requirements would be rejected or reprocessed). With such screening, we expect that a 31.5 MV/m gradient and Q of 1 $\times 10^{10}$ would be achieved on average in a linac made with eight-cavity cryomodules.

We are embarking on an aggressive globally coordinated R&D program to understand the process well enough to get a more consistent cavity gradient than has so far been obtained. We expect to either demonstrate this gradient or possibly change the baseline at the time we undertake a detailed engineering design in a couple years.

This assumes that: (1) the rf system would be capable of supporting 35 MV/m operation throughout the linac; (2) some of the poorer performing cavities would be de-Q'ed so the associated cryomodule can run at a higher gradient; and (3) the cryomodule

power feeds would include attenuators so the average gradient in each unit can be maximized.

For a future upgrade to 1 TeV, we assume that cavities of the low-loss or reentrant type will be fully developed and can be used. They will be qualified to at least 40 MV/m with $Q > 0.8 \times 10^{10}$ in order to achieve 36 MV/m and $Q = 1 \times 10^{10}$ on average in the linac

The baseline rf unit is a 10 MW klystron driving 24 cavities. This configuration allows 35 MV/m operations with 7% rf distribution losses and an 11% power overhead (below klystron saturation). This basic unit is three cryomodules, each containing 8 cavities.

2.1.4.2   *The Electron Source*
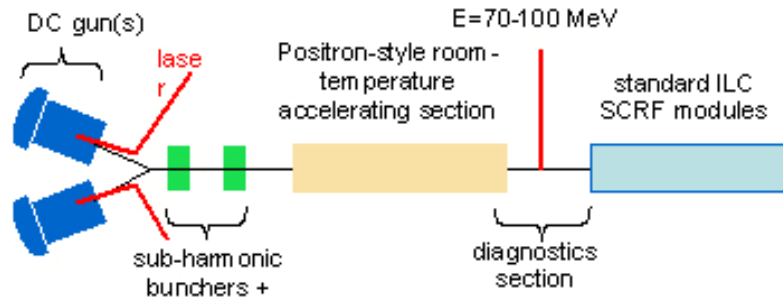
Figure 3: Configuration for the ILC Electron Source

A conventional source using a DC Titanium-sapphire laser emits 2-ns pulses that knock out electrons. An electric field focuses each bunch into a 250-meter-long linear accelerator that accelerates up to 5 GeV. The produced long electrons microbunches (~ 2 ns) are bunched by two sub-harmonic bunchers and then accelerated in a room-temperature linac to approximately ~100 MeV, followed by further acceleration in a standard ILC-type superconducting section to 5 GeV before injecting into the damping ring.

2.1.4.3   *The Positron Source*

A helical undulator-based positron system was chosen for the baseline, because it can run at higher current and has promise of creating polarized beams. The 100-meter-long undulator will be placed at the 150 GeV point in the electron linac. For collider beam energies below 150 GeV, electrons of 150 GeV are still passed through the undulator and then the beam is decelerated in the remainder of the linac to the required energy.
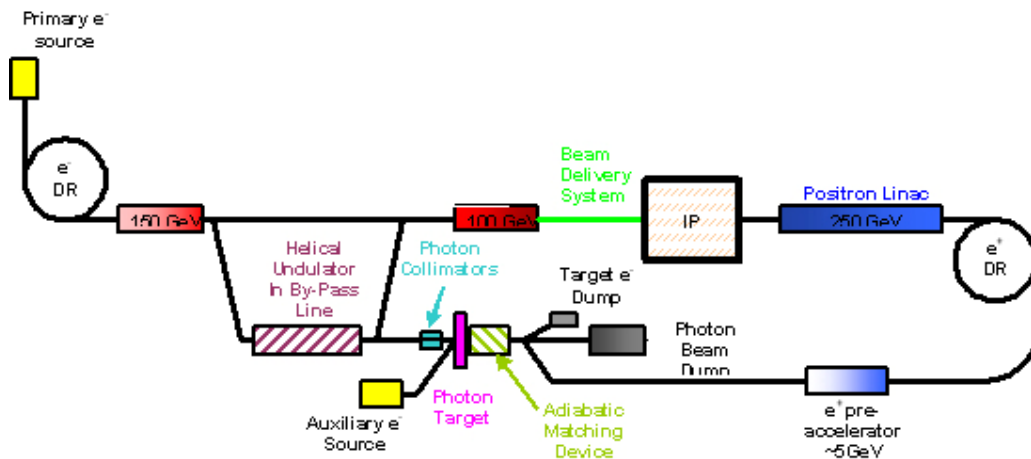
Figure 4: The helical undulator configuration for producing positrons for the ILC

The ILC electron beam passing through this undulator generates circularly polarized photons. It makes photons that then hit a titanium alloy rotating wheel target of 0.5 radiation lengths to produce positrons.

Positrons are captured downstream in an L-band RF linac with operating gradient of 15 MeV/m. After acceleration to 250 MeV, the captured positrons are separated from captured electrons in a magnetic chicane and injected into the 4.75 GeV booster linac for acceleration to the full damping ring energy of 5 GeV.

A yield into the damping ring of 1.5 positrons per electron through the undulator has been chosen for the design as an operational safety factor. This overhead is manifested in extra photon beam power incident on target and in the power and peak energy handling capabilities of the pair-production target system as well as the power load considerations of the downstream capture systems.

The scheme also contains a "keep alive" conventional source at 10% of the design current to keep the machine tuned during periods when the positron source is not operational.

Recently, we have gotten our first reliable costing information and are now doing various studies to optimize cost to performance, including physics potential. For the positron source, we were very much influenced in our decision by the potential to obtain polarized positrons in the future using an undulator source. Now, we are evaluating the cost, complexity and reliability of this system *vs*. alternate methods of producing positrons, as well as the importance of polarized positrons in terms of physics considerations.

2.1.4.4   *The Damping Rings*

Two circular 6-kilometer positron damping rings, and one circular 6-kilometer electron ring, will be located on either end of the linac. This is the most challenging subsystem from an accelerator physics point of view. A fast (~ 5 ns) rise time kicker must be used to inject and extract beam bunches and the close spacing between bunches creates issues with electron cloud effects.
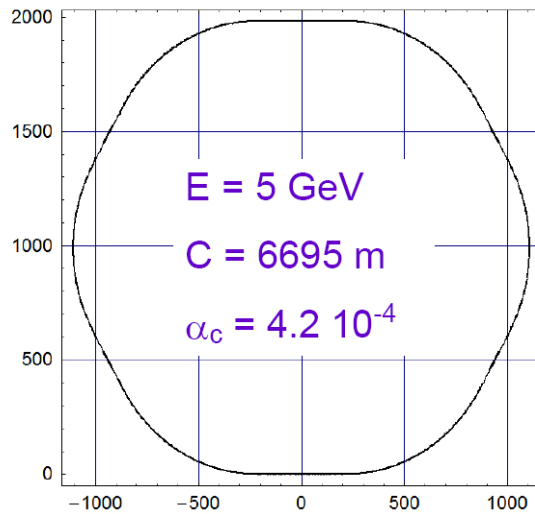
Figure 5: The Damping Ring has a six-fold symmetry with six straight sections. Four contain wigglers and RF cavities; one has injection and extraction systems, while the final one has the abortion line. The arcs each have 18 TME cells and dispersion suppression.

The electron damping is accomplished in a single 6 km ring, where the fill pattern allows a sufficient gap for clearing ions. The exact circumference of the damping rings will be chosen to allow flexibility in the fill patterns and number of bunches in a bunch train.

The positron damping ring in the original baseline established in December 2005 consisted of two (roughly circular) rings of approximately 6 km circumference in a single tunnel. The two damping rings were employed to mitigate electron-cloud effects, until possible mitigation techniques can be studied and evaluated. Using two positron rings the injected bunches can be alternated between the rings to mitigate this effect.

A recent preliminary study by Mauro Pivi and Lanfa Wang (SLAC) that was presented at the Vancouver GDE meeting suggests that by using clearing electrodes, electron cloud effects could be suppressed in the damping rings. This might allow the use of a single 6 km positron damping ring, rather than the present baseline. Although these studies are preliminary, at the time of this writing, the damping ring group is already considering whether to submit a configuration change request. It is worth emphasizing that such a change would be very desirable, since it would both simplify our configuration and significantly reduce costs.

The damping ring energy has been chosen to be 5 GeV. A lower energy would increase the risks from collective effects; while a higher energy makes it more difficult to tune for low emittance and could reduce the acceptance.

An injected beam having maximum transverse emittance up to 0.09 m-rad and energy spread up to 1% (full width) is preferred to a distribution with larger energy spread but smaller transverse emittance. Achieving good off-energy dynamics in the damping ring lattices is likely to be more problematic than achieving a large on-energy dynamic aperture. A smaller energy spread is likely to improve the margin for the acceptance of the injected beam.

A train length of around 2800 bunches or lower is preferred because of difficulties with the kickers, ion effects and electron cloud. If more bunches are needed, there may

be solutions between 2800 and 5600, but this needs more study to specify the gaps in the fill, in order to keep ion effects under control. To mitigate single-bunch collective effects, a bunch length of 9 mm bunch is preferred; however a 6 mm bunch also appears viable.

The baseline damping ring kickers are based on "conventional" strip-line kickers driven by fast pulses, without the use of RF separators (due to possible adverse effects on beam dynamics). The basic technology is available, and is close to a demonstration of most of the performance specifications.

The baseline damping wigglers are based on superconducting technology. The requirements for field quality and aperture have been demonstrated in existing designs, and the power consumption is low. The main magnets are electromagnets, because use of electromagnets will simplifies tuning and will allow polarity reversal.

A superconducting RF system will be employed, because it requires fewer cavities, having cost and technical advantages. The damping rings RF frequency was chosen to be 500 MHz for the initial baseline, but have been since changed to 650 MHz. This change went through our formal change control process and the reason for the change is to better accommodate the fill patterns and ability to achieve the Low-Q parameter set.

A chamber diameter of (not significantly less than) 50 mm in the arcs, 46 mm in the wiggler and 100 mm in the straights is required. The wiggler chamber needs a large aperture to achieve the necessary acceptance, and to suppress electron cloud build-up. The large aperture also reduces resistive-wall growth rates, and eases the requirements on the feedback systems.

2.1.4.5 *The Beam Delivery Systems*

The baseline configuration has two interaction regions fed by two separate beam delivery systems having crossing angles of 20 mrad and 2 mrad. The two detectors are to be mounted in two independent and longitudinally separated halls.

The 20 mrad interaction region has a more mature design, where the separate incoming & extraction beam lines facilitate high luminosity and potentially cleaner downstream diagnostics. This beam configuration has minimum risk to achieve the nominal parameters and will be upgradeable in the future for gamma-gamma.

The 2 mrad crossing angle would provide better background and detector hermeticity, however it will have lower luminosity and the downstream diagnostics will have higher background.

The two interaction points are longitudinally separated in the baseline configuration by about 130 m, and this provides the flexibility to work on one detector while another is taking data. This longitudinal separation will present some problems. For example, for the undulator positron source, there may be difficulties providing collisions at both detectors with appropriate time separations.
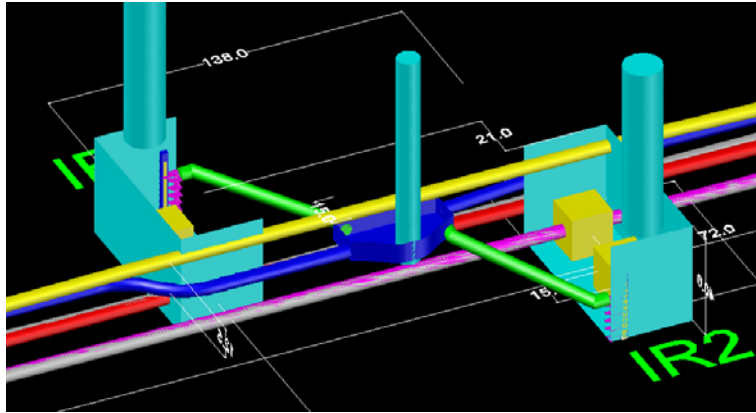
Figure 6: Baseline Configuration having two interaction regions with 138 m longitudinal separation

The linacs in the baseline layout point at the large 20 mrad crossing interaction region. This will facilitate a multi-TeV upgrade, but may not in itself provide multi-TeV compatibility.

Recent costing information has prompted us to propose a change request to two interactions regions at 14mrad. This would result in a considerable cost saving, plus an easier to implement magnet system (because the disrupted beam for the 2mrad crossing puts severe requirements on the magnets close to the IR). We are presently working with the detector *World Wide Study* to evaluate the loss of physics potential of such a change, before making a decision.

2.1.4.6   *ILC Detectors*

Large Scale 4π detectors with solenoidal magnetic fields will be developed for the interaction regions. There are presently four concepts for such detectors, using somewhat different philosophies and technologies.

It is still too early to form collaborations and specific designs. So, instead there are several concepts being developed and coordination provided by the *World Wide Study* (WWS) that represents all the regions and is helping to provide workshops and other mechanisms for developing both the components through R&D programs and the concepts to the level that the requirements for final detectors are being developed.

For the accelerator design, the WWS provides us an ongoing body for us to interact with as we weigh design changes that can affect the experiments. As part of our change control process, if proposed design changes might impact science performance we are soliciting input from through the WWS.

Lastly, we have formed a joint group we call *Machine Detector Interface* (MDI) which has representatives from the accelerator and detector community and where we are working the interface issues, especially for the beam delivery systems.
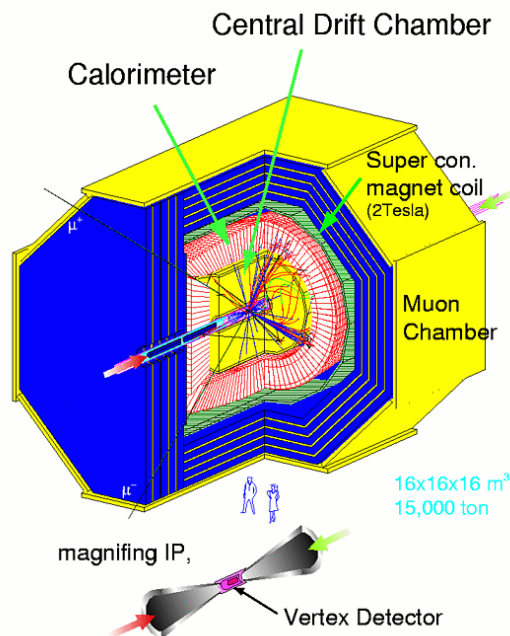
Figure 7: ILC Detectors will be 4π detectors with precision tracking and calorimetry

In order to take full advantage of the ILC ability to reconstruct, one need to improve resolutions, tracking, etc. by a factor of two or three. To reach these goals, new techniques in calorimetry, granularity of readout etc. are being developed in a worldwide R&D program.

2.1.5   Other issues for the Design

2.1.5.1   *Upgrade Path to 1 TeV*

The footprint of the facility will be for 1 TeV, but the initial tunnel construction will be ~30 km for the 500 GeV configuration. The baseline includes the necessary features to enable a 1 TeV upgrade, for example beam dumps scaled for 1 TeV, bends and length scaled for 1 TeV, etc. However, the upgrade will require new tunnelling to reach the full 50 km. Alternate upgrade schemes are still under consideration.

2.1.5.2   *Laser Straight vs. the Earth's Curvature*

The main linac will follow the curvature of the earth, instead of being laser-straight. The cryogenics system, helium system and civil construction are more straightforward with a curved tunnel, but we must prove that we can control emittance growth in the main linac.

New studies by K. Ranjan, F. Ostiguy, N. Solyak, K. Kubo, P. Tenenbaum, P. Eliasson, A. Latina and D. Schulte show that it is possible to make beam designs that minimize emittance growth in the main linac by injecting a dispersive beam that compensates for the dispersion and vertical orbit in the linac. This encouraging result could be critical to our achieving the very small spot sizes at the interaction regions.

2.1.5.3   *One Tunnel vs. Two Tunnels*

The initial baseline uses two parallel tunnels that allow radiofrequency equipment and other support instrumentation to be located in a separate tunnel adjacent to the beam tunnel. This configuration would enable access for repairs without turning off the beam line. However, this whole question will need to be revisited after we get costing information.

2.1.6   The Next Steps

This baseline configuration presented here is not final and will evolve both as the design/costing develops and as the R&D program demonstrates improvements over the baseline in performance, cost or risk. The Baseline Configuration Document (BCD) is therefore a living document. It is not intended for funding agencies at this early stage, but rather our best view of the globally agreed to configuration at any point in time. This document will migrate to an Engineering Design Management System at the time we begin a detailed engineering design.

The next goal is to produce a Reference Design Report (RDR) that is based on the BCD and one that has reliable cost estimates. This means that in addition to the configuration defined in the BCD, we will have determined the number and specifications of the elements and other details that will enable first reliable costing.

The RDR will also contain sections on siting, industrialization, detector concepts, performance and options for the machine, including upgrade plans to 1 TeV. In order to accomplish this next step, the GDE has been reorganized and expanded somewhat to bring in some missing skills. At this point, the program to develop the reference design report is well-underway.

The BCD was "frozen" after it was agreed upon last December and has been put under formal configuration control. This step was necessary in order to maintain a stable configuration during the design and costing effort. A Change Control Board and process have been established to make and document changes in an orderly manner, and that is now working well. A number of changes have already been made and the BCD is expected to continue to evolve, as more is learned through the design process and later through improvement established in the R&D program that will improve the performance or reduce the costs.

We are just on the verge of getting our first costing information and folding costs into the picture will undoubtedly result in further changes to the baseline, as we optimize cost to performance and strive toward an affordable machine.

2.1.7   References

1. ICFA Subcommittee Report, "Parameters for the Linear Collider" September 2003
   http://www.fnal.gov/directorate/icfa/LC_parameters.pdf

2. International Technology Recommendation Panel Report September 2004
   http://www.fnal.gov/directorate/icfa/ITRP_Report_Final.pdf

3. The ILC Baseline Configuration Document
   http://www.linearcollider.org/wiki/doku.php?id=bcd:bcd_home

2.2   International Accelerator School for Linear Colliders

Barry Barish, Weiren Chou and Shin-ichi Kurokawa
mail to: barish@ligo.caltech.edu, chou@fnal.gov, shin-ichi.kurokawa@kek.jp

On 19-27 May 2006, the *International Accelerator School for Linear Colliders* took place at Sokendai, the Graduate School for Advanced Studies in Hayama, Japan. (http://www.linearcollider.org/school/) It was the first truly international school that focused on the International Linear Collider (ILC). This school was jointly organised by the ILC GDE, the International Linear Collider Steering Committee (ILCSC) and the ICFA Beam Dynamics Panel.

The path to becoming an accelerator physicist is not straight-forward. Accelerator schools not only provide enrichment for young accelerator physicists, they also play a central role in teaching future generations. Most universities do not have accelerator physicists on their faculties, and therefore do not offer courses or PhD theses in the field. Most accelerator physicists have converted from other areas of experimental physics through learning at schools like Sokendai, and by on the job training at accelerator laboratories. Therefore, we felt obliged to sponsor the Sokendai School to help augment the pipeline for young potential accelerator physicists.

We aimed the school at PhD students, postdocs and young researchers, especially young experimentalists. The school was generously supported by funding agencies and laboratories in Asia, Europe and the U.S., who provided support for all the students and lecturers. This was an excellent example of successful global collaboration for the ILC. The school also resulted from two years of Japanese efforts to host an accelerator school for linear colliders.

By any measure, the school was a spectacular success. Interest in the school was very high. There were over 500 applicants from 44 countries. Through a very difficult but rigorous selection process, the Curriculum Committee accepted 74 students. (http://www.linearcollider.org/files/ilc_school/student_list.pdf) Students from 18 countries participated giving the school a global atmosphere. The students were excellent. Their enthusiasm and abilities were higher than expected. The curriculum consisted of an 8-day program, 6 days for lectures and 2 days for visiting several facilities (ATF, B-Factory, Photon Factory and SCRF) and working on real machines at KEK. (http://www.linearcollider.org/files/ilc_school/curriculum_v9.pdf) Covered were both basic and advanced topics with the focus on accelerators, but also with lectures on detector concepts and physics. The Curriculum Committee recruited a first-class set of lecturers from the linear collider community, many of whom were GDE members. (http://www.linearcollider.org/files/ilc_school/lecturers_list_v6.pdf) The set of lectures were well organized and excellent. A video stream of the lectures will be available. (http://www.linearcollider.org/cms/?pid=1000272)

The Local Organising Committee did an excellent job and provided most of the logistics for the school. This success is also due in part to Fermilab's Cynthia Sazama and KEK's Yoko Hayashi, who worked very hard to support the school. We appreciate all of their efforts.

The school assigned two goals to the students before it started. The first goal was to learn as much as possible about the ILC. The other was to make as many new friends as possible. For the students, this could be an once-in-a-lifetime opportunity to meet with so many other young talented people from different origins who shared the same

interest (accelerators) and career goals (ILC). From past experience, some of the friendships nurtured at the school will last a lifetime.

Most instructors assigned homework and required the students to finish it on the same day when the lecture was given. And they made sure that these assignments were not easy. (http://www.linearcollider.org/cms/?pid=1000296) With a serious attitude, a majority of the students wrestled with the homework until midnight or even dawn. In response, the Committee modified the curriculum such that some of the homework was tackled in a group session, which helped the students to communicate with each other. While doing homework is an irreplaceable part of any successful school, it appeared that we were too demanding and gave too much homework, not giving students adequate time for informal contacts (or maybe even sleep!). This was a main complaint from the students and a lesson we learned for the next school.

On the last school day, we selected the top ten students based on their homework grades and had an award ceremony. Each of these ten students received a certificate as well as a *Handbook of Accelerator Physics and Engineering* (edited by Chao and Tigner, World Scientific).

At the end of the school, a student survey was conducted. The feedback was encouraging: 85% ranked the school "excellent" or "very good," 86% would recommend the school to their fellow students or colleagues, and 88% planned to work on the ILC or linear colliders in the future if there is the opportunity.

Based on the interest, demand and success of the first school and in view of a real need to develop young accelerator physicists, we are now planning a 2nd linear collider accelerator school in either Europe or the U.S.
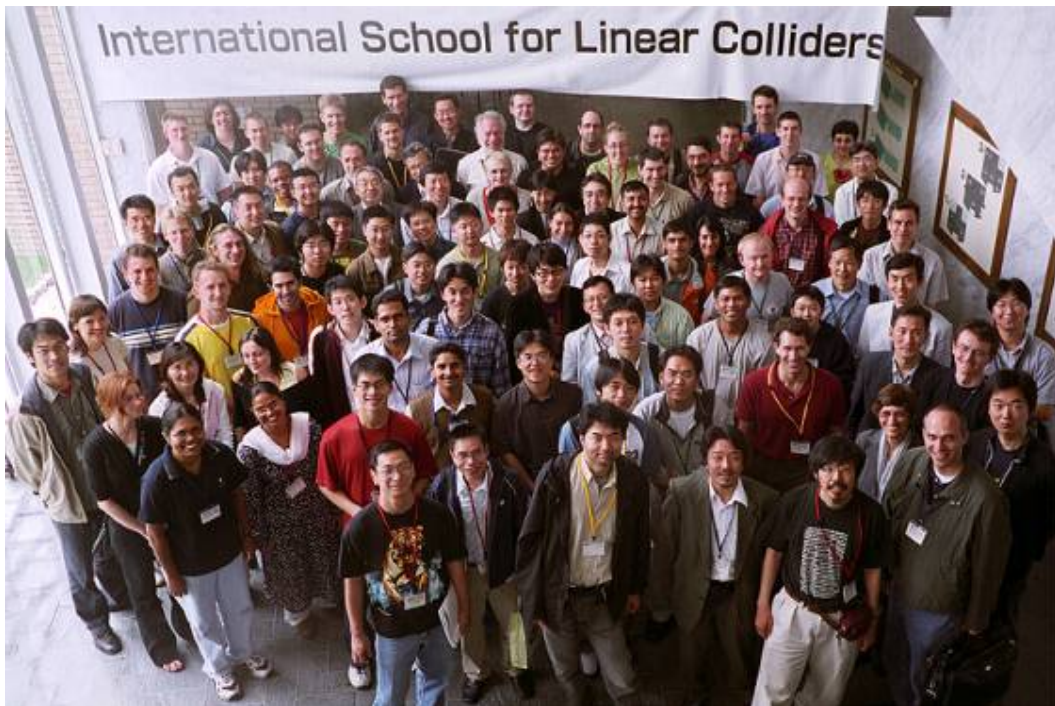
2.3   ILC Accelerator Related R&D Activities in IHEP

J. Gao, IHEP, CAS, Beijing, China
mail to: gaoj@ihep.ac.cn

2.3.1   Introduction

The decision of using super-conducting accelerator technology to build an International Linear Collider (ILC) was announced in August 2004 in Beijing; Chinese accelerator scientists endorse the decision and are interested by the project. Even the projects like BEPCII and Beijing Spallation Neutron Source (BSNS) absorb most of the skilled Chinese accelerator scientists at IHEP; in 2005 an ILC-IHEP group was formally formed under the leadership of Prof. J. Gao, ILC GDE member and ILC RDR Area leader. Started from Jan. 2005, strong regional ILC-Asia collaboration was established among China, Korea, and Japan. As for IHEP, the emphasis was put to ILC parameter choice, damping ring study, SC cavity R&D, bunch compressor, ATF2 magnet fabrication, students training (SC cavity technology, SCLLRF, positron source, BD for Main Linac, etc). In the following some main works and status are reported.

2.3.2   ILC Parameter Choice

In the second ILC workshop at Snowmass J. Gao proposed a set of formulation [1] to determine a linear collider parameter started from the limitation at interaction point. As for ILC, to ease the difficulties in different subsystems such as positron source, damping ring, main linac, etc, a new ILC parameter is proposed named as Very Low Charge Case in addition to existed 5 parameter sets proposed in Ref. 2. In fact, the newly proposed parameter is more similar to the Low-Q case in Ref. 2; consequently, the Low-Q case is underlined and taken as the most important alternative parameter to the nominal one. In ILC BCD studies subsystems have been required to accommodate Low-Q case.

2.3.3   ILC Damping Ring

As one of the most important sub-systems of ILC, damping ring design work is one of the battlefields of IHEP. During BCD stage in 2005, before making a final recommendation, to avoid space charge effect in TESLA type 17 km damping ring, a 7 GeV 17 km damping ring has been studied [3] and the results support adopting 6 km damping rings as baseline. During RDR stage in 2006, to reduce the cost of damping ring the BCD damping ring lattice (TME) has been replaced by FODO type and the wiggler sections have been reduced from 8 to 4 (FODO3) and to 2 (FODO4), progressively [4]. The aim of these efforts is to reduce the number of quadrupoles and to reduce the number of cold stations. Fig. 1 shows the lattice of FODO lattice with 2 wiggler sections (FODO4), Fig. 2 illustrates the FMA results in analyzing the FODO4 working point, Fig. 3 gives the comparison results of three lattices, OCSv6 (4 wiggler sections), FODO3, and FODO4, and Table 1 provides more detailed parameters of these three lattices.
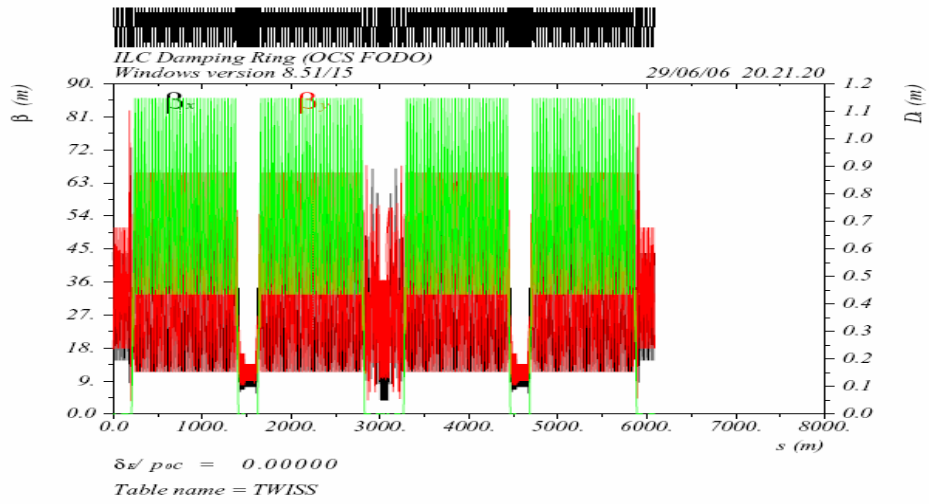
Figure 1: FODO lattice with 2 wiggler sections (FODO4)
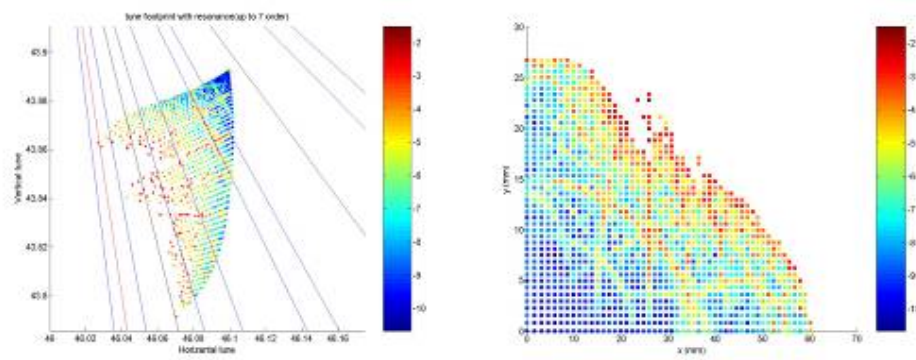
Figure 2: The FMA analysis of the working point of FODO4
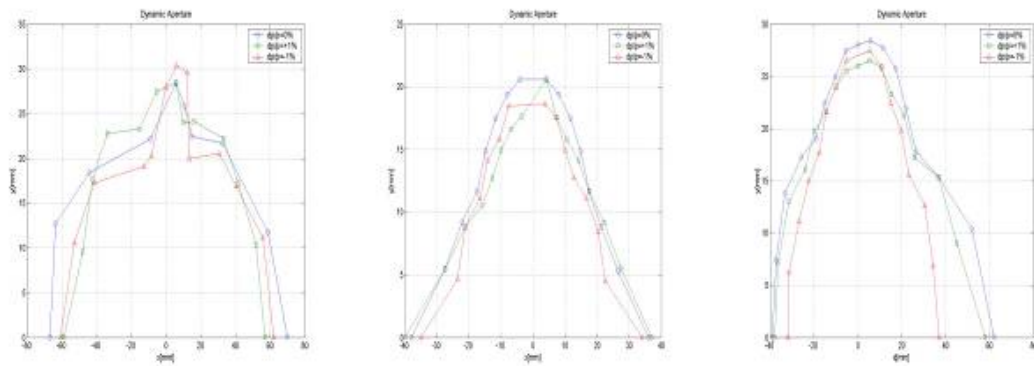
(a) OCSv6   (b) FODO3   (c) FODO4

Figure 3: Dynamic aperture comparisons for OCSv6, FODO3, and FODO4

Table 1: Detailed parameter for three lattices

	OCS6	FODO3	FODO4
Circumference [m]	6695.057	6249	6088.8
Arc cell	TME	FODO	FODO
Q magnets length totally (ARC)	480*(0.3 m)	240*(0.3 m)	240*(0.3 m)
Wiggler section number	4	4	2
Tune	52.4 / 49.31	48.35/45.32	46.09/43.89
Natural chromaticity	-62.6 / -61.7	-58.8/-60.3	-56/-58.15
Momentum compaction [10-4]	4	4.5	4.4
Norm. Natural emittance [mm-mrad]	4.6	4.4	4.2
RF voltage [MV]	46	46	46
Natural bunch length [mm]	5.9	5.9	5.9

2.3.4 ATF2 Magnets Fabrication [5]

The ATF2 experimental facility at KEK is one of the most important international collaboration programs dedicated to studying ILC final focus subsystem. In ATF2, the beam will be extracted from a damping ring, ATF, and then focused transversely to less than 40 nanometers, the smallest transverse beam size ever obtained. (ILC required vertical beam size at the interaction point will be approximately 10 times smaller.)

To contribute actively to this important ILC R&D related program, the Institute of High Energy Physics (IHEP) of Chinese Academy of Sciences, having a great deal of experience producing high quality magnets and having contributed to such projects as PEP-II and SPEAR3, fabricated the ATF2 required 24 quadrupole magnets. The total 24 quadrupole magnets were shipped to KEK in March and June, 2006 in two batches. During the production of the magnets, experts from IHEP, KEK, and SLAC collaborated efficiently to solve problems in fabrication and measurement. Even though that IHEP was also occupied with fabricating magnets for its own BEBC-II and the Shanghai Light Source, the scientific managers, engineers and factory technicians tried very hard to guarantee the schedule and quality of the ATF2 quadrupole magnets. For the Chinese ILC Collaboration Group, the ATF2 magnet becomes their first milestone in ILC international collaboration. Chinese scientists expect to make more contributions to the ILC in the future.
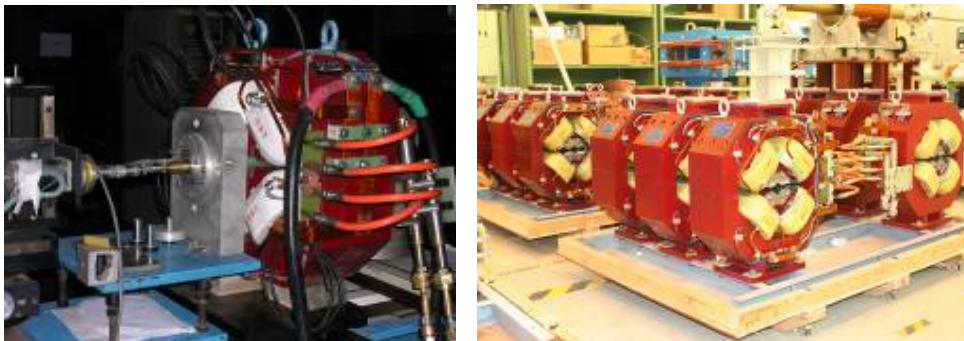
Figure 4: ATF2 quadrupole magnets fabricated by IHEP. Left – Magnets at IHEP under measurement; right – Magnets arrived at KEK.

2.3.5   Bunch Compressor

Another important subsystem of ILC is Bunch Compressor which is used to compress the bunch length at the exit of damping ring into the bunch length required by the interaction point. For example, the extracted bunch length from the damping ring is 6mm and the bunch length at IP corresponding to Low-Q case is 150 μm. Fig. 5 illustrates a two stage bunch compressor for ILC [6].
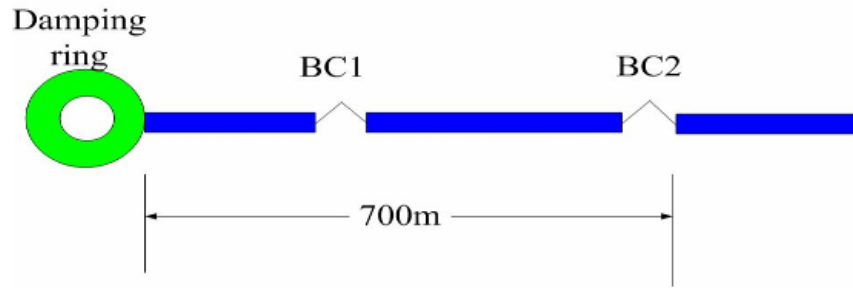
Figure 5: A schematic view of two-stage BC for ILC

Fig. 6 shows the numerical simulation result of the two-stage BC. It is seen that a Gaussian bunch of 6mm is compressed down to 150 μm.
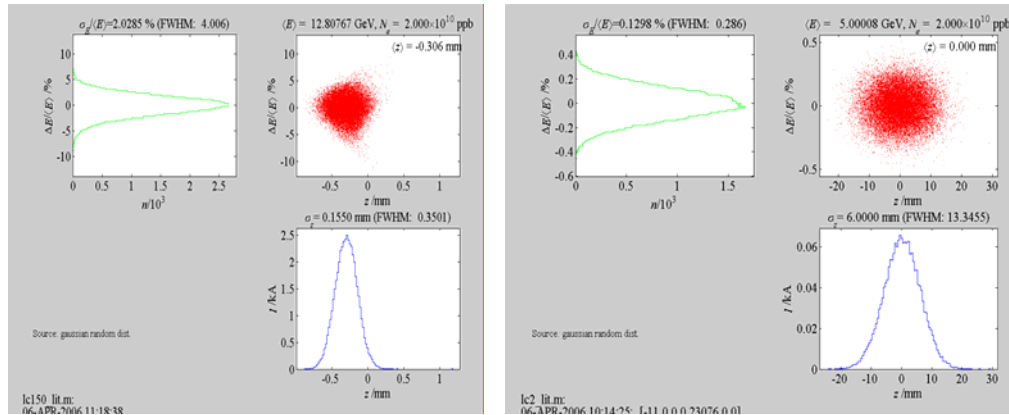
Figure 6: Bunch compressor design for ILC. Left – the bunch at the exit of ILC damping ring; right – the bunched beam at the exit of 2nd BC.

2.3.6   SCRF LLSC Studies [7]

At IHEP a Low Loss Superconducting Cavity R&D program has started. Fig. 7 is the computer modeling of the cavity; Figs. 8-10 show the dies and the copper test cavity. Materials from Japan and Chinese Ning Xia large grain Nb materials will be used as shown in Fig. 11. The aim of this study is to prepare for 9 cell cavity studies later. The SC laboratory at IHEP is equipped with single cell cavity experimental study facilities except for EP. For 9 cell cavity studies essential modifications should be made within the laboratory. Right now a close collaboration with KEK SC laboratory has been established and two students have been trained on SC technologies. As for large grain

Ning Xia materials, it is decided that IHEP-KEK will collaborate to make single cell cavity studies soon.
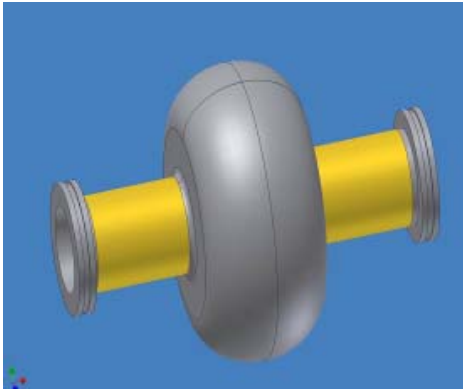
Figure 7: IHEP designed LLSC

Figure 8: Die of LLSC

Figure 9: Die measurement

Figure 10: Test copper cavity

Figure 11: Chinese Ning Xia large grain Nb. Left – RRR300 Grade Nb Ingot; right – Slices of RRR300 Ingot.

2.3.7 Miscellaneous

In addition to the above mentioned activities, other starting research areas have been planned. They are: 1) Positron source study in collaboration with KEK ATF, 2) SCLLRF in collaboration with KEK STF, 3) ILC main linac BD, and 4) Costing.

IHEP as a world-wide known normal conducting magnet constructor, during ILC damping ring RDR, IHEP magnet and power source groups contribute to the costing of magnets and their power sources.

2.3.8 Young Accelerator Physicist Training

2.3.8.1 *ILC Accelerator School*

On 19-27 May 2006, the first ILC Accelerator School was held in Sokendai, Hayama, Japan, and 74 students were selected from over 500 applicants. Among the 74 selected students 7 were from China – 6 from mainland China and 1 from Taiwan. Due to their hard work and training in China on accelerator physics and technologies three of them won the top 10 prizes and were ranked 2nd, 4th, and 8th, respectively. Prof. B. Barish wrote especially to Chinese ILC Accelerator School Curriculum Committee member (J. Gao) to encourage Chinese students taking more works in ILC after the school.

Figure 12: Top ten students of the ILC Accelerator School.

2.3.8.2 *Visitor Exchange Program*

Another efficient way to train Chinese young accelerator scientists on ILC is to send them to other foreign accelerator laboratories, such as KEK. In the frame of ILC-Asia collaboration a prioritized visitor exchange plan has been discussed and applied starting from the beginning of new fiscal year of 2006. Till now, there are already more than five visitors from IHEP to KEK that have been proved.

2.3.9 References

1. J. Gao, "Parameter Choice for International Linear Collider (ILC)", SNOWMASS-2005-ILCAW0806, Aug. 2005, or High Energy Physics and Nuclear Physics, Vol. 30, Supp. I, Feb., 2006, p. 156.

2. T. Raubenheimer, Talk given at the First ILC Workshop, Japan, Nov. 13-15, 2005.
3. Y.P. Sun and J. Gao, "7 GeV TESLA dogbone damping ring study", ILC WG3b meeting, CERN, Nov. 2005.
4. Y.P. Sun and J. Gao, "ILC DR lattice (FODO) with 4(2) wiggler sections", internal report to be presented in VLCWS06, July 19-22, 2006, Vancouver, Canada.
5. ILC Newsline: http://www.linearcollider.org/newsline/archive/2006/20060525.html.
6. X.W. Zhu, ILC BC studies, IHEP internal report, 2006.
7. M.Q. Ge, S.C. Zhao, H. Sun, J. Gao, "Design Study on 1.3GHz Mono-cell High Gradient Low Loss Superconducting Cavity", High Energy Physics and Nuclear Physics, Vol. 30, No. 4, April 2006, pp. 354-358.

3   High Luminosity e$^+$e$^-$ Factories

3.1   Crab Crossing Scheme at KEKB

Y. Funakoshi
KEK 1-1 Oho, Tsukuba, Ibaraki, 305-0801, Japan
mail to: yoshihiro.funakoshi@kek.jp

3.1.1   Introduction

KEKB adopted a horizontal crossing angle of ±11 mrad [1]. There are two motivations of the crossing angle. The first is that effects of parasitic collisions can be alleviated with the crossing angle. The second is that the IR (Interaction Region) design can be simpler, since we do not need bending magnets for beam separation. In the design phase of KEKB, however, it was widely believed that the crossing angle collision was dangerous, since it may cause instability due to synchrobetatron resonances based on experiences at DORIS. Unlike the case of DORIS that employed a vertical crossing angle, we showed that the horizontal crossing angle scheme has less harmful effects and work well in KEKB using beam-beam simulations [2]. As a backup plan which might be important in the case that the horizontal crossing angle brings unexpectedly harmful effects, we continued R&D's of a crab cavity system. An idea of the crab crossing scheme had been originally proposed for the linear collider in 1988 [3]. Soon after this, its effectiveness was shown also for ring colliders [4]. With the crab crossing scheme, we can effectively recover the head-on collision even with the finite crossing angle. Fortunately, the history of KEKB shows that the horizontal crossing angle does work and we have successfully obtained the vertical beam-beam parameters higher than 0.05 without the crab crossing [5]. This seemed to indicate that the crab crossing scheme was not needed at KEKB. However, recent studies on the beam-beam effects opened a new aspect on the effectiveness of the crab crossing.

3.1.2   Studies on Beam-Beam Effects

The beam-beam effects related to the crab crossing scheme have been studied mainly by K. Ohmi [6]. Both the weak-strong and strong-strong beam-beam simulations were

carried out for the studies, although it is believed that the strong-strong simulation gives more reliable prediction on the beam-beam performance. Both methods treat the beams in three-dimensional space and slice the bunch along the longitudinal direction using the so-called synchrobeam map [7]. In the strong-strong simulations, 100,000 macroparticles were tracked up to 20,000 turns (5 times of the transverse damping time) with the radiation damping and excitation processes. The potential of the beam-beam interaction is calculated with the PIC method. The transverse plane at the IP was divided into 128 x 256 grids with unit mesh size of 20 μm x 0.4 μm. The number of longitudinal slices was five. In the weak-strong simulations, 100 macroparticles were tracked up to 40,000 turns.

An achievable beam-beam parameter or luminosity has been estimated by using the strong-strong simulation method with and without the crossing angle. In the simulations, machine parameters used were the same as those of present KEKB except that the energy transparency condition on the beam currents was kept to avoid complexity on behavior of the beams. The simulations showed that we can obtain a vertical beam-beam parameter higher than 0.1 and double the luminosity if we eliminate the crossing angle. The head-on collision can be realized by installing the crab cavities even with the crossing angle. Another point of the high beam-beam parameter is that the horizontal tune must be very close to the half integer resonance. In the simulations in ref [6], the fractional part of the horizontal tune of both rings was set at 0.515. The latest values of KEKB are 0.511 and 0.505 for HER and LER, respectively. Further beam-beam simulations showed that an even higher beam-beam parameter than 0.1 can be obtained with a closer horizontal tune than 0.515 to the half integer. The conclusion of the strong-strong simulation is that we can expect a twice as high as beam-beam parameter or a doubled luminosity with the crab crossing scheme at the present working points.

Effectiveness of the horizontal tune close to the half integer for raising the luminosity has been proven in high luminosity colliders such as CESR, PEP-II and KEKB [8]. Usually its effect is explained in the context of the dynamic beta and dynamic emittance effects. Recently, another qualitative explanation has been given by K. Ohmi [9]. The point of this explanation is that the degree of freedom of the transverse beam-beam kick in the x-y plane is reduced from two to one in the limit of the horizontal tune on the half integer or the integer, since the absolute value of x becomes constant in this limit.

The crossing angle is interpreted as a dispersion that couples to z at the IP contrasted with the ordinary dispersion that couples with p(z). These dispersions as well as liner x-y coupling parameters at the IP, which are ideally zero, degrade the luminosity, if their values are significantly large [10]. Most of machine tuning time in daily operations at KEKB is devoted to that on those coupling or dispersion parameters. The crossing angle can be regarded as a kind of coupling parameters. Like other coupling parameters, tolerance for the crossing angle was also estimated by the strong-strong simulation. The simulation showed that the luminosity degradation is not negligible even with a half crossing angle of 1mrad, while the present value is 11mrad. It is desirable to keep the crossing angle small enough compared with 1 mrad. Another point of the effects of those coupling parameters is whether the tolerances for the x-y couplings and the dispersion at the IP will get severer with the vertical beam-beam parameter as high as 0.1. The simulations showed that their tolerances do not change so much even with the thus high beam-beam parameter. Degradations of the luminosity due to those coupling parameters including the crossing angle are explained in terms of the non-linear

diffusion [6]. To estimate the diffusion rate due to the crossing angle and to study its nature, the weak-strong simulation has been used with synchrotron radiation turned off. It was found that the crossing angle, which causes the x-z coupling, causes not only the horizontal diffusion but also the vertical one. The weak-strong simulation also gave some insights into the origin of the beam-beam limit by comparing their results with those of the strong-strong simulation [11].

3.1.3 Location of Crab Cavities and Optics Development

In the original plan, we planed to install a pair of crab cavities in each ring so that the crabbing orbits are localized near the IP. To this end, however, we need to construct a cryogenic system near the IP or to transport liquid helium from the Nikko area, where a cryogenic system for the superconducting RF cavities of HER is located, to the IP. We gave up both of these for a financial reason. Instead, we revised the plan to install one crab cavity for each ring in the Nikko section as is shown in Fig. 1. In this case, the crabbing motions are not localized near the IP and are extended to all over the rings. Even in this case, the crab crossing scheme can be realized by properly choosing kick voltages of the crab cavities and horizontal betatron phase advances between the crab cavities and the IP. This new scheme enabled us to largely reduce the cost for realizing the crab crossing scheme. Possible problems with this scheme are reduction of dynamic aperture due to the synchrobetatron resonances and head-tail instability. These issues are described below.
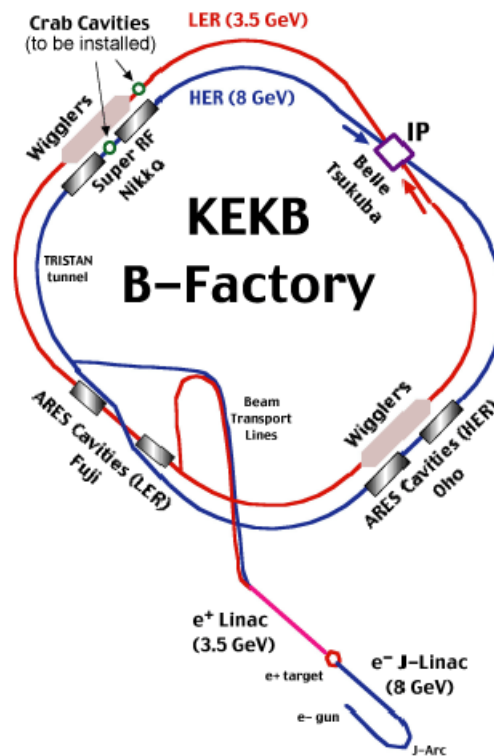

Figure 1: Schematic view of KEKB

Prior to installation of the crab cavities, we have already developed optics compatible with this new scheme. Table 1 summarizes requirements to the optics and some related

machine parameters. The bottom condition is required to measure the crab angle at the positions of streak cameras. We needed to alter the optics of HER, which should have a higher horizontal beta function at the crab cavity, more largely. For this purpose, we increased the number of families of the quadrupole magnets in the Nikko RF section from 8 to 14. This increase was needed to disorder a regular structure of the RF cells and make a higher beta at the place where the crab cavity will be installed. On the other hand, in the case of LER, we did not need to change the number of families of quadrupoles, since the required value of the beta function at the crab cavity is not much different from the original value. However, we changed a design orbit of LER so that the synchrotron light from the bending magnets does not hit the crab cavity directly, since the planed location of the cavity is near to the arc section. For this purpose, we removed chicane bending magnets, which used to be used for circumference tuning, in Nikko section from operation. Without these, circumference tuning can be done by using another set of chicane magnets installed on the opposite side of the ring (Oho section). In addition, we newly installed four weak bending magnets in this section. Another change of the optics in LER is that of the horizontal dispersion. In the original optics, we had a dispersion of about +/- 0.5m in peak-to-peak value in the Nikko wiggler section. To remove the dispersion at the crab cavity location, which may induce additional difficulty, we made the whole of the Nikko wiggler section virtually non-dispersive. Also in this case, the dispersion in the Oho wiggler section was made larger so that a design horizontal emittance is preserved.

Table 1: Requirements to crab optics and related machine parameters

	LER	HER
β_x^* [cm]	59	56
Crab kick voltage [MV]	1.4	1.44
β_x^{crab} [m]	40	200
$\Delta\phi_x$ [crab - IP]	$2n\pi +/- \pi/2$	
$\Delta\phi_x$ [streak - IP]	$n\pi$	

With the crab optics, the dynamic aperture issue was investigated by using the SAD code [12]. The simulations were done in the neighborhood of the present working points, where the most important resonance line is that with the condition of $2\nu_x+\nu_s$=integer. This resonance has been giving a performance limitation to KEKB particularly in HER. A poor beam lifetime from narrow dynamic aperture prevents us from lowering the horizontal tune in HER, although the beam-beam simulation predicts that a higher luminosity would be obtained with the lower horizontal tune. In the case of LER, this resonance line is relatively weak thanks to the local chromaticity correction scheme adopted only in LER and usually does not give any performance limitations. Our main interest on the dynamic aperture issue is whether the strength of the resonance lines is changed or not with the crabbing motion around the rings. The tracking simulation including tune surveys around the present working points showed that there is no significant difference in dynamic aperture with the crab cavities on and off. We concluded that the crabbing motion around the rings would be safe from the viewpoint of dynamic aperture.

Hardware works for the crab optics were done during the summer shutdown in 2005. In autumn in 2005, we actually operated the machine with the crab optics without the

crab cavities. We confirmed that we can obtain a luminosity equivalent to that before the change of the optics, although we made some modifications to the crab optics. The largest modification was a change of the integer part of the horizontal tune in HER. This change was done as a part of efforts to investigate into poor luminosity recovery after the summer shutdown, although it is not clear how important this change was for the luminosity. In the present crab optics, the condition of the horizontal phase advance between the streak camera and the IP is not exactly satisfied, although we still maintain enough sensitivity for measuring the crabbing angle.

3.1.4   Beam Instability

A possible problem with the present crab crossing scheme where the crabbing motion is not localized near the IP is a head-tail instability originated from this crabbing motion. To study this problem, a multi-particle tracking study has been done in HER using SAD by A. Morita [13]. In this simulation, a short range linear wake was assumed with the potential of 10^{16} V/Cm per ring. The impedance was distributed to the accelerating cavities of the ring. The number of macroparticles was 1000 representing 3.3×10^{10} particles per bunch. The particles were tracked through 32,000 turns that correspond to 8 damping time. Dipole moments, head-tail moments and emittances were observed with the crab cavity on and off. We found no indications of the instability regardless of the presence the crab cavity. The assumed value of the wake potential is that assumed at the design phase of the KEKB and the real value may be somewhat higher than this. In the simulation, however, the head-tail instability was observed with more than one order higher impedance. And even in this case, no enhancement of the instability by the crabbing motion in the ring was seen. Based on this simulation, it is believed that no head-tail instability from the crabbing motion will occur with the crab cavity. Another possible instability originated from the crab cavities is coupled bunch instability due to trapped modes of the cavities. So far, however, no dangerous modes have been found in calculations and bench tests.

3.1.5   Plans for Beam Commissioning with Crab Cavities

Since the effect of the crab crossing scheme was demonstrated by the beam-beam simulations, the R&D works for the crab cavity system have been accelerated at KEKB. And they are now at the final stage [14]. In the present plan, the crab cavities for a beam test will be installed in the rings during the coming winter shutdown. After the installation, a beam test of the crab cavities will be conducted. Main purposes of the beam test are hardware tests of the crab cavity itself and studies on the beam dynamic issues with the crab crossing scheme. For these purposes, about one month will be devoted. Since a concrete plan of the beam test has not been made yet, a rough plan is described in the following. Basically, the crab cavities to be installed in the next winter are considered as a test version. After the beam test, they will be removed from the rings, unless their performance is unexpectedly good under the condition of high beam currents comparable with the level of the usual operation. The beam test will start with very small beam currents and the beam currents will be gradually increased. In the process, conditioning of the crab cavities with the beams and vacuum scrubbing will be done. From the viewpoint of the hardware test, it is important to check that basic functions of the crab cavity work well with sufficient stability in the presence of the

beams. In the high beam current condition, we will investigate into performance of some key components such as HOM absorbers, RF contacts and coaxial tuners and their tolerance against the high beam currents. The goal of the beam test is not an actual use of the crab cavities in the physics run but finding of problems that will be feedback to the next version.

From the viewpoint of the beam dynamics, the most important point will be to confirm that the high beam-beam parameter predicted by the beam-beam simulation can be actually attained with the crab crossing scheme. For this study, high beam currents are not needed. In principle, we can study the maximum attainable beam-beam parameters with a single bunch collision. However, our present plan is to conduct this study with medium beam currents that are about 1/6 of those in the usual physics run. This is because collision tuning tools are tuned to work at relatively high beam currents. In the case that these medium beam currents are not possible to be stored due to some hardware problems of the crab cavities, we will do the study with smaller beam currents. In this study, in addition to usual collision parameters such as the x-y coupling parameters at the IP, the IP vertical dispersion or the betatron tunes, the crab voltage and its phase should be optimized so that we can maximize the beam-beam parameters or the luminosity. Although the crabbing angle can be adjusted using the streak camera, this is a rough tuning. Due to the transition from the crossing angle to the head-on collision using the crab cavities, the methods of the luminosity tuning may be altered. To find effective methods of the luminosity tuning is also one of the purposes of the beam test. Another point of the beam test is to study the single bunch instability possibly induced by the crabbing motions in the rings. The dynamic aperture issue should be also investigated by observing the beam lifetime. These studies can be done with relatively small beam currents and will be done before we go for critical tests of the crab cavities with the high beam currents. With the high beam currents, the coupled bunch instability due to trapped modes of the crab cavity should be also studied.

3.1.6   References

1. KEKB B-Factory Design Report, KEK Report 95-7, June 1995.
2. K. Hirata, Phys. Rev. Lett. 74, 2228 (1995).
3. R.B.Palmer, SLAC-PUB-4707, 1988.
4. K. Oide and K. Yokoya, Phys. Rev. A 40, 315 (1989).
5. Y. Funakoshi et al., Proceedings of EPAC2006, Edinburgh, Scotland, June 2006 pp. 610.
6. K. Ohmi et al., Phys. Rev. ST Accel. Beams 7, 104401 (2004).
7. K. Hirata et al., Part. Accel. 40, 205 (1993).
8. Beam Dynamics Newsletter No. 31, August 2003.
9. K. Ohmi, private communications.
10. K. Ohmi et al., Proceedings of PAC2005, Knoxville, Tennessee, May 2005 pp. 925.
11. K. Ohmi et al., Phys. Rev. Lett. 92, 214801 (2004).
12. A. Morita et al., Proceedings of PAC2005, Knoxville, Tennessee, May 2005 pp. 865.
13. A. Morita, private communications.
14. K. Hosoyama, http://agenda.kek.jp/fullAgenda.php?ida=a0653.

3.2   Status of the BEPCII Project

Chuang Zhang for BEPCII Team
Institute of High Energy Physics, Chinese Academy of Sciences
P.O.Box 918, Beijing 100049, China
mail to: Zhangc@ihep.ac.cn

3.2.1   Introduction

As a natural extension of the Beijing Electron-Positron Collider (BEPC), the BEPCII project has started its construction since the beginning of 2004. The BEPCII will operate in beam energy of 1-2.1 GeV, so that its physical potential in τ-charm range is preserved. Its design luminosity is $1 \times 10^{33} cm^{-2}s^{-1}$ at 1.89 GeV with double-ring structure. The upgraded collider will also provide improved synchrotron radiation performance with higher beam energy and intensity. Some key technologies, such as superconducting RF, low impedance vacuum devices, superconducting micro-β quadrupoles, etc. are developed. The injector linac commissioning was carried out, and its design performance is expected in the summer of 2006. Manufacturing of most storage ring components is completed. The upgrading of the utility for BEPCII is finished. The cryogenic system commissioning and then test/measurement of the superconducting devices are on the critical path of the BEPCII schedule. The commissioning of the storage rings is planned to be started in the autumn of 2006. The Physics run of BEPCII/BESIII is scheduled to start by autumn 2007.The BEPCII will be operated in the beam energy region of 1.0-2.1 GeV The storage ring design is optimised at the beam energy of 1.89 GeV, and the details can be found in its design report [1]. The layout of the BEPCII storage rings with BESIII detector is shown as Fig. 1.


Figure 1: The layout of the double ring of the BEPCII.

The inner ring and the outer ring cross each other in the northern and southern IP's. The horizontal crossing angle between two beams at the southern IP, where the detector locates, is 11mrad×2 to meet the requirement of sufficient separation but no significant degradation to the luminosity. While in the northern IP, the two beam cross horizontally with angle of 11mrad×2 and a vertical bump is used to separate two beams, so that the optics of the two rings can be symmetric. For the dedicated synchrotron radiation operation of the BEPCII, electron beams circulate in the outer ring, so in the northern IP, a bypass is designed to connect two half outer rings and in the southern IP, a pair of bending coils in superconducting magnets serves this purpose.

In order to obtain a high average luminosity, top-off injection is adopted up to 1.89 GeV, and the positron injection rate should be higher than 50 mA/min. Table 1 summarizes the main parameters of the BEPCII.

Table 1: Main Parameters of the BEPCII

Parameters	Unit	Collision	SR
Optimum Energy	GeV	1.89	2.5
Circumference	m	237.53	241.13
RF frequency	MHz	499.8	499.8
RF voltage	MV	1.5	3.0
Bunch number		93	200-300
Beam current per ring	A	0.91	0.25
Injection energy	GeV	1.89	1.89
β function at IP	m	1/0.015	–
Crossing angle	mrad	11×2	–
Beam-beam Parameter		0.04	–
Luminosity	$cm^{-2}s^{-1}$	1.0×10^{33}	–

3.2.2 The Injector Linac

The BEPC injector is a 202-meter electron/positron linac with 16 RF power sources and 56 S-band RF structures. The BEPCII requires the injector in two aspects. One is the full energy injection to the storage rings, i.e. $E_{inj} \geq 1.89$ GeV; the other is that the positron intensity satisfies the required injection rate of 50 mA/min. To realize the full energy top-off injection up to 1.89 GeV, the klystrons are replaced with the new 45-50 MW devices and the modulators upgraded with new pulse transformer oil tank assembly, PFN, thyratron, charging choke and DC power supplies. In order to compensate the RF phase drift due to various factors, a RF phasing system is developed.

The technical measures taken for increase of positron intensity in the BEPCII injector can be summarise as: to increase the e$^-$ beam current on e$^+$ target from 2.5A to 6A, the repetition rate from 12.5Hz to 50Hz, the bombarding energy for e$^+$ from 140MeV to 240MeV; adopt new positron source to increase the yield from 1.4% to 2.7%, and two bunch injection scheme. Though the pulse length reduced from 2.5 ns to 1ns, the total gain factor on the e+ intensity can be about 20 times higher than BEPC.

All the new hardware subsystems, including the electron gun, 40MeV pre-injector, 200MeV booster section and the positron source of the BEPCII linac were installed in the summer 2004 after dismounting of old devices. Figure 2 shows the BEPCII linac injector.

It took less than one month to start up the machine and process the new systems before the linac provided electron beam for the dedicated SR operation of the BEPC storage ring starting from the beginning of the December 2004. The commissioning of the linac for the positron beam has been carried out during the machine studies. The first positron beam of 50mA was obtained at the linac end on March 19th, 2005. The electron beam out of gun is ~10A, and ~ 6A at the positron converter target as simulation predicted. Almost all of 16 RF power sources have been rebuilt, and stably work at 50pps. New control and beam instrumentation make the machine commissioning and operation much easier. The commissioning results of the linac are listed in Table 2 showing that its design specification is reached.

Figure 2: The BEPCII linac injector

Table 2: The results of the linac commissioning

	Unit		Measured	Design
Energy	GeV		1.89	1.89
Current	mA	e$^+$	63	37
		e$^-$	>500	500
Emittance	mm·mrad	e$^+$	0.32	0.4
		e$^-$	0.09	0.1
Energy spread	%	e$^+$	0.50	0.50
		e$^-$	0.55	0.50
Repetition rate	Hz		50	50
Pulse length	ns		1.0	1.0

3.2.3 The Storage Rings

The design of the BEPCII storage rings aims at a high luminosity, shown in Table 1. The luminosity of an e$^+$-e$^-$ collider is expressed as

$$L(\text{cm}^{-2}\text{s}^{-1}) = 2.17 \times 10^{34}(1+r)\xi_y \frac{E(GeV)k_b I_b(\text{A})}{\beta_y^*(\text{cm})}$$

where $r = \sigma_y^*/\sigma_x^*$ is the beam aspect ratio at the interaction point (IP), ξ_y the vertical beam-beam parameter, β_y^* the vertical envelope function at IP, k_b the bunch number in each beam and I_b the bunch current. The strategy for the BEPCII to reach the design luminosity is to applying multi-bunch collisions with double rings (k_b=93), micro-β at IP with short bunches whose length is compatible to the β_y^* value. The machine physics issues for intensive beams and high luminosity are intensively studied [2].

3.2.3.1   *RF System*

The superconducting RF cavities are chosen for its advantage on large accelerating gradient and well-damped HOMs. Two superconducting cavities are needed in the BEPCII with one cavity installed on each ring to provide necessary RF voltage of 1.5 MV to shorten bunch length. The structure of the superconducting cavity is similar to that of KEKB style with frequency of 499.8 MHz instead of 508 MHz. Each cavity is powered with a 250 kW klystrons. The refrigeration capability of 300W is required for two superconducting cavities, so a 500W refrigerator is equipped in the cavity side. The cavity assembly has been completed and horizontal high power test is in progress. Figure 3 pictures the first cavity in the test station.

Figure 3: A RF cavity in test

Figure 4: New PM wiggler

3.2.3.2   *Magnets and Power Supplies*

Due to limited space in the BEPC existing tunnel, except the old BEPC magnets reused, both the longitudinal and transverse size of the newly built magnets should be small enough. In addition, the magnets are designed to give room for the antechamber on horizontal plane. At present, over 97% of the ring magnets have been fabricated and field measured. There are three permanent magnet wigglers in the storage rings for SR operation, two out-vacuum and one in-vacuum. The new permanent magnet wiggler 1W1 is shown in Fig. 4. All others are electric magnets.

To provide required flexibility for BEPCII operation with various modes, each arc quadruple is excited with its independent power supply. There are all together 345 power supplies in the BEPCII storage rings. Most of ring power supplies have been delivered, installed and tested.

3.2.3.3   *Injection Kickers*

In order to meet the challenges both on the filed uniformity and low coupling impedance, a modified slotted pipe kicker has been designed with the coating strips on ceramic bar instead of metallic plates as the beam image current return paths. With careful design and manufacture, the measured magnet quality is better than that of the design specifications. All of the kicker magnets and their pulsed power supplies were completed. Figure 5 shows a kicker installed in the BEPCII tunnel.

Figure 5: A kicker installed in the BEPCII tunnel

3.2.3.4 *Vacuum System*

The BEPCII poses two challenges to the vacuum system, one is the vacuum pressure, and the other is the impedance. The design values of the dynamic vacuum pressure are 8×10^{-9} Torr in the arc and 5×10^{-10} Torr in the IR. Antechambers are chosen for both electron and positron rings. For the positron ring, concerning the ECI, the inner surface of the beam pipe in the arc is coated with TiN in order to reduce the secondary electron yield (SEY).

Up to now, all 80 arc chambers are delivered, most of straight section chambers of total 120 are completed. TiN coating for the vacuum chambers of the positron ring is completed. Measurement results show that the maximum SEY are 1.6-1.9. Figure 7 shows an aluminium antechamber in coating.

Figure 6: An aluminium antichamber in coating

3.2.3.5   *IR and Superconducting Insertion Magnets*

The design of interaction region (IR) has to accommodate competing and conflicting requirements from the accelerator and the detector. Many types of equipment including magnets, beam diagnostic instruments, masks, vacuum pumps, and BESIII detector must coexist in a very small region.

A special pair of superconducting IR magnets (SCQ's) are designed with main and skew quadrupoles, compensation solenoid and dipole coils to squeeze the β function at IP, compensating the detector solenoid and to serve as the bridge connecting outer ring in SR operation, respectively. Some special warm bore magnet in IR such as septum bending magnet and two-in-one quadrupoles have been manufactured. The magnetic field measurement results confirm the design. The horizontal test of the SCQ's will start soon. Figure 5 shows two SCQ's and some warm magnets installed in the IR.

Figure 7: SCQ's and some warm magnets installed in IR

3.2.3.6   *Instrumentation and Control*

The instrumentation system consists of 136 beam position monitors (BPM's), 2 DCCT's, 2 bunch current monitors and 2 synchrotron radiation monitors. Transverse feedback systems are equipped in order to damp beam instabilities. Majority of the monitors and their electronics are completed and ready for installation. The software development is in progress.

The control system is based on the EPICS environment providing a friendly man-machine interface for operators. Control hardware is installed and software is being developed. The system is being prepared for commissioning scheduled to start in October 2006.

3.2.3.7   *Installation*

The magnets, vacuum chambers and other components are pre-aligned in laboratory before they are installed into the tunnel. There are altogether 80 arc units in two rings. About 80% the units have been installed in the BEPCII tunnel. Figure 7 shows a part of the installed units.

Figure 8: Installed accelerator units in the BEPCII tunnel

3.2.4   Budget and Schedule

The budget of the BEPCII project is estimated as 640 million RMB. Physics run of BEPCII/BESIII is scheduled to start by autumn 2007.

3.2.5   References

1. BEPCII Group, BEPCII Design Report, IHEP-Proceedings, Aug. 2001.
2. G. Xu, et al, Accelerator Physics Design of BEPCII, Beam Dynamics Newsletter, No. 31, pp. 32-41, August 2003.

4   Light Sources

4.1   Progress on the Australian Synchrotron Project

Alan Jackson
Technical Director
mail to: alan.jackson@synchrotron.vic.gov.au

On Thursday, 8th June 2006 – just before midnight, electrons were coaxed around the Australian Synchrotron storage ring for the first time, soon there-after many more turns were observed – see figure 1. This event marked the start of storage ring commissioning with beam of a facility that began its life with the announcement of funding just 3 ½ years earlier, at the end of January 2003.
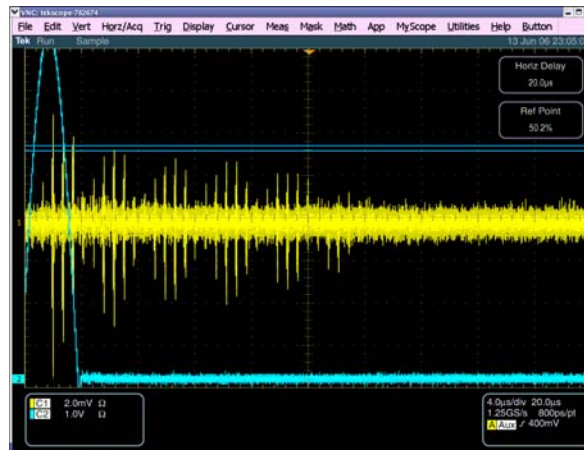
Figure 1: The injection kicker pulse (blue), and the first 30+ turns of electrons in the AS storage ring.

The Australian Synchrotron (AS) is a 3-GeV third-generation synchrotron facility being built in the SE suburbs of Melbourne, and is being delivered by Major Projects Victoria (MPV), a part of the Victorian State Government. The layout of the facility is shown in figure 2, and the main design parameters of the storage ring are listed in Table 1. The funding for the construction of the facility, announced by the State Treasurer John Brumby on 30 January, 2003, totals ~A\$206M (~ US\$150M), of which A\$157M is for the building and accelerators, and A\$49M for the first phase of nine beamlines. The funding for the building and accelerators has been provided by the Victorian State Government, whilst the beamlines are being funded by a group of interested parties, including universities, research organizations and other state governments.

Table 1: Key design parameters

Energy	3 GeV
Beam current	200 mA
Circumference	216 m
Number of straights	14
RF frequency	500 MHz
Beam size (in bending magnets) (σ)	87 μm x 58 μm
Natural Emittance ($\eta = 0.10$ m) (σ)	10 nm
Injection Energy	3 GeV
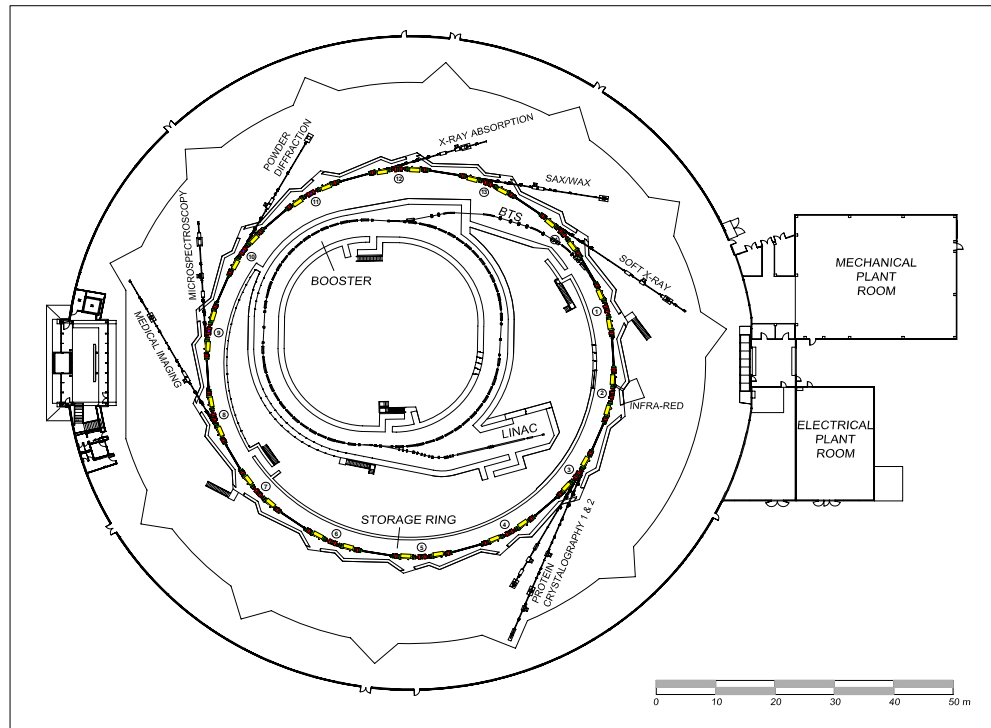
Figure 2: General layout of the Australian Synchrotron

The AS is being delivered on a green-field site with a small team of relatively inexperienced staff. The number of staff started at 3 in January 2003 and has grown almost linearly to 54 at the end of 2005. Figure 3 shows the team (not all present!) assembled in front of the Synchrotron main entrance. This team has been augmented by specialist contractors and consultants as required. The organizational structure of the project delivery team is shown in Figure 4. Due to the relatively small number of staff, much of the responsibility for the design and project management has been placed on suppliers, with turn-key contracts, that included elements of design, engineering, project management, installation and commissioning.

Contracting turn-key systems has meant that great attention needs to be paid to controlling the interfaces between systems, and to the quality of documentation and training provided by the contractors, to ensure that AS staff has the capability to maintain the facility to give the required level of performance for reliability and availability.

Figure 3: The Australian Synchrotron Delivery Team, March 2006
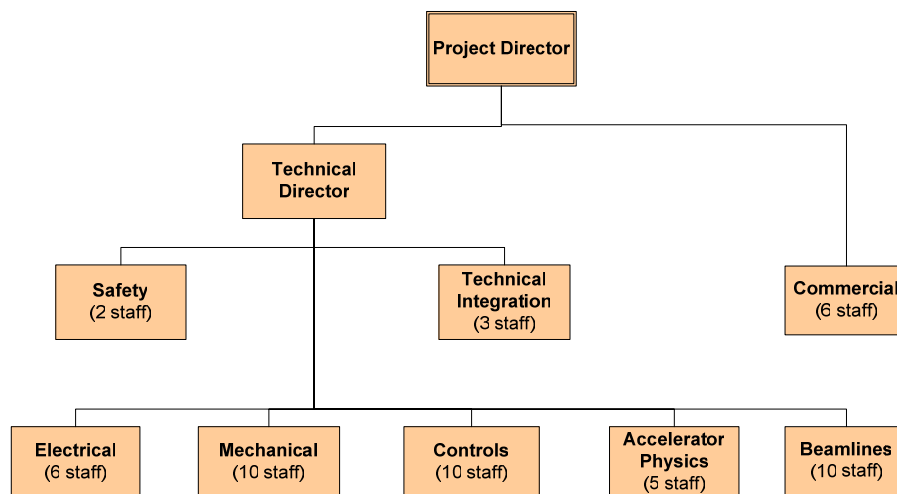
Figure 4: Organisation of the AS Project Delivery Team

During the past 3 ½ years most of the project milestones have been met on schedule: The building contract was let July 2003 and completed in February 2005, with all the accelerator shielding enclosures complete. Staff moved into their new premises in March 2005, and accelerator installation commenced in April. Installation of all the accelerators was complete by May 2006, and commissioning of the storage ring with beam started in June – hitting a milestone that had been set three years previously. Hand-over for operations, with at least four beamlines with beam on target, is scheduled for March 31, 2007.

Funding for the first nine beamlines is in place and contracts for many of the insertion devices, photon delivery systems, shielding enclosures (hutches), and end station equipment have already been awarded. Construction of the hutches will start in September 2006, and installation of optical elements and detectors will follow immediately thereafter. Commissioning of the beamlines is scheduled to start in January 2007.

Table 2 lists the first nine beamlines, identifying the technique to be used on the beamline, and the source of radiation. Figure 5 shows a cut-away drawing of the Powder Diffraction Beamline. The hutch roofs have been "removed" to reveal the focusing optics and monochromator contained the "first optical enclosure", and the detector systems housed in the first and second shielded experimental end-stations.

Table 2: The first Australian Synchrotron Beamlines

Beamline ID	Technique	Source
2IR	Infrared Spectroscopy	Bending Magnet
3BM	Protein Crystallography	Bending Magnet
3ID	Protein Crystallography	In-vacuum undulator
8ID	Imaging & Medical Therapy	Superconducting wiggler
9ID	Microspectroscopy	In-vacuum undulator
10BM	Powder Diffraction	Bending Magnet
12ID	X-ray Absorption Spectroscopy	Wiggler
13ID	Small & Wide Angle X-ray Scattering	In-vacuum undulator
14ID	Soft X-ray Spectroscopy	APPLE II Undulator

Much work remains to be completed before the facility becomes operational early next year. However, with the on-time start of the commissioning of the storage ring, and with contracts for the beamline systems on schedule, the delivery team is confident that it will meet all the acceptance criteria required for a successful transition into operations.

Figure 5: Cut-away layout of one of the Powder Diffraction Beamline, showing the optical components housed in the first hutch, followed by two experimental hutches.

4.2   Status of PAL-XFEL Design

In Soo Ko
Pohang Accelerator Laboratory, POSTECH, Pohang, Kyungbuk, 790-784 Korea
mail to: isko@postech.ac.kr

4.2.1   Abstract

Pohang Accelerator Laboratory has a plan to build an X-ray FEL machine. This new machine will utilize the existing 2.5 GeV injection linac to the storage ring by upgrading its energy up to 3.7 GeV and using an in-vacuum undulator. The target wavelength will be 3 Å and its third harmonic 1 Å will also be used. The project will proceed in two stages: In the first stage, a VUV SASE machine with 385 MeV will be

constructed and tested for the proof-of-principle. The full X-ray machine will be constructed in the next stage.

4.2.2   Introduction

Pohang Accelerator Laboratory (PAL) is going to build a new X-ray FEL machine based on SASE (self amplified spontaneous emission) scheme. This new machine called PAL-XFEL will utilize the existing 2.5 GeV electron linac by upgrading its energy and performance. The linac is currently used for injection to the 2.5 GeV storage ring of Pohang Light Source (PLS). The X-ray community, which is the biggest synchrotron user community in Korea, has demanded that the target wavelength be in 1-1.5 Å range, which put quite a challenge for the PAL-XFEL design. Since the available linac energy of PAL is limited, we decided to utilize third harmonic radiation of SASE. The existence and usefulness of SASE higher harmonic radiation was verified in VUV-FEL at DESY [1]. The fundamental wavelength of PAL-XFEL will be 3 Å and the third harmonic will be 1 Å, both of which will be used. A PAL-XFEL layout is shown in Fig. 1. In the figure, the current linac building is shown and the new 1.2 GeV linac is drawn outside the existing building. We are going to build the new part of PAL-XFEL while still running PLS.
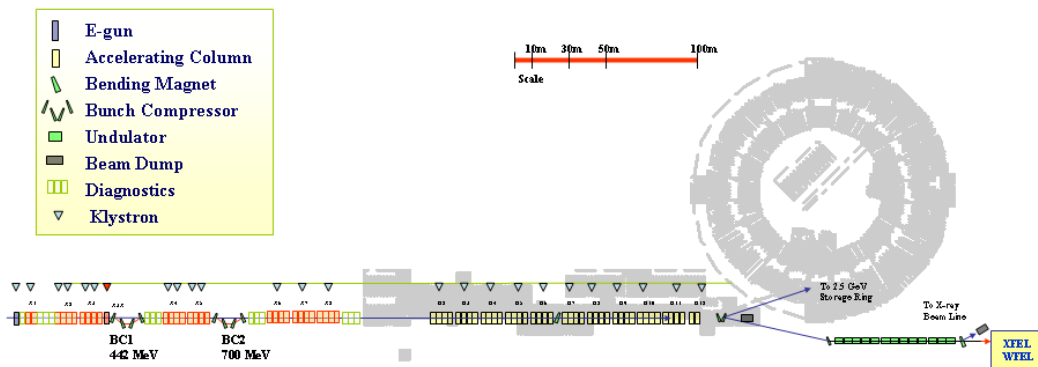
Figure 1: Layout of PAL-XFEL. The current linac building is shown in the figure. The beam transport dog-leg has approximately 0.5°, although it is exaggerated in the figure.

It is still not easy to obtain 3 Å SASE radiation with 3.7 GeV electron beam. Both the undulator period and the undulator parameter should be small enough to be allowed only for an in-vacuum undulator. Therefore PAL-XFEL will adopt an in-vacuum undulator with small period.

The PAL-XFEL project will proceed in two stages. In the first stage, only a separate 385 MeV SASE machine will be constructed. The purpose is to test and prove the design strategy of PAL-XFEL. Hence, this test machine (TM) will use the same undulator as PAL-XFEL. Only in the second stage, the full PAL-XFEL will be constructed. Design of the two machines (TM and PAL-XFEL) is still on-going. In this status report, overall design and major parameters of the two machines will be presented.

4.2.3 PAL-XFEL

4.2.3.1 *Overview*

Recall that the resonant wavelength of an undulator is given by

$$\gamma_r = \frac{\lambda_u}{\gamma^2}\left(1+\frac{K^2}{2}\right),$$

where λ_r is the resonant frequency, λ_u the undulator period, γ the Lorentz factor, and K the undulator parameter. From this relation, it is clear that 3 Å radiation is generated by 3.7 GeV electron beam only with an in-vacuum undulator. Therefore, PAL-XFEL will adopt an in-vacuum undulator with $\lambda_u = 1.5$ cm. Fundamental parameters of PAL-XFEL are listed in Table 1.

Table 1: Parameters of PAL-XFEL.

Beam Parameter	Value	Unit
Electron energy	3.7	GeV
Peak current	3	kA
Normalized slice emittance	1	mm mrad
RMS slice energy spread	0.01	%
Full bunch length	270	fs
Undulator Parameters		
Undulator period	1.5	cm
Segment length	4.5	m
Full undulator length	80	m
Peak undulator field	1.19	T
Undulator parameter, K	1.49	
Undulator gap	4	mm
Average β-function	10	m
FEL Parameters		
Radiation wavelength	3	Å
FEL parameter, ρ	5.7×10^{-4}	
Peak brightness	5×10^{31}	photon/(sec mm^{2}mrad^2 0.1%BW)
Peak coherent power	1	GW
Pulse repetition rate (Max.)	60	Hz
1D gain length	1.2	m
Saturation length, L_{sat}	45	m

Computer simulation with GENESIS code [2] shows that the SASE power gain proceeds properly and the saturation is reached at a reasonable length of 45 m. The GENESIS output is shown in Fig. 2.
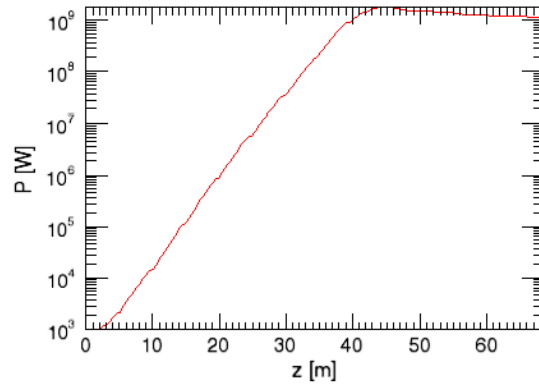
Figure 2: Power gain and saturation of PAL-XFEL.

4.2.3.2 *Linac*

The PAL-XFEL linac is composed of two sets of bunch compressors, one X-band accelerating section that is needed to compensate non-linearities, and conventional S-band accelerating columns. In the current design, the 1st bunch compressor (BC1) is located at the point of 430 MeV and the 2nd one (BC2) is located at 630 MeV. The X-band structure is located just before BC1. BC1 compresses the 10 ps injector output to around 200 μm and BC2 compresses it further to 80 μm. A layout of PAL-XFEL injector and linac is shown in Fig. 3. As is well known, a serious problem in the bunch compressor design is the effect of coherent synchrotron radiation (CSR) in the bending magnets, especially the CSR instability which can develop for very cold beams [3]. The PAL-XFEL bunch compressors have been designed to minimize the CSR effect. However, a possible use of a laser heater as a back-up plan is reserved. After BC2, the full bunch length of the almost rectangular beam is longer than 80 μm.
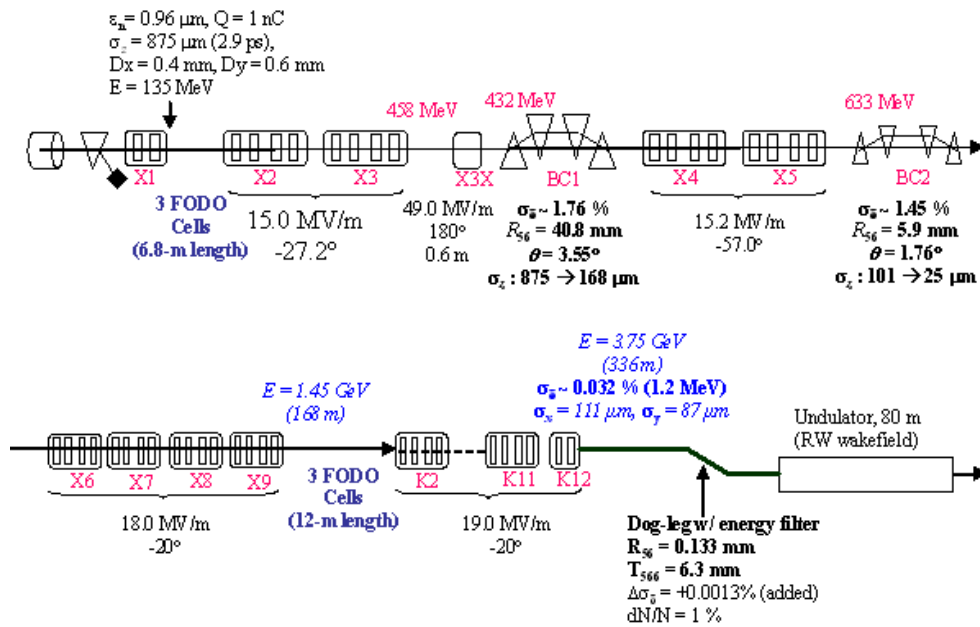
Figure 3: Layout of the PAL-XFEL injector and linac.

There are two FODO cells in the linac, one is 6 m long and located just after the injector and the other one is 12 m long and located right after the 9th accelerator column as shown in Fig. 3. These two FODO cells will be used for the diagnostic purposes. After the linac, there places 36 m long beam transport line to the undulator. It includes a dog-leg composed of 4 bending magnets, each of which bends 0.5°.

4.2.3.3 *Undulator*

The PAL-XFEL undulator will be a hybrid planar undulator with the material of vanadium permendur. Basic parameters of PAL-XFEL undulator are listed in Table 1. As shown there, each undulator segment is 4.5 m long. Between segments, a 0.5 m space is reserved for diagnostic equipments and a quadrupole for the beam focusing. Also, either a corrector magnet or trim windings on the quadrupole is planned. The average β function of the undulator lattice is optimized to 10 m for minimal saturation length and maximal power gain.

4.2.4 Test Machine

The purpose of TM is to prove, in the low energy, that PAL-XFEL is achievable. Hence, TM will have a low energy of 385 MeV, approximately a tenth of PAL-XFEL energy, but the undulator will be the same as in PAL-XFEL except the segment and total length. Beam parameters are chosen to give comparable magnitude of energy spread to the PAL-XFEL case. The optimal average β function of the undulator lattice is reduced from 10 m of PAL-XFEL to 2 m. A few fundamental parameters of TM are shown in Table 2.
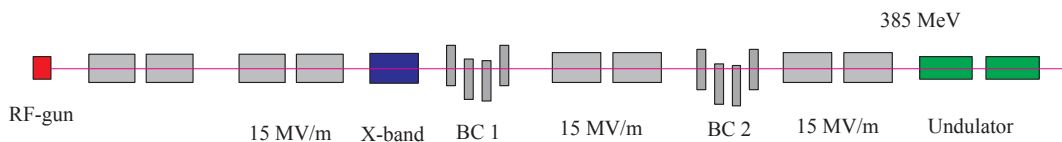
Figure 4: Layout of the test machine.

Table 2: Parameters of the test machine.

Beam Parameter	Value	Unit
Electron energy	0.385	GeV
Peak current	0.8	kA
Normalized slice emittance	0.8	mm mrad
RMS slice energy spread	0.01	%
Full undulator length	8	m
Average β-function	2	m
Radiation wavelength	28	nm
FEL parameter, ρ	3.4×10^{-3}	
1D gain length	0.2	m
Saturation length, L_{sat}	45	m

4.2.5 Injector

The photo-cathode RF gun is one of the essential elements for the success of SASE FEL. Our aim is to achieve normalized slice emittance of 1 micron or smaller for 1 nC bunch charge. The design pulse length is 10 ps and the final energy of the injector is 135 MeV. The PAL-XFEL photo-cathode gun is currently under development. Currently the R&D place is in a test stand separate from the XFEL site. The gun R&D facility consists of a 1.6-cell photocathode RF gun, a Ti:Sa laser, and special beam-diagnostic devices. The first beam was obtained in November 2005. Since then, much effort has been made for improving laser-beam qualities including timing and pointing stabilities, transverse uniformity, and remote control capabilities. Details of PAL-XFEL injector R&D status are presented in separate papers [4,5].

4.2.6 Summary

PAL-XFEL will provide 3 Å FEL by expanding and upgrading the existing linac up to 3.7 GeV. It will use an in-vacuum undulator. The photo-cathode RF gun is under development. Linac has been designed to compress the bunch to a very short length and to keep the emittance low at the end of the linac. The whole project will proceed in two stages. In the first stage, only a 385 MeV TM will be constructed to prove the validity of PAL-XFEL design. The full PAL-XFEL will come in the second stage.

4.2.7 References

1. Y. J. Kim, Talk given at Pohang Acceleratory Laboratory.
2. S. Reiche, Nucl. Instr. and Meth. A, 429 (1999) 242.
3. S. Heifets et al., SLAC-PUB-9165, 2002.
4. S. J. Park, J. Y. Huang, C. Kim, I. S. Ko, and T.-Y. Lee, to be appeared in the proceedings of the ICFA Beam Dynamics Workshop 37 (Future Light Source) held at DESY on May 15-19, 2006.
5. C. Kim, J. Y. Huang, I. S. Ko, and S. J. park, to be appeared in the proceedings of the ICFA Beam Dynamics Workshop 37 (Future Light Source) held at DESY on May 15-19, 2006.

4.3 Accelerator-related Activities at Singapore Synchrotron Light Source

H.O. Moser, C.Z. Diao, P.D. Gu, Z.W. Li
Singapore Synchrotron Light Source
National University of Singapore
mail to: slshom@nus.edu.sg

4.3.1 Introduction

The Singapore Synchrotron Light Source (SSLS) is a university-level research institute at the National University of Singapore (NUS). It is dedicated to generating and exploiting synchrotron radiation for research and development purposes, and provides services for customers including research institutions, industry and institutions of public interest. At present, synchrotron radiation is produced by a compact 700 MeV

electron storage ring with two 4.5 T superconducting dipoles. Routinely, initial currents stored are well in excess of 400 mA with a lifetime of 11 hours which can increase to 17 hours at smaller currents. Electron beam emittance is about 1.3 μm·rad due to the large bending angle of 180° [1, 2]. It covers a spectral range of 7 orders of magnitude from hard X-rays to the far infrared.

4.3.2   Present Status

Meanwhile, the scope of activities at SSLS is mainly divided into three directions: Micro/nanofabrication of materials and devices using lithography technique is covered with the LiMiNT facility (Lithography for micro/nanotechnology) [3] while the characterisation of materials and processes relies, currently, on four beamlines, namely, the white-light hard X-ray phase contrast imaging and tomography beamline (PCIT beamline) [4]; surface, interface, and nanostructure science (SINS beamline) [5] in the soft X-ray spectral range; a hard X-ray facility for diffraction, absorption spectroscopy and fluorescence (XDD beamline) [6] and an infrared spectro/microscopy facility (ISMI beamline) [7]. A further beamline for electron beam diagnostics will be in operation by the end of 2006. This portfolio of experimental facilities makes SSLS rather attractive for a wide variety of research disciplines including micro/nanotechnology and semiconductor manufacturing, materials science and engineering, life sciences, data storage, environmental science and engineering, biomedical engineering, catalysis.

Beyond the exploitation of synchrotron radiation from the storage ring, SSLS is working at the development of superconducting miniundulators (supramini). Hardware progress was made with SSLS' prototype supramini featuring 50 periods of 14 mm period length. The technical test and training phase for it was successfully completed. Upon signing a Memorandum of Understanding on 27 April 2005, SSLS and the Shanghai Institute of Applied Physics (SINAP) have joined efforts to perform a proof of technology (POT) experiment by installing SSLS' supramini at SINAP's 100 MeV electron linac. The POT experiment will allow studying the essential issues of electron beam transport and radiation generation in a supramini, besides using its VUV radiation for experiments. In the meantime, the fabrication tolerances determining the performance of supraminis are being studied by analytical and numerical means to clarify, e.g., the influence of the finite length, and of mechanical fabrication and positioning errors on the magnetic field, the spectral output, and the phase error [8].

4.3.3   Future Work

The development of supraminis being a part of, SSLS envisions a 4th generation synchrotron light source to complement and, eventually, replace the current facility. This vision includes an accelerator system based on a superconducting linear accelerator with up to 5 recirculation loops for energy multiplication and recovery with the distinguishing feature that the light would be generated by superconducting mini- and micro-undulators. The facility would enable Free Electron Laser operation in the spectral ranges mid infrared to vacuum ultraviolet, extreme ultraviolet at 13.5 nm, water window (284 – 543 eV), and soft X-rays around the L edges of the transition metals (700 – 900 eV), and beyond. The respective R&D programme is called LIULI which stands for Linac Undulator Light Installation and has the Chinese meaning of flow power [9].

4.3.4   References

1.   H.O. Moser, V.C. Kempson, Yang Ping, Chew Eh Piew, Li Zhiwang, Tun Nyunt, B.T.G. Tan, R. Rossmanith, I.J. Underhay, "Status and Planned Development of the Singapore Synchrotron Light Source", Proc. 2nd Asian Particle Accelerators Conference (APAC'01), pp. 31-34, Beijing, China, 2001
2.   H.O. Moser, E.P. Chew, V.C. Kempson, J.R. Kong, Z.W. Li, Tun Nyunt, H.J. Qian, R. Rossmanith,P. H.   Tor, O. Wilhelmi, P. Yang, H.W. Zheng, I.J. Underhay , " Singapore Synchrotron Light Source: status, first results, program", Nuclear Instruments And Methods B 199, 536-540 (2003)
3.   H.O. Moser, B.D.F. Casse, O. Wilhelmi, B.T. Saw, "Terahertz Response of a Microfabricated Rod-Split-Ring-Resonator Electromagnetic Metamaterial ", Physical Review Letters 94, 063901 (2005)
     A. Yeo, P. Yang, A.G. Fane, T. White and H.O. Moser, " Non-invasive observation of external and
4.   internal deposition during membrane filtration by X-ray microimaging (XMI)", Journal of Membrane Science 250, Issues 1-2 , 189-193 (2005)
5.   Xiao Jiang Yu, Oliver Wilhelmi, Herbert O Moser, Singanallur V. Vidyaraj, Xing Yu Gao, Andrew T.S. Wee, Tun Nyunt, Haijie Qian, Hongwei Zheng, "New soft X-ray facility SINS for surface and nanoscale science at SSLS", Journal of Electron Spectroscopy and Related Phenomena 144-147, 1031-1034 (2005)
6.   P. Yang, D. Lu, B. Ramana Murthy and H.O. Moser, "High-resolution synchrotron X-ray reflectivity study of the density of plasma-treated ultra low-k films", Surface and Coatings Technology 198, Issues 1-3, 133-137 (2005)
7.   Mohammed Bahou, et al, "Infrared Spectro/Microscopy at SSLS – edge effect source in a compact superconducting storage ring", The 9th International Conference on Synchrotron Radiation Instrumentation, Daegu, Korea, 2006
8.   H.O. Moser, C.Z. Diao, "Finite-length field errors and its compensation in superconducting miniundulators", Nuclear Instruments And Methods A 535, 606-613 (2004)
9.   H.O. Moser, C.Z. Diao, "Towards light sources featuring superconducting miniundulators", ICFA 38th Advanced Beam Dynamics and 9th Advanced & Novel Accelerators Joint Workshop, Taipei, 2005

5   Proton and Heavy Ion Accelerators

5.1   Beam Dynamics Design of CSNS/RCS

Sheng Wang for CSNS/AP team
Institute of High Energy Physics,Chinese Academy of Sciences, Beijing,100049,China
mail to: wangs@ihep.ac.cn

5.1.1   Abstract

Rapid Cycling Synchrotron (RCS) is a key component of China Spallation Neutron Source (CSNS). It accumulates and accelerates protons to design energy of 1.6 GeV, and extracts high energy beam to the target. As a high beam density and high beam power machine, low beam loss is also a basic requirement. An optimal lattice design is

essential for the cost and the future operation. The lattice design of CSNS is presented, and the related dynamics issues are discussed. The injection/extraction scheme the beam collimation system design, and the longitudianl dynamic design are introduced.

5.1.2 Introduction

China Spallation Neutron Source (CSNS) accelerator [1, 2] consists of a low energy linac and a high energy Rapid Cycling Synchrotron (RCS). As a compromise among proton current, kinetic energy and the upgrade capability, CSNS linac output energy is chosen as 81 MeV in the first phase and the extraction energy from the RCS is 1.6 GeV. The primary parameters of CSNS accelerator complex are shown in Table 1. At the repetition rate of 25 Hz, the accelerators can deliver beam power of 120 kW at phase I, and will be updated to 240 kW (phase II) or 500 kW (phaseII') by increasing the injection beam energy and intensity of RCS. The beam dynamics design of RCS is presented in this paper.

Table 1: The primary parameters of CSNS

Project Phase	I	II	II'
Beam power (kW)	120	240	500
Repetition rate (Hz)	25	25	25
Average current (μA)	76	151	315
Beam energy on target(GeV)	1.6	1.6	1.6
LINAC energy (MeV)	81	134	230
Linac RF frequency (MHz)	324	324	324
Linac length (m)	41.5	67.6	77.6
Linac duty factor (%)	1.1	1.1	1.7
Accum. particles (10^{13})	1.88	3.76	7.8
Target	1	1	1 or 2

5.1.3 Lattice Design for RCS

5.1.3.1 *Linear Lattice*

The lattice design of the RCS should meet the basic requirements of the injection, accumulation, acceleration and extraction of beam, and can provide the beam a reasonable chromatic correction, closed orbit correction, coupling correction and beam collimation to promote the performance of beam.

The 3-fold or 4-fold symmetric lattice are investigated and compared in the RCS design. As a compromising of the magnetic field quality and the volume of the dipole, the length of the bending magnet is chosen as 2.1 m, and totally 24 dipoles are used for RCS. For accommodating momentum collimator, a gap with large dispersion function is required. In case of a four fold symmetry structure, there are 6 bending magnets at each arc, and with one or two missing dipole gap for momentum collimation, each arc shall be consisted by 3.5 or 4 90°phase advance FODO cells. To have large dispersion in

missing dipole gap, the gap should be located in the middle of the arc, so a 4-fold symmetry lattice with 3.5 FODO cells at each arc is adopted [3, 4]. Compare with the 3-fold symmetry structure, the 4-fold structure is also good for reducing the impact of the structure resonance, and the transverse collimation system can be accommodated in a separated straight section.

As shown in Fig. 1, the dispersion is suppressed by using two groups of 3 half-cells (90° horizontal cell phase advance) located on each side of a missing-dipole half-cell.
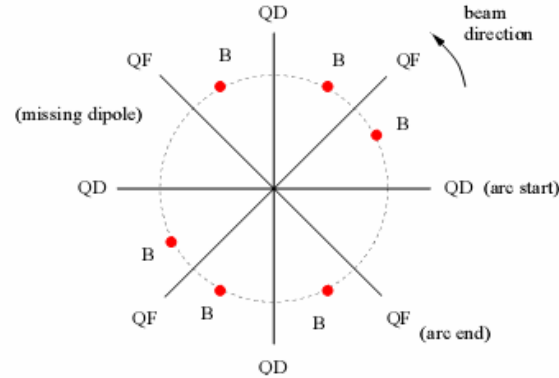

Figure 1: Dispersion suppression with a single missing dipole at each arc

Figure 2 gives the twiss parameters of one super-period. For there are 3.5 cells at each arc, the lattice function are anti-symmetric. It contains 24 dipoles and 48 quads. The circumference is 230.8 m. The base tunes are (5.82, 5.80). The straight section adopts doublet structure, and each straight section consists of two 6 m and one 9 m long drift space. The total dispersion free long straight section is 84 m. In the middle of the arc the missing dipole form a 4.1m straight section for momentum collimation. The peak dispersion is 5.4 m and the peak beta is < 25 m in the straight, and < 16 m in the arc. The FODO arc should allow easy lattice correction. Table 2 indicates the primary parameters of the RCS lattice.
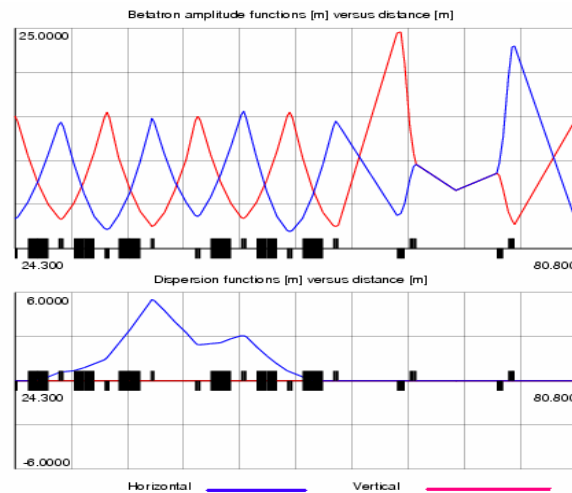

Figure 2: Twiss parameters for RCS lattice in one super-period

Table 2: The primary parameters of the RCS lattice

Injection energy (GeV)	0.081-230
Extraction energy (GeV)	1.6
Repetition rate (Hz)	25
Circumference (m)	230.8
Lattice Superperiod	4
Lattice type	Anti-symmetric
Arc structure	Single-gap, 3.5 FODO cells
Straight Structure	2 doublets
Number of dipoles	24
Number of quadrupoles	48
Number of long drift	12
Total length of long drift (m)	84
Betatron tunes (h/v)	5.82/5.80
Chromaticity (h/v)	-6.64/-7.27
Momentum compaction	0.041
Rev. periods (inj/ext, μs)	2.059/0.811

Figure 3 shows the geometry of the RCS. One of the four straight sections is for transverse collimation, and the other three straight sections are for injection, extraction and RF station. One missing dipole gap in the middle of the arc is for the momentum collimation, and the other three can be left for dual harmonic cavities or other device in the future upgrade. To decrease the circumference of the RCS, the cell length in the arc is set to 10.2 m, and the effective length between quardrupole and dipole is only 0.6 m. These short straight sections are used for dipole correctors, trim quadrupole , sextupoles, beam position monitors (BPM) and vacumm bumps, and the space is very tight. There are 4 sextupoles, 8 quardrupoles, 8 dipole correctors, 8 BPMs and 4 vacuum bumps at each arc. To save space, all the BPMs are planed to be installed under the sextupole and dipole correctors, and the vacuum bumps are planed to be installed under the dipole correctors.


Arcs: 3.5 DOFO cells, 315 degrees phase advance

Straights: doublet, 6×2+9 m long drifts at each straight

Dipole : <1.0 T
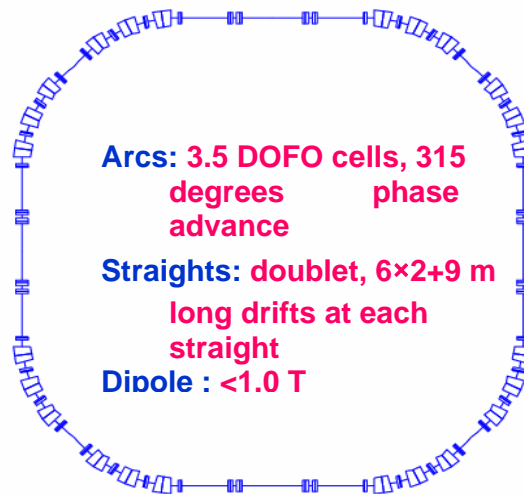
Figure 3: The geometry of RCS

5.1.3.2   *Chromaticity Correction*

Although the nature chromaticity is not so large, as shown in table 2, to reduce the tune spread and correct the off-axis lattice functions, especially in the low energy part, 4 families sectupoles are used to correct the chromaticity to -0.5. The phase advance between two adjacent F sextupoles is nearly 90°, and the phase advance between two adjacent D sextupoles is also nearly 90°. The arrangement of the setupoles is interleaving. During one cycle of RCS, the importance of chromaticity correction is decreased with the energy increased, so the sextupoles are designed as DC magnets. Figure 4 and figure 5 respectively show the horizontal and vertical beta functions for $\Delta p/p=0$, $\pm 1\%$, with and without chromaticity corrections. One can find that, without chromaticity correction, the deviation of vertical beta function is nearly 20%, after the proper chromaticity correction, these deviations become very small.
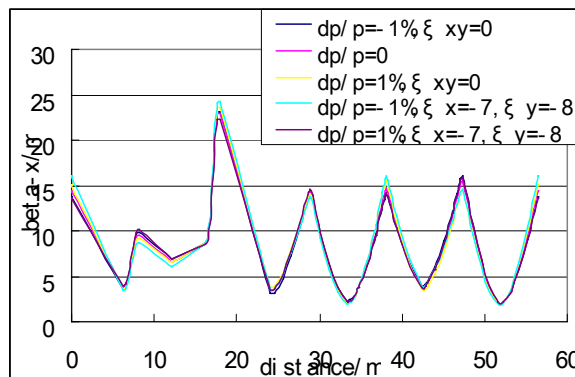
Figure 4: Horizontal on- and off-axis beta function for one super-period
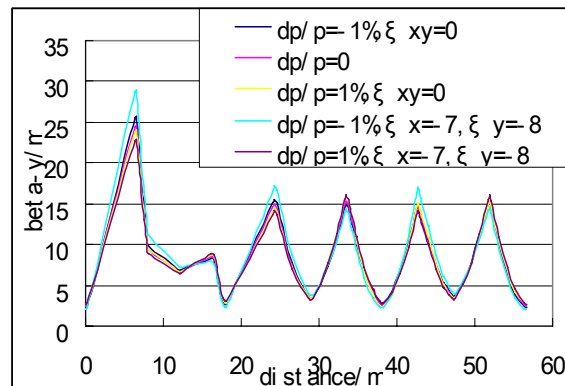
Figure 5: Vertical on- and off-axis beta function for one super-period

The tracking was done for checking the dynamic aperture with only the nonlinear effect of the sextupoles. In two dimensional case (*x-y*), the tracking results show that the dynamic aperture for particles of $\Delta p/p=\pm 1\%$ is large than $5\sigma_x \times 5\sigma_y$, where σ_x and σ_y are horizontal and vertical beam size.

5.1.3.3   *Closed Orbit Correction and Trim Quadrupoles*

There are 48 BPM in the whole RCS ring; each of them is installed just nearby a quadrupole. The number of dipole correctors in RCS is 40, in which 20 are for horizontal plane and 20 for vertical plane. The power supply for dipole corrector is programmable, and the dipole corrector should be ramped 10 to 20 steps during one RCS cycle. The maximum correction ability of dipole corrector is 1mrad at 1.6GeV. With these BPM and correctors, the closed orbit distortion can be well corrected.

For adjusting tune during ramping process, 32 trim quadrupoles are arranged in the RCS. The ISIS [5] has some experience on using the trim quadrupoles, which are from the commissioning and normal operation. The operation mode of trim quadrupoles shall be further investigated.

5.1.4   Beam Loss and Collimation

In the whole design, beam losses should be controlled in a very low level. Based on the past operational experience, to allow hands-on maintenance for most accelerator components, an average uncontrolled beam loss should be not exceeding about one watt of beam power per tunnel meter. For CSNS case, in the first phase, one watt of beam power per tunnel meter corresponds to a fractional uncontrolled beam loss of 2×10^{-3}. To control the beam loss to this level, both longitudinal and transverse collimation systems are required to reduce the uncontrolled beam loss within the acceptable level for hands-on maintenance. By using the momentum collimators located at straight section in the middle arc and the transverse collimation located at long straight section, it is expected to obtain more than 95% collimation efficiency.

There is one momentum collimator located in the missing dipole gap of the arc. The type of the momentum collimator is direct absorber made of graphite and copper. The transverse collimation system adopts the two-stage collimation system. It consists of one primary collimator and four secondary collimators. The transverse collimation system takes a separate straight section, just downstream of the momentum collimators. Halo particles are scattered by the primary collimators, and the secondary collimator absorb these scattered particles. It is expected to have a collimation efficiency of over 95% for the whole collimation system. Fig 6 [6] shows the layout of the two-stage transverse collimation system which is located in one straight section of RCS.
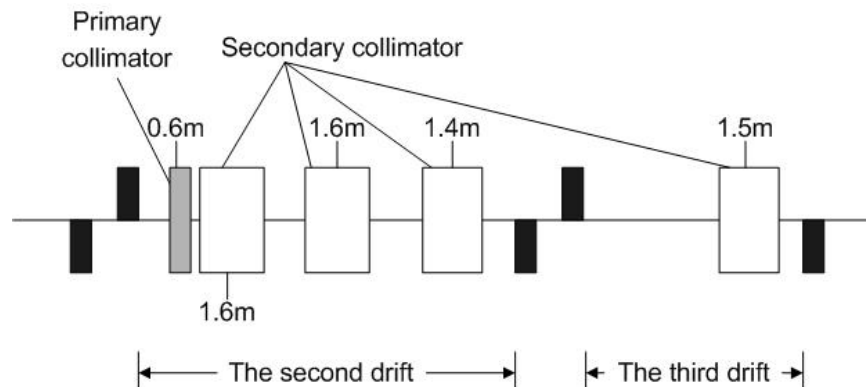

Figure 6: The layout of the transverse two-stage collimation system in the straight section

5.1.5 Injection and Extraction

In order to reduce the tune depression and tune spread due to strong space charge effect, injection into the RCS is by using H⁻ painting method in both horizontal and vertical planes.

Figure 7 gives the injection scheme [7]. The whole injection chain is arranged in a 9 m long drift space, consists of four horizontal painting magnets (BH), four vertical painting magnets,(BV) and four fixed field bumping magnets (BC). The BC magnets are used to facilitate the design for the septum magnets and reduce the proton traversal in the stripping foil, and it will be switched off after the injection period. Beside of an injection septum magnet, another septum magnet is used to direct the non-stripped or partially stripped H⁻ particles in the main stripping foil to a beam dump. A second stripping foil converts almost 100% the unusable particles states into protons. A very small fraction of H0 and H⁻ particles in high excited states are stripped by the magnetic field of BC3, and will form beam halo in the ring that will be finally stopped by the collimators.
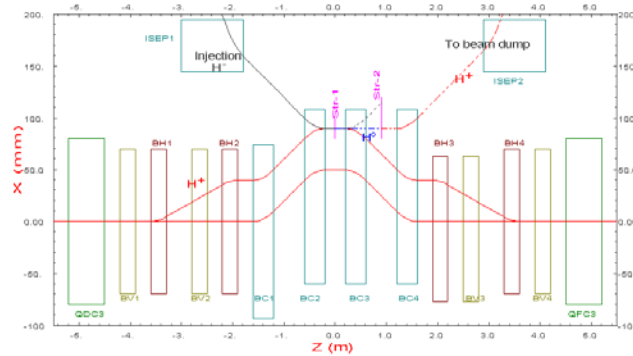

Figure 7: Injection scheme (BC1~BC4: closed-orbit bump magnets , BH1~BH4: horizontal painting bumpers, BV1~BV4: vertical painting bumpers, QDC3 & QFC3: quads, ISEP1&2: septa)

At the end of injection, the transverse emittance will be within 320 πmm.mrad, and for uniform distribution, the designed space charge tune shift is 0.28. The designed RCS physical acceptance is 540 πmm.mrad while the acceptance of collimation system is 350 πmm.mrad, and the painting emittance is about 250 πmm.mrad. A careful design of the painting scheme is very importance to control the emmitance blow up and beam loss. Both correlated and anti-correlated painting schemes are available [8]. In the correlated painting scheme, the beam fills the emittance from inner to outer for both the horizontal and vertical painting, and the beam distribution in the *x-y* space is nearly rectangular. In the anti-correlated painting scheme, the beam fills the vertical emittance from outer to inner, while fills the horizontal emittance from inner to outer and the beam distribution in *x-y* space is elliptical. Fig. 8 shows the beam distribution in phase spaces at the injection end with anti-correlated painting [8].

Case = , turn = 125
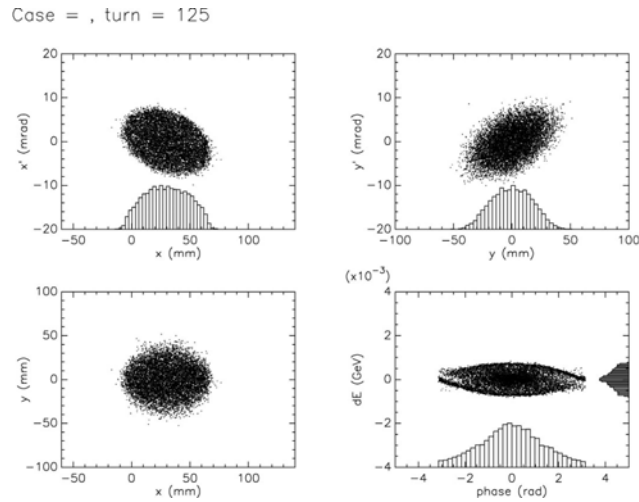
Figure 8: Beam distribution in phase spaces at the injection end (anti-correlated, Ip= 15mA, VRF=15kV)

The one-turn extraction from the RCS can be obtained by using a series of fast kickers followed by a Lambertson septum [9]. Pre-extraction orbit bumping is considered to reduce the strength requirement for the kickers and the beam loss in case of firing failure of one thyratron.

5.1.6   Longitudinal Dynamics Design [10]

The waveform of magnetic field variation is sinusoidal in the RCS, as shown in Fig. 9. In phase I, the single harmonic RF cavity will be adopted to reduce the RF voltage demand, and in the future upgrade for higher beam power, dual harmonic cavities will be added. The design of RF voltage and phase curves is an import issue to decrease the beam loss due to the space charge and phase changes. An RF acceleration period consists of three stages: injection, capture and acceleration. Totally there are 10 single harmonic cavities in the phase I with total RF voltage of 165 kV.
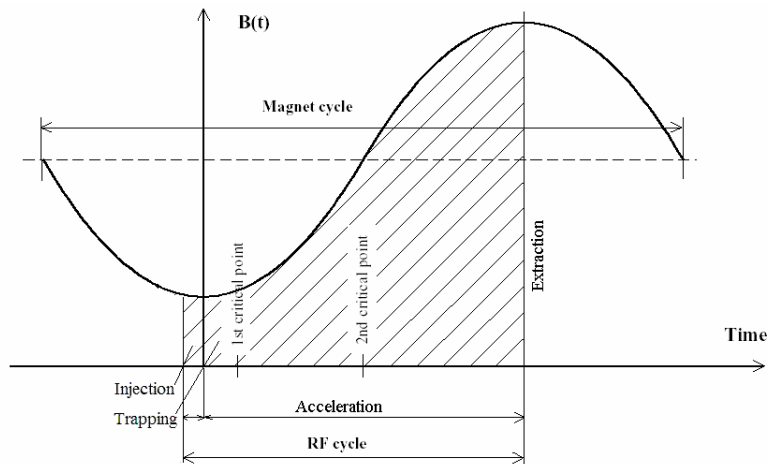

Figure 9: One cycle of magnetic field of RCS and its RF acceleration period

The RF voltage curve and the corresponding RF phase curve are calculated by using the code of RAMA. In the beginning of the acceleration, the bunching factor is about 0.4, and with the increasing of RF voltage, the bunching factor is decreased to 0.12. The filling factor used in the calculation is 0.8. Fig. 10 shows the variation of RF voltage and energy gain during half RCS cycle, as well as the variation of RF phases and bunch phases.
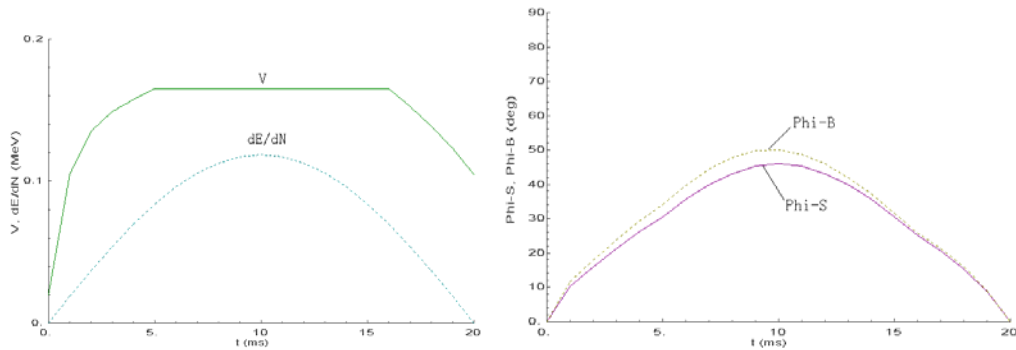

Figure 10 : The curves of RF voltage and energy gain during half RCS cycle(left), and the curves of RF phase (Phi-S) and bunch phase (Phi-B) (right)

To decrease the beam loss during the RF capture, the RF voltage should be increased rapidly in the beginning of the RF acceleration, as shown in the Fig. 10, during the first 0.5 ms, the RF voltage is increased to 70 kV from 21 kV, while the change of the magnetic field is very small. If the initial RF voltage is high, the beam loading factor will be large, so the initial RF voltage is set to 20 kV. The RF voltage is increased to 165 kV during the 5 ms, and the RF voltage is 100 kV at the end of the acceleration. 1-D ORBIT is used to simulate the beam loss during one RCS cycle. The painting procedure is not included in the simulation. With chopping rate of 50%, there are only 3 particles lost in 20280 macro-particles during the acceleration. Fig. 11 shows the longitudinal phase space at the initial and end of acceleration.
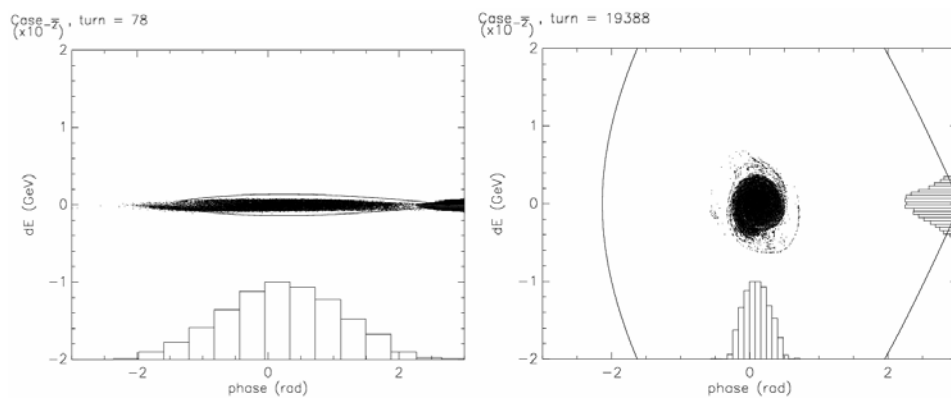

Figure 11: The longitudinal phase space at the initial and end of acceleration

5.1.7 Summary

An FODO cell and doublet hybrid structure lattice is presented for CSNS/RCS. It has a four-fold symmetry structure, and the lattice functions are anti-symmetry. The FODO cell arc ease to lattice correction and doublet straight section makes long uninterrupted straight for injection and extraction. The missing dipole gap in the middle of arc is suitable for momentum collimation. The lattice correction, beam collimation system, and injection/extraction system of RCS are discussed, and the longitudinal dynamics design is introduced.

5.1.8 References

1. CSNS Conceptual Design Report (IHEP, China, 2005)
2. J.Wei, S. Fu, S. Fang, EPAC'06, Conf. proceedings, Edinburgh, UK 26-30 June 2006 .
3. S. Wang, et, al, EPAC'06, Conf. proceedings, Edinburgh, UK 26-30 June 2006.
4. J.Wei, S.Wang, et, al, EPAC'06, Conf. proceedings, Edinburgh, UK 26-30 June 2006.
5. C.M. Warsop, AIP Conf. Proc. 448 (1998) 104
6. T. Wei, Design of the two-stage collimation system for CSNS/RCS, to be published in NIM-A.
7. J.Tang, et al; S.Wang et al, EPAC'06, Conf. proceedings, Edinburgh, UK 26-30 June 2006.
8. J.Qiu, J.Tang, S.Wang, J. Wei, EPAC'06, Conf. proceedings, Edinburgh, UK 26-30 June 2006.
9. J.Tang, et al; S.Wang et al, EPAC'06, Conf. proceedings, Edinburgh, UK 26-30 June 2006.
10. Q.Qin, private communication.

5.2 Dynamic Studies and the Initial Commissioning of CSRm

J.W. Xia, Y.J.Yuan, J.C. Yang, Y. Liu, Y. He, and the CSR commissioning group
Institute of Modern Physics (IMP), Chinese Academy of Sciences (CAS)
P.O. Box 31, Lanzhou, 730000, People's Republic of China
mail to: xiajw@impcas.ac.cn

5.2.1 Abstract

CSRm is the first storage ring of the new double ion Cooler-Storage-Ring (CSR) system in China IMP. The heavy ion beams from the existing cyclotrons will be injected in to CSRm for accumulation, cooling and acceleration. To ensure the stability of beam storage in CSRm, the dynamic effects caused by the dipole and quadruple errors have been investigated. In this paper, a beam-dynamic review for a real machine was made, including the lattice modification, closed orbit distortion, chromaticity correction and dynamic aperture tracking in different error cases. Based on the dynamic discussions, the initial commissioning of CSRm in 2006 was introduced.

5.2.2 Introduction

CSRm is the first storage ring of the new double ion Cooler-Storage-Ring (CSR) system in China IMP [1]. The heavy ion beams from the existing cyclotrons will be accumulated, cooled and accelerated in CSRm. After the acceleration those ion beams will be extracted to the second storage ring CSRe, or used for internal and external

target experiments. Figure 1 is the lattice layout of CSRm, and Table 1 is the major parameters of the ring.

Table 1 Major parameters of CSRm

| Circumference (m)	161.00	
Geometry	Race-track	
Ion species	p–U	
Max. energy (MeV/μ)	2800(p), 500 (U^{72+})	
Intensity (Particles)	10^5–10^9	
Bρ$_{max}$ (Tm)	12.05	
B$_{max}$ (T)	1.6	
Ramping rate (T/s)	0.05–0.4	
Accumulation time (s)	$\sim$ 10	
Acceptance	Fast extraction mode	
A$_h$ (π mm-mrad)	200 ($\Delta P/P = \pm 0.15$ %)	
A$_v$ (π mm-mrad)	40	
$\Delta P/P$ (%)	1.4 (ε_h= 50 π mm-mrad)	
E-cooler		
Ion energy (MeV/μ)	7–50	
Length of cooling (m)	4.0	
RF system	Accel.	Accum.
Harmonic number	1, 2	16, 32, 64
f$_{min}$/f$_{max}$ (MHz)	0.24 / 1.81	6.0 / 14.0
Voltages (n $\times$ kV)	1 $\times$ 7.0	1 $\times$ 20.0
Vacuum pressure (mbar)	3.0×10^{-11}	
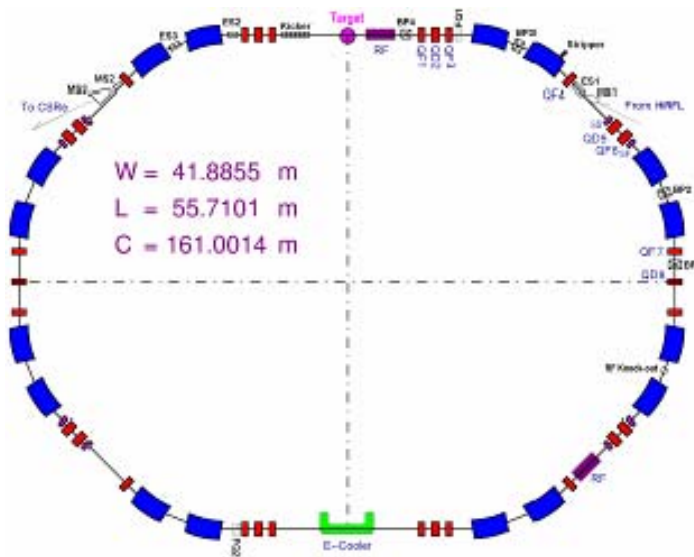
Figure 1: Lattice layout of CSRm

5.2.3   Error Free Dynamics

5.2.3.1   *Ideal Lattice*

CSRm is a racetrack shape, as shown in Fig. 1, and consists of four arc sections. Each arc section consists of four dipoles, two triplets and one doublet. The lattice of each arc section is given as follows,

----- L_1-----FDF--B--B--F---- L_2---DF--B--B—F (1/2D)

Where, $2L_1$ is the long-straight section with dispersion free and moderate β amplitude for e-cooler or extraction kicker and internal target. L_2 is the dispersion drift for beam multi-turn injection and RF-stacking [2], or for the beam extraction and RF cavity. In the injection arc-section, 4 bump magnets (BP1, BP2, BP3, BP4) and one static-electric septum (ES1) were used for the multi-turn injection with a horizontal acceptance of 150π mm-mrad. Fig. 2 is the distributions of the β-functions and the dispersion for the error free lattice, and Table 2 is the ideal lattice parameters of CSRm.
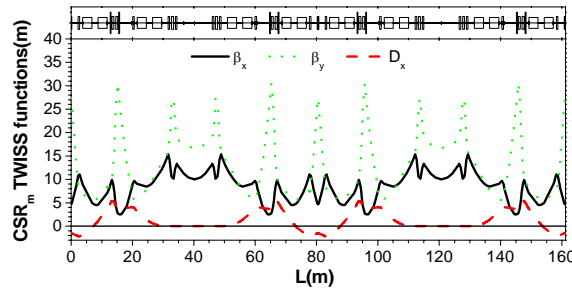
Figure 2: β and dispersion of CSRm

Table 2: Lattice parameters of CSRm

Transition gamma	γ_{tr} = 5.418
Tune values	Q_x / Q_y = 3.64 / 2.61
Chromaticity	Q'_x / Q'_y = -3.17 / -5.37
Max. β (m)	β_x / β_y = 12.1 / 13.5 (B) β_x / β_y = 15.3 / 30.5 (Q)
Dispersion (m)	$D_{max}(x)$ = 3.1(B, β_x = 9.0) $D_{max}(x)$ = 5.4(Q , β_x = 9.9)
Injection (m)	β_x= 8.0 , D_x = 4.1 (SM) β_x= 9.7, D_x=3.9 (Q)
E-cooler (m)	β_x / β_y=10.0/16.7, D_x = 0
Target (m)	β_x / β_y = 10.0/16.0, D_x = 0
RF station (m)	β_x / β_y = 8.0 / 22.5, D_x = 4.0

5.2.3.2 *Tune and Chromaticity Correction*

The ideal tune of CSRm is chose at the value of 3.64/2.61. It is closed to the 1/3 resonance line in the horizontal plane, in order to do the slow extraction of 1/3 resonance. The natural chromaticity is -3.17/-5.37, and will cause large tune distribution in the range of momentum acceptance. Fig. 3 shows the tune distribution caused by the natural chromaticity in the ΔP/P of ±0.6%.
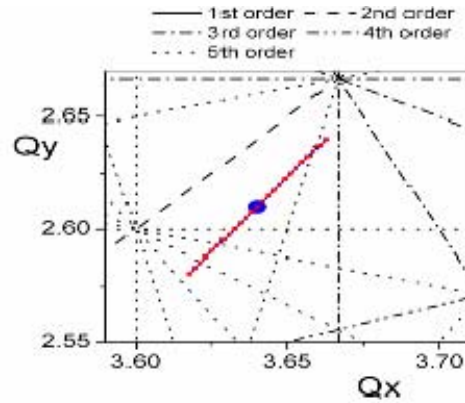
Figure 3: Tune distribution with ΔP/P of ±0.6%

In order to shrink the tune spread in a large momentum range, two families of sextuple in each arc section are used to correct the natural chromaticity. The sextuple lattice in each arc section is given as follows.

$$B\text{--}B\text{--}F\text{-----}S_D\text{-}DF\text{-}S_F\text{--}B\text{--}B$$

5.2.3.3 *Error Free Dynamic Aperture*

Fig.4 is the tracking results of the dynamic aperture (DA) for the ideal lattice. The 1000-turns DA before chromaticity correction is large, and after the correction with chromatic sextuples the DA become small from 0.5m/0.8m to 0.25m/0.4m, but also larger than the physical aperture.
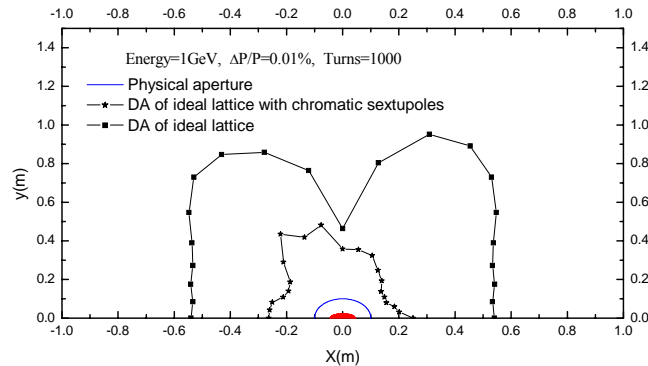
Figure 4: The DA of CSRm with error free.

5.2.4   Dynamics with Magnet Errors

5.2.4.1   *Field Distribution in Dipole*

The dipole field of CSRm was measured in the range of 500 Gs to 1.65 T with the exciting current from 76A to 3000A. It is larger than the working region of 0.1 T to 1.6 T. Fig. 5 shows the dipole integral-field distribution versus the radius. According to the measurement results, the good-field width with the homogeneity of 7×10^{-4} is 140 mm below the field level of 1.3 T, and it will be shrunken to 120 mm within the field range of 1.3 T~1.6 T.
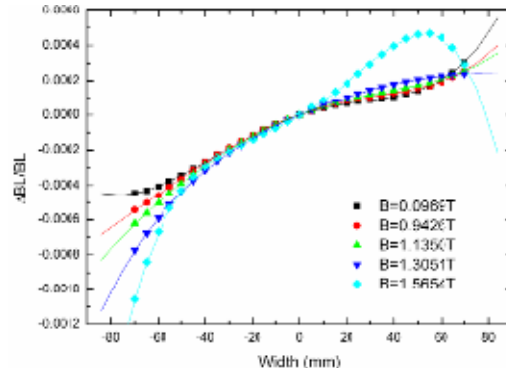
Figure 5: Dipole field distribution versus the radius.

From the field results the quadruple component is obvious in the dipole, and the b_2-coefficient [3] of the quadruple component is from 3.2×10^{-4} to 5.7×10^{-4} within the working region. This will cause the change of the storage-ring lattice. Fig.6 is the b_2-coefficient versus the exciting current, and the tune-shift caused by the a_1-component error in dipole is shown in Fig. 9.

The multiple-components errors in dipole also can be analysed from the measurement result. Fig.7 shows the b_i-coefficients [3] of the multiple components versus the exciting current, and the values of the b_i-coefficient are less than 5×10^{-4} in the used range of 150A to 2700A.
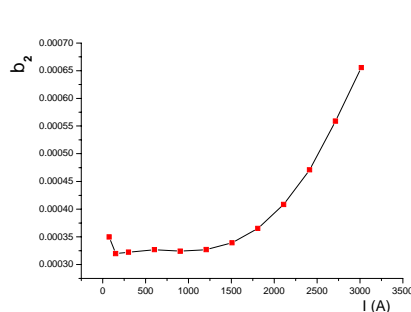
Figure 6: b_2-coefficient versus the exciting current.
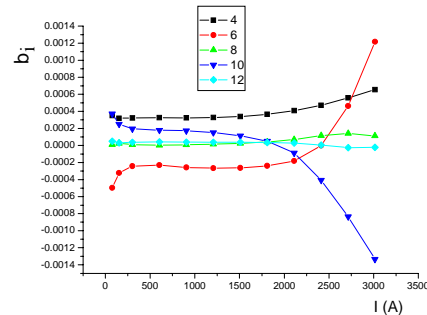
Figure 7: Multiple component errors in dipole.

5.2.4.2 *Fringe-Field Coefficient of Dipole*

The fringe-field FINT-coefficient [3] is not a constant, and will increase with the exciting current. Fig.8 is the FINT-coefficient in dipoles versus the exciting current. The Value of FINT is from 0.46 to 0.64 in the working region, and the variety of FINT-value will also cause the change of storage-ring lattice. The tune-shift caused by the variety of FINT-value in dipole is shown in Fig. 9.
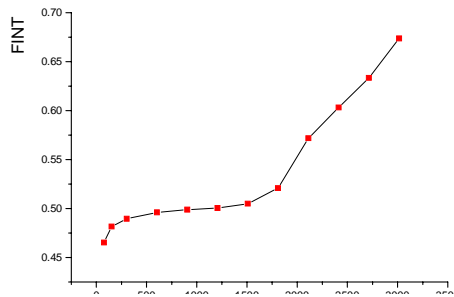
Figure 8: FINT-coefficient versus the exciting current.
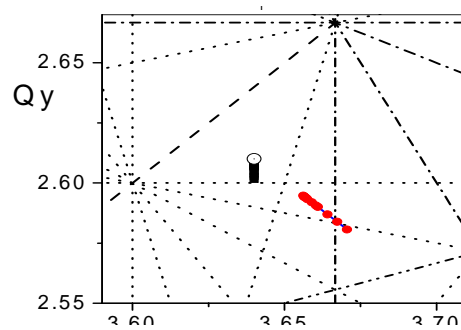
Figure 9: Tune-shifts caused by b_1 and FINT of dipole from 0.1T to 1.5T.

5.2.4.3 *Original Lattice Modification*

The original lattice of CSRm was designed with the quadruple-component error of zero and the FINT-coefficient of 0.4 in dipoles. But in the real case, they aren't the constant, and will be a range during the acceleration. Originally the values of b_1 and FINT aren't in the middle of the working region, and the tune-shift area will be very large, shown in Fig. 9.

According to the practical case, we can adjust the original values to $b_1=4.5\times 10^{-4}$ and FINT=0.55, and keep the lattice to be same as the original design by adjusting slightly the K_1-values of the 8 families quadruples in CSRm. After the adjusting the tune-shift area shrinks to a small area around the original point of $Q_x/Q_y=3.64/2.61$. Fig.10 shows the tune-shift area after the lattice modifying. Of cause during the actual acceleration, the tune value can be kept at the design point by adjusting the strength of only two family quadruples instantaneously.
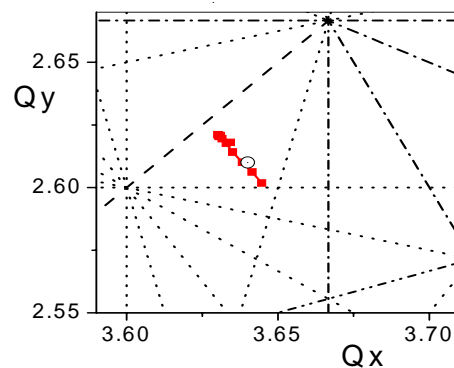
Figure 10: Tune-shift after the lattice modifying.

5.2.4.4 *Dipole-Field Reproducibility*

Owing the manufacture error, the field difference should be occurred between the 16 dipoles and one reference dipole. From the measurement results, the dipole-field reproducibility is less than 3×10-4 below the field level of 1.0T, and this value will reach to 8×10-4 while the field level at 1.5T. Fig.11 is the reproducibility of CSRm dipoles at the level of 1000Gs.
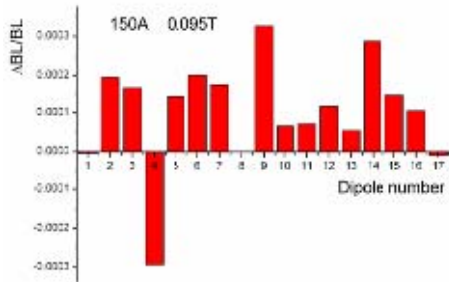
Figure 11: Reproducibility of CSRm dipole at 0.1T.

The reproducibility between dipoles will cause the closed-orbit distortion (COD) in storage ring. Fig.12 is the COD results caused by the dipole reproducibility in CSRm. The COD will less than 1mm blow the field of 1.0T, and it will reach to 4mm at the high field level.
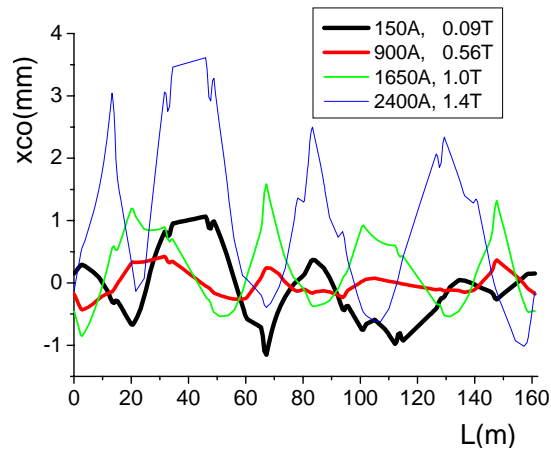
Figure 12: COD caused by dipole reproducibility.

5.2.4.5 *Dynamic Aperture with Dipole Errors*

Considering the high-order component errors in dipoles, the dynamic aperture of CSRm should be investigated. Fig. 13 and Fig. 14 show the dynamic aperture.

68
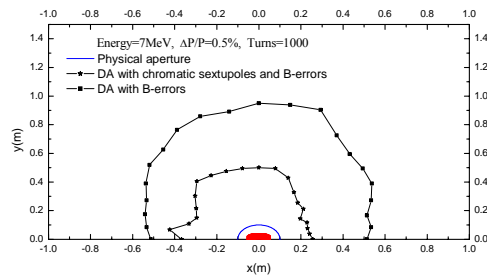
Figure 13: DA with B-errors at low energy.
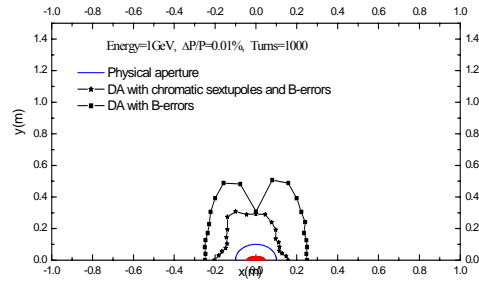
Figure 14: DA with B-errors at high energy.

5.2.4.6 *Results of Quadruple Field*

The maximum quadruple gradient of CSRm is reched to 10 T/m with the exciting current of 690A, and the multiple components error are less than 5×10^{-4} in the working region of 20A~600A. Fig. 15 is the multiple-component errors versus the whole exciting current from 15A to 690A.
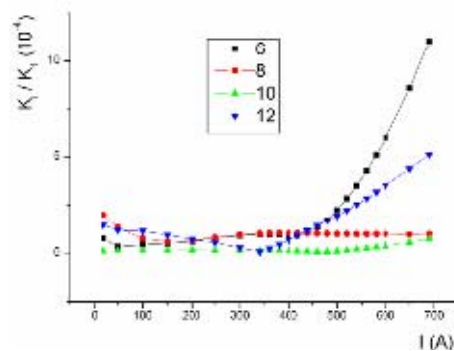
Figure 15: Multiple component errors in quadruple.

5.2.4.7 *DA with Dipole and Quadruple Errors*

Considering the multiple component errors in dipoles and quadruples, the dynamic aperture of CSRm should be investigated. Fig. 16 and Fig. 17 show the dynamic aperture.
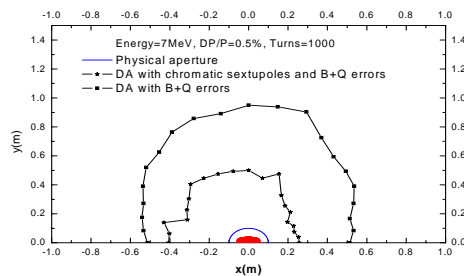
Figure 16: DA with B+Q errors at low energy.
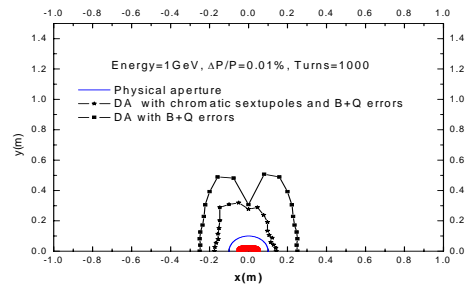
Figure 17: DA with B+Q errors at high energy.

5.2.5 Initial Commissioning Results of CSRm

5.2.5.1 *Project Status*

The construction and installation of the two storage rings were finished in the end of 2004. Since that time many offline tests have been done. For example, e-cooler, RF station, power supply, Ultra-high vacuum, magnetic field measurement and ring alignment, etc. For the e-cooler, the hollow electron beam can be obtained to partially solve the problems due to space charge effect and reduce the effect of recombination between the ions and the e-beam. In CSRm the vacuum pressure already reached to $5 \times 10\text{-}12$ mbar.

Up to now, several subsystems will be delayed, for example, control and diagnosis systems, and fast extraction kicker.

5.2.5.2 *First Beam Storage in CSRm*

In the beginning of 2006, the main ring CSRm was under the preliminary commissioning. At January 18 of 2006, the single-turn stripping injection beam of C^{6+}-6.89MeV/u was stored successfully in CSRm with bumping orbit. Fig. 18 is the stored beam signal from a BPM. In this case the RF system of CSRm wasn't used, thus the bunched beam from the cyclotron SFC would be become as a costing beam gradually after the single-turn injection, and the beam signal from BPM also became weak turn by turn.

From the result of the Fig.18, we can see that the beam signal of the 20th turn had already become very weak.

Based on the single-turn beam storage, at January 23 of 2006, the multi-turn stripping injection beam of C^{6+}-6.89MeV/u was stored successfully in CSRm with bumping orbit. Fig. 19 is the stored beam signal from the spectrum analyser connected with a BPM in the zero-span mode.
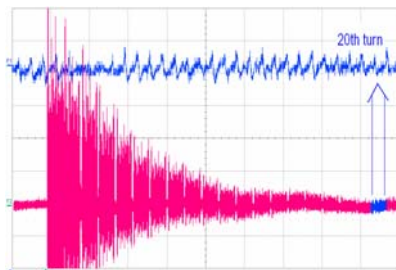
Figure 18: The stored beam signal from BPM.
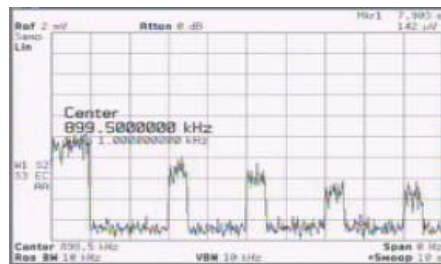
Figure 19: The stored beam signal from the spectrum analyser with 5 times of RF modulating.

In order to observe the stored beam signal from BPM in a long time, the stored costing beam should be re-bunched by the RF system of CSRm with the harmonic number of 4 and the RF voltage of 1.3KV. By the RF modulating, the stored beam signal can be obtained from the spectrum analyser connected with a BPM in the zero-span mode. As the showing in Fig. 19, after the multi-turn stripping injection, the stored beam was modulated by RF five times in 10 seconds. The first modulating period was 1

second, and after that every period was 0.5 seconds. According to Fig. 19, the 1/e life time of stored beam was about 10 seconds.

5.2.5.3 *Preliminary Beam Accumulation of CSRm*

In the spring of 2006, the new controller DSP developed by ourselves was used in the power supply control system of dipole, quadruple, bump and RF system. By using this new DSP, the synchronous times between the dynamic bumping orbit which used to cross the stripper, the period of injection beam and the RF system can be controlled accurately. Fig. 20 is the synchronous signal between RF, bumping orbit and injection beam.

At April 20 of 2006, just after the bumping injection with the accumulation period of 15ms, the RF system switched on to capture the stored beam. In this case, the accumulated beam of C^{6+}-7.185MeV/u with a high intensity can be observed on the spectrum analyser. Fig. 21 is the stored beam signal from the spectrum analyser in the 5 seconds of RF modulation.
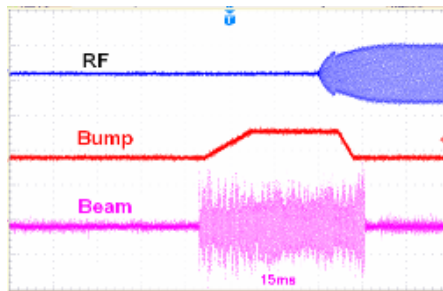
Figure 20: The synchronous signal between RF, bumping orbit and injection beam.
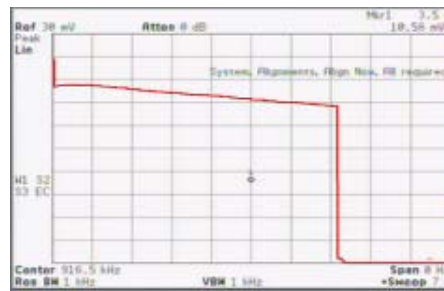
Figure 21: The stored beam signal from the spectrum analyser just after the bumping injection.

As the results shown in Fig. 21, the 1/e beam-life is about 37 seconds, and the beam intensity is about 100eμA, namely the stored C^{+6} particles can be reach to 10^9 in the storage ring CSRm.

5.2.5.4 *First Ramping Injection in CSRm*

After the success of the static injection, the ramping injection was done. During the ramping injection, the current of dipole power supply was increased from 80A to 160A, and 30 quadruple power supplies also ramped from 10A to 17~33A. Fig. 22 shows the work mode of the dipole power supply during the ramping injection.

At April 23 of 2006, the ramping injection got the success. Fig. 23 is the result of stored beam with the ramping injection mode. In the case of ramping injection, the beam current stored in CSRm reached to about 50 eμA, and the 1/e beam-life was 167 seconds.
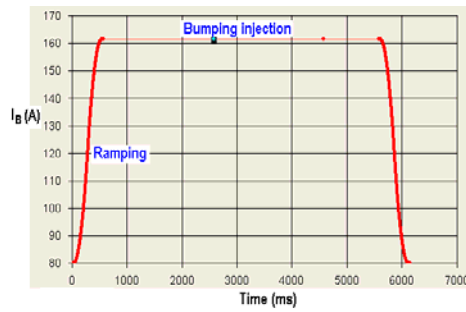
Figure 22: The work mode of the dipole power supply during the ramping injection.
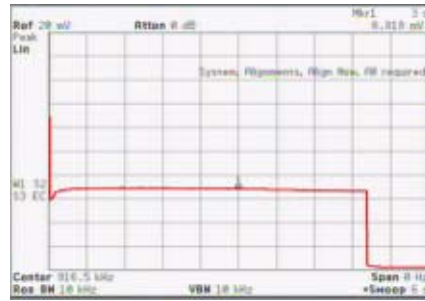
Figure 23: The stored beam signal from the spectrum analyser during the ramping injection. Initial ramping of CSRm

In May of 2006, the dynamic scale for all quadruple power supplies was finished. After that a short acceleration test was done. In the test, the C^{6+}-beam energy was increased from 7MeV/u to 14MeV/u. Fig.24 is the exciting currents of dipole and quadruple's power supplies. Fig.25 shows the RF voltage and frequency during the ramping test.
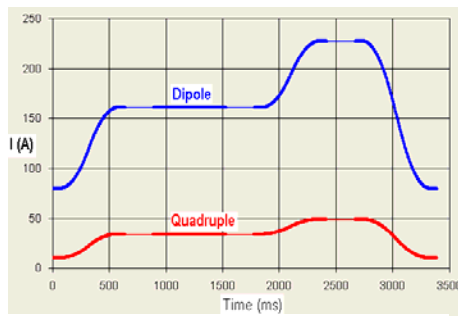
Figure 24: The exciting currents of B+Q-PS.
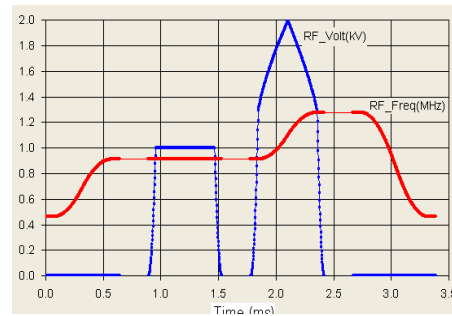
Figure 25: The curve of RF voltage and frequency.

The short ramping test consists of two steps, the first step is the ramping injection, and the second one is the accelerating. At June 16 of 2006, the first accelerated beam-signal was observed on the spectrum analyzer with a wide-band range of 300 KHz. Fig.26 is beam signal of ramping injection and acceleration from the spectrum analyzer during the acceleration test.
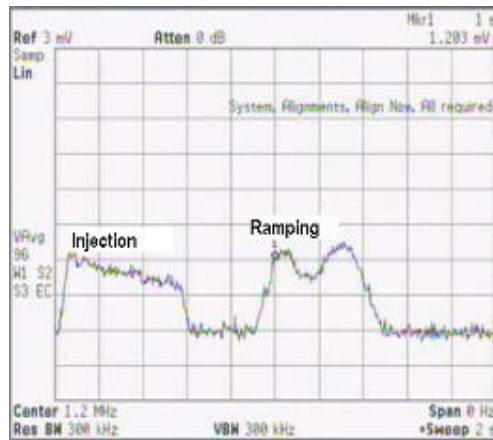
Figure 26: The beam signal of the acceleration test.

5.2.5.5   *Commissioning Schedule of CSRm*

2006 is the first commissioning time for CSRm, and in the end of 2006 the whole acceleration will be finished.

5.2.6   References

1   J.W.Xia, W.L.Zhan, B.W.Wei, et. al., The Heavy ion Cooler-storage-Ring Project (HIRFL-CSR) at Lanzhou, NIM A 488(2002) 11-25.
2   Y. J. Yuan et al., Simulation of RF Stacking and Multiple Single-Turn Injection and Multi-turn Injection, Proc. of the 14th Inter. Conf. on Cyclotrons and Their App., South Africa, 1995, 479pp.
3   Hans Grote, F.Christoph Iselin, The MAD Program, CERN/SL/90-13 (AP), 1993.

5.3   Accelerator Development at VECC

Bikash Sinha, VECC
mail to: bikash@meghdoot.vecc.ernet.in

5.3.1   Introduction

The Variable Energy Cyclotron Centre at Kolkata is a premier institute in the country for nuclear science having excellent infrastructure for advanced research and development in accelerator technology. This Centre indigenously developed the first big accelerator in the country, the room temperature cyclotron K-130 during seventies (commissioned in 1977). After delivering light ions beams to the users for almost twenty years it was shutdown in 1997 and has undergone many changes. Now it delivers a variety of heavy ion beams with external ECR ion sources. It is also planned to use the cyclotron as primary source for a Radioactive Ion Beam (RIB) Facility in the near future.

VECC, with its vast experience and expertise in accelerator design, fabrication and operation, took up the challenging task of constructing the first superconducting cyclotron in the country some ten years back. Now this superconducting cyclotron is

under commissioning. Most of the subsystems have been installed and tested sucessfully. It will provide heavy-ion beams of energy 80 MeV/nucleon for light ions.

Radioactive Beams (RIB) are indispensible tools for nuclear science. They provide the possibility to study structure of unstable nuclie that are very neutron rich or proton rich. At VECC an ISOL based RIB facility is under-construction. Several components of this facility have already been tested and installed.

Thorium cycle power reactors based on the principle of Accelerator Driven Sub-critical System (ADSS), require a proton driver capable of 1GeV energy and 10MW total power and cyclotron is one of the options. Studies on using cyclotrons to achieve high power proton beam has been undertaken at the center. At present we are developing ion source and injection system of a high current 10MeV injector cyclotron.

VECC is also setting up a medical cyclotron to produce proton beam with energy up to 30 MeV and current up to 350 mA, to produce various isotopes for medical applications. This cyclotron will also be used for R&D in material science and to settle the various problems related with handling of high beam current on ADS related components.

5.3.2 K-130 Cyclotron

The Variable Energy Cyclotron (VEC) at Kolkata is a medium energy AVF cyclotron. It can accelerate protons up to 60 MeV, deuterons up to 65 MeV and heavier ions up to $130\,Q^2/A$. The energy of the particles from the machine can be varied by varying both the magnetic field and the radio-frequency electric field used for acceleration; hence the name Variable Energy Cyclotron. The design of the VEC is based on the 88-inch cyclotron at Lawrence Berkeley National Laboratory in USA with modifications incorporated for facilitating indigenous fabrication and for improved performance. More details about the cyclotron can be obtained in references [1,2].

The cyclotron is an assembly of various subsystems such as magnet, rf system, power supplies, ion source, injection and extraction system, vacuum and control systems, beam transport and data processing systems etc. The rf system of the cyclotron consists of the dee, the dee stem, the fixed and movable panels, all enclosed in a large vacuum chamber and a high power tetrode RCA4648 as the final amplifier (MOPA system). It has a frequency range of 5.5 MHz to 16.5 MHz and a working voltage of 70 kV (max.). Frequency variation is accomplished by using panel movement. The H shaped dc electromagnet with pole diameter of 224 cm and weighing 262 tons is the heaviest component of the cyclotron. It has three hills on each pole with a maximum spiral angle of ~55 degrees. The maximum average magnetic field is 17 kG. The main magnet coils, 17 trim coils and 5 sets of valley coils all have independent power supplies. The working pressure inside the machine is of the order of 5×10^{-6} torr, which is obtained by using two freon cooled 89 cm oil diffusion pumps backed by roots and rotary pumps.

Figure 1: View of the K-130 cyclotron with three beam lines.

The first beam of 50 MeV α-particles using an internal hot cathode PIG type ion source was accelerated on 16th June, 1977. It started regular operation for proton, deuteron and alpha beams towards the end of 1981 and is since then being used by a large number of users from all over India.

Since its inception, scientists at this center planned to accelerate heavy ions using this cyclotron, but the efforts became visible only during the late years of 80's when the development of 6.4 GHz ECR ion source was funded. Though this source became operational in 1991, it could not be connected to the cyclotron due to the commitment of beam time to large number of users requiring light ion beams for experiments. Cyclotron was shut down in the early 1997 to install the injection line and to do certain modifications in the central region to accelerate heavy ion from ECR source. The first heavy ion beam of 115 MeV O^{5+} was accelerated during mid 1998 and since then this machine is providing variety of heavy ions to users. At present, the cyclotron is operating with two ECR ion sources; the indigenously developed 6.4 GHz ion source (Fig. 2) for gaseous light heavy ions and 14 GHz source for gaseous as well as metal ions. Table 1 shows the various ion species, their energies and the extracted beam current used by various users for experiments.

Figure 2: The 6.4 GHz ECR ion source and the initial portion of injection line together with the charge state analyser.

In the meantime a programme has been taken up to modernize the technical systems of the cyclotron and several modifications have already been carried out in many subsystems to improve the over all performance of the machine. The old synthesized signal generator as well as 1 kW power distributed amplifier both are replaced for better stability of the rf system. A PC-based Data-Acquisition system has been developed to monitor all rf parameters in the control room. There is a programme to replace most of the 30 years old power supplies connected to various systems to improve the stability and reduce the down time of the beam. A programme has also been initiated to computerize the operation of various subsystems.

Table 1: List of ion species accelerated with K-130 cyclotron for experiments.

Ion Species	Q	Energy (MeV)	Current (enA)
N^{14}	5+	105	070
O^{16}	5+	160	300
O^{16}	6+	140	1000
O^{16}	6+	160	530
O^{16}	6+	180	410
Ne^{20}	6+	170	200
Ne^{20}	7+	200	310
Ne^{20}	7+	210	260
Ne^{20}	7+	225	005
S^{32}	10+	230	060
Ar^{40}	12+	288	060
Ar^{40}	12+	350	007

VEC is operating as a national facility. A large number of research institutions and universities spread all over the country have been using VEC for research in basic nuclear physics, isotope production, solid state physics, radiation damage, radio chemistry, radiation chemistry, biophysics and many other related fields. A typical experimental setup known as INGA (Indian National Gamma Array) used by several institutes is shown in Figure 3.


Figure 3: The Indian National Gamma Array setup in Ch#3 using clover detectors.

5.3.3 Superconducting Cyclotron

The success achieved with the commissioning and streamlining the operation of K-130 cyclotron, motivated the scientists at VECC to extend their R&D activities. They started searching for a machine of high energy in the range of ~ 80-100 MeV /nucleon for light heavy ions. Two options were available at that time: either to develop a seperated sector cyclotron or a superconducting cyclotron. A systematic and rigorous study was carried on both the options. The involved technological challenges and an opportunity to develop and learn a new technology in the cryogenic field, motivated them to choose the superconducting cyclotron. This cyclotron is presently in the commissioning stage.

The superconducting cyclotron [3] has bending limit K_b of 520 and focusing limit K_f of 160. It will deliver heavy ion beams of 80 MeV/nucleon energy (for light ions) which are not presently available in the country. The basic design features of this machine are similar to the cyclotrons operating at Michigan State University and Texas A&M University in USA [4,5]. It is being constructed, primarily, for nuclear physics experiments with heavy ion beams at intermediate energies. With the advent of ECR ion source this cyclotron can deliver species and energy suitable for new class of experiments and is expected to satisfy the experimental nuclear physics community as a whole. Figure 4 depicts the energies available for different mass numbers with the superconducting cyclotron. With improved ion source performance the the mass range can also be extended to the higher mass in the periodic table.
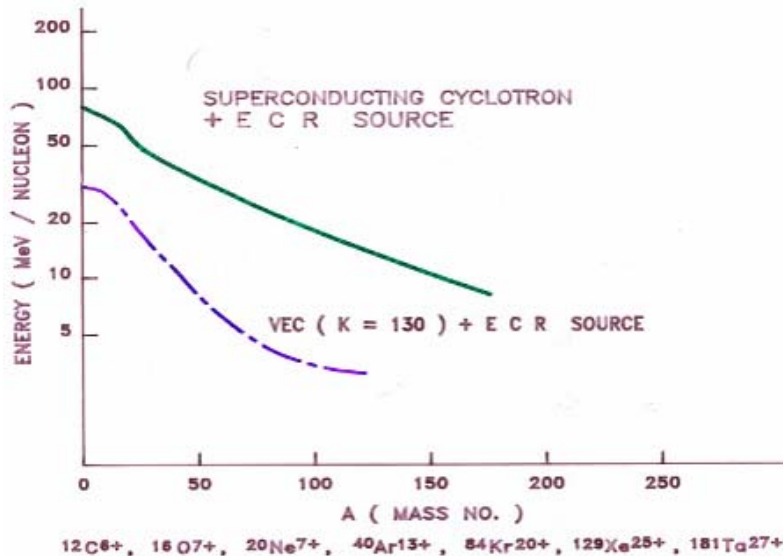
Figure 4: Energy/nucleon vs mass number for heavy ion beams at the VEC Centre.

The 80 tonne main magnet iron structure has been successfully fabricated and installed in the new cyclotron building at VECC campus (Fig. 5). The superconducting coil was wound on the cryostat bobbin using a specially developed winding set up. The liquid helium chamber housing the coil has been welded shut. The cryostat containing the superconducting coil has been assembled. The cryogenic delivery system both for LHe and LN2 for the main magnet cryostat is already installed. The 200W (at 4.5K)

helium liquefier/refrigerator has been re-commissioned in the main accelerator building complex. Main magnet power supply along with dump resistors has been installed and tested in position. Trim coil power supplies are commissioned. Development of the elaborate magnetic field measurement set up is also complete. Extensive measurement of magnetic field and its harmonics has been planned to evaluate the errors and its correction. Magnetic field measurements will be carried out over the next several months. Fabrication of the intricate RF cavities that will operate at room temperature is in progress. Various groups are engaged in the development of other systems such as RF amplifiers, LHe cooled cryopanels, ECR ion source and injection, extraction, diagnostics, controls, beamlines etc. All other systems of the cyclotron are in an advanced stage of fabrication or development.

Figure 5: 80 tonne cyclotron magnet with cryostat installed in it.

Cooling of the coils was started in mid-December 2004. It took about three weeks to fill the liquid helium chamber - fully immersing the coils. All the four temperature sensors embedded in the coil are steady at about 4.4K. The helium liquefier/refrigerator of 200W capacity has been functioning well and so is the network of vacuum jacketed and liquid nitrogen cooled cryogenic transfer lines.

The main magnet was energized in the beginning of 2005. A computer controlled magnetic field measurement set up was used for elaborate field mapping. The magnetic field mapping process, which included shimming of the iron part for correction of the unwanted harmonics and generation of data at various current levels for operation, continued for almost six months. Few results of field measurements are shown in Figures 6 and 7. At present assembling and testing of rf resonators and vacuum system is going on.
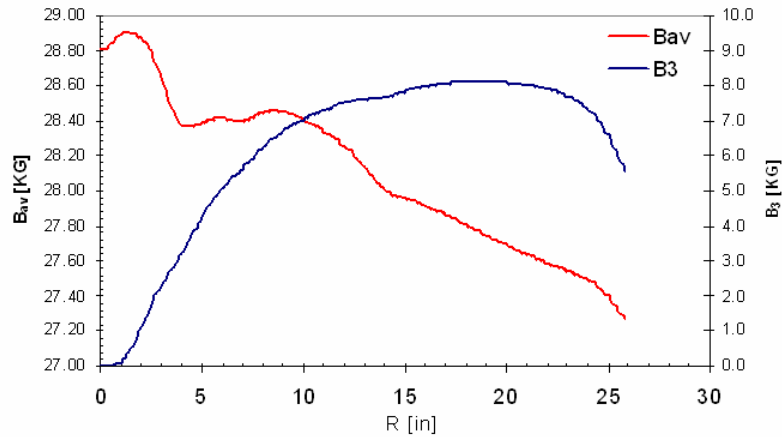
Figure 6: Average magnetic field and third harmonic field profile ($I_\alpha = I_\beta = 300$ A)
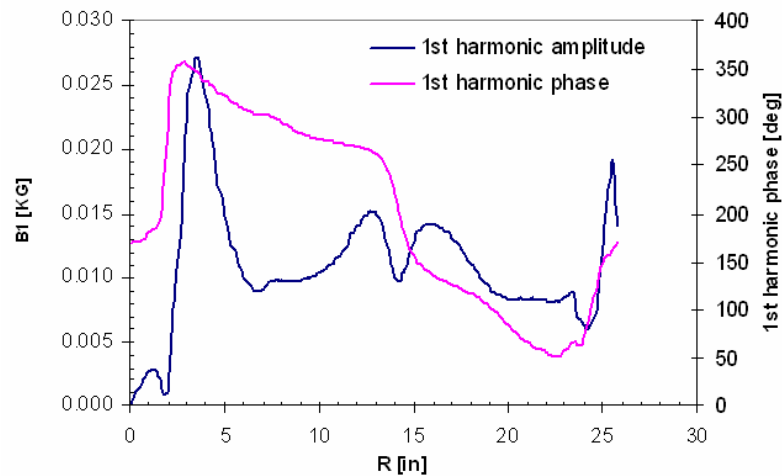
Figure 7: First harmonic field and amplitude ($I_\alpha = I_\beta = 300$ A)

5.3.4   Radioactive Ion Beam Facility

The physics and experiments with Radioactive Ion Beams (RIB) are the emerging frontier in nuclear physics and allied sciences. It is expected to address some basic questions regarding the nature of nuclear interaction, the origin of elements in the universe etc. The development of accelerator facilities for producing RIB is the major activity in all the leading nuclear physics laboratories around the world. Technologically the development of a RIB facility is extremely challenging which involves extensive R&D and VECC accepted this challenge in 1998 to build an ISOL-post accelerator type RIB facility with the existing K=130 room temperature cyclotron [6], VEC, as the primary beam source.

A schematic layout of the RIB facility to be built in phase-1 is shown in Fig 8. Proton and alpha beams from the cyclotron will bombard a thick production target placed inside an integrated surface ion-source. Radioactive ions with charge state 1^+ extracted from the target-ion-source will be injected into an on-line ECR ion source "charge

breeder" for further ionization to q+. The RIB of interest (1keV/u, q/A=1/16) will be selected in an isotope separator downstream of the ECR ion source and accelerated initially to about 86 keV/u in a Radio Frequency Quadrupole (RFQ) linac and subsequently to about 400 keV/u in three IH-LINAC tanks.
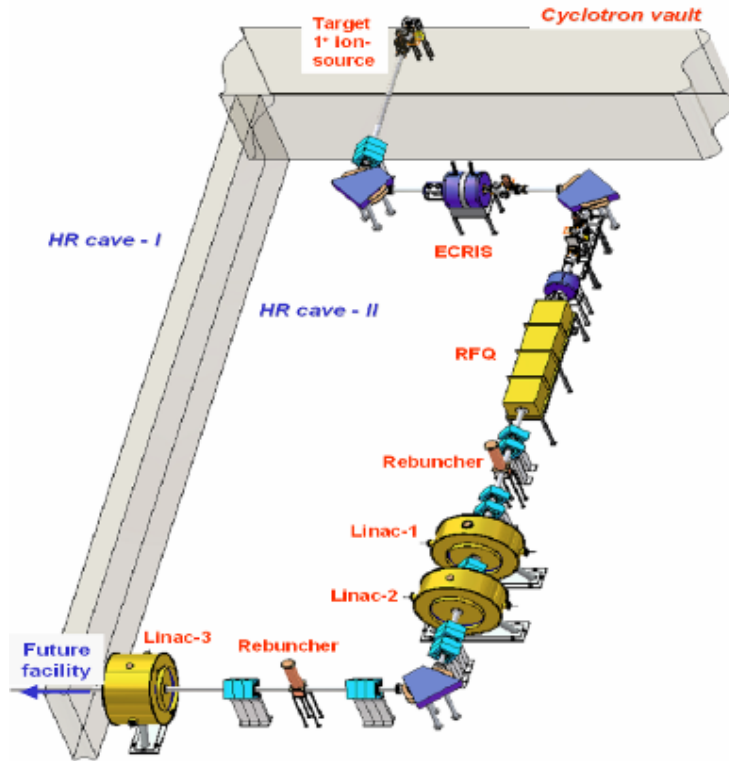
Figure 8: A schematic layout of the RIB facility to be built in Phase-1.

Thick target R&D and in-beam RIB production and release measurements have been initiated at the VECC He-jet ISOL system. We can produce proton-rich nuclei four to five neutrons away from stability as well as neutron-rich nuclei with A/Z~2.5 in the range of $28 \leq Z \leq 50$ with cross-sections of a few tens of millibarns. The initial attempt however, has been limited to develop a few targets like Al_2O_3, MgO, Graphite and HfO_2 and the actinide targets will be developed in future.

The charge breeder [7] for the VEC RIB facility consists of a surface ionization source coupled to a 6.4 GHz on-line ECRIS. The 1^+ ions from the first ion-source are decelerated to about 20-50 eV and focused into the ECRIS plasma. The ECRIS is operated in the "High B mode" having a peak solenoidal field of 1.0 Tesla at the injection end and 0.7 Tesla at the extraction end. The radial field at the surface of the plasma chamber is 0.7 Tesla. The installation of the ECRIS has been completed. In the first beam test, about 20 μA, O^{4+} beam was measured at the focal plane F2.

Figure 9: A half-scale model of the RFQ with un-modulated vanes.

A four-rod type Radio Frequency Quadrupole (RFQ) linac has been designed for an input beam energy of 1.0 keV/u and $q/A \geq 1/16$. The output energy will be $\approx$ 86 keV/u for a 3.2 m long, 35 MHz structure. A half-scale model of the RFQ with un-modulated vanes has been fabricated to carry out RF structure studies and the tests confirm the design [8]. The measured Q and R_p values are both slightly more than 50% of the values calculated by MAFIA as expected. The RFQ cold model is shown in Figure 9. The preliminary beam test of the full-scale model RFQ was tested during Dec 2005 using oxygen beam at low rf power level and ~75% of beam transmission through the RFQ was observed.

The design of the first three LINAC tanks has been frozen and the fabrication of cold model for the Linac first tank has been completed. The RF power tests on this cold model are in excellent agreement with the design. For Linac tank -1 a 40 kW, 35 MHz transmitter has been indigenously developed and installed.

5.3.5   High Current Cyclotron for ADSS

The Department of Atomic Energy has emphasized the need to pursue a program for large-scale utilization of thorium fuel for nuclear power generation through Accelerator Driven Sub-critical Systems (ADSS). The most important component of such a system is the development of a high energy high current (1 GeV, 10 mA) proton accelerator. A combination of cyclotrons (injector, intermediate stage and final booster) is considered an excellent option [9] for delivering high power as needed by ADSS. VECC is working on the development of the first stage of this complex accelerator system, a 10 MeV compact proton cyclotron [10,11]. The basic aim of this project is to study and settle various physics and technological problems associated with the production and handling of high intensity beams.

In the first phase we are developing a 2.45 GHz microwave ion source, which will deliver a 30 mA proton beam at 100 keV. This beam will be transported by a low energy beam injection line and will be injected axially into a 10 MeV, 5-10 mA compact radial sector cyclotron. The important design parameters of the cyclotron are shown in Table 2. The layout of the injection line, ion source, and high voltage deck is shown in Figure 10.

Table 2: Parameters of the 10 MeV Cyclotron

Injection Energy	100 keV	Final Energy	10 MeV
Hill Field B_H	1.5 T	Valley Field B_V	0.1 T
Hill gap	3 cm	Valley gap	46 cm
Min. hill angle	35.6°	Max. hill angle	36.0°
No. of Dee	2	Dee voltage	100 kV
Injection radius	6.6 cm	Phase width	30°
Radial tune υ_r	1.121	Axial tune υ_z	0.743

An efficient low energy beam transport system will be used to match the extracted beam into the subsequent accelerator structure and to give the beam the desired radial size and angle. A drift tube type sinusoidal buncher will be used to bunch the dc beam from the source. For inflecting the beam by 90° in the median plane we have chosen a spiral inflector because of its large admittance and relatively low voltage requirement on the electrode. In order to fully characterize the low energy beam before it is injected into the cyclotron, we planned to study the space charge effects in detail through simulations and experiments.
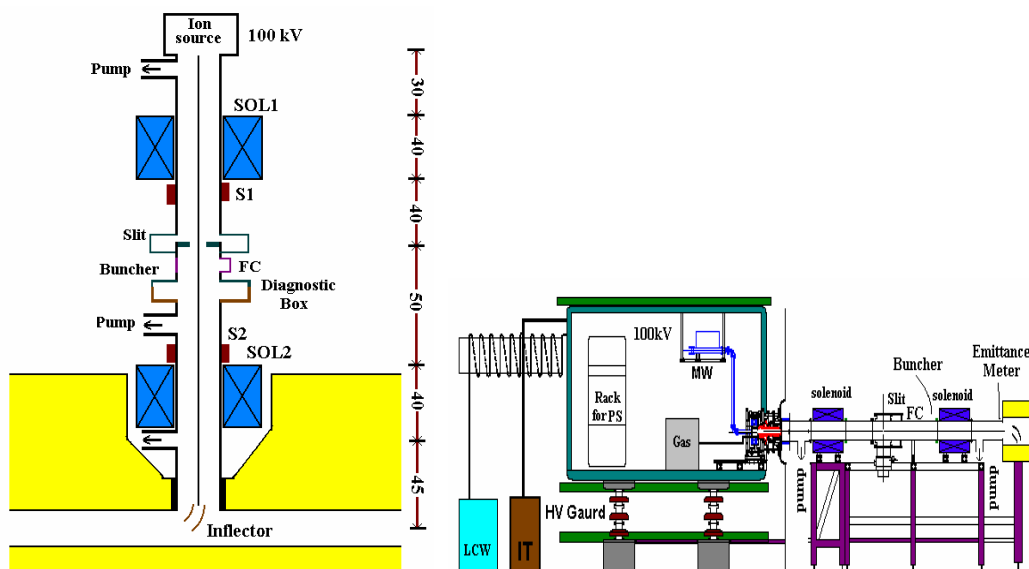
Figure 10: Scheme of injection and layout of the high voltage deck, source and Low Energy Beam Transport for preliminary study.

Most of the components of the ion source, extraction system, high voltage deck and LEBT have already been procured/fabricated. We hope to start assembling and testing of the source by the end of 2006.

5.3.6 Medical Cyclotron

The VEC Centre is in process to establish medical cyclotron facility in Kolkata. The main objective of the facility will be to produce radioisotopes and subsequently to

process radio-pharmaceuticals, which will be used in nuclear imaging for medical diagnostic purposes. The facility will also be used for various research and development purposes.

Medical cyclotron will produce proton beam with energy up to 30 MeV and current up to 350 mA. The negative ions, produced in an external ion source, will be axially injected into the cyclotron. Two RF cavities, called dees, will accelerate the negative ions. At the extraction radius carbon stripper foils will be used to extract two simultaneous proton beams from the machine. The extracted beam energy will be adjustable from 15 MeV up to 30 MeV and the beam current will be tunable up to 350 μA.

5.3.7 Recovery and Analysis of Helium from Hot Spring and Seismic Monitoring Activities

Scientist at VECC, are also engaged on a project of recovery and purification of helium collected from hot springs of Bakreshwar and Tantloi. Helium is an essential commodity in many modern technological processes and research, particularly in atomic energy. Its usefulness combined with its general scarcity has made it a strategic material. After purification to cryogenic grade (99.995%), it will be utilized in the superconducting cyclotron and hence will reduce the burden of import by a substantial amount.

Scientists of VECC and SINP have also set up an advanced experimental facility at Bakreswar, Birbhum for geochemical observations to be used as precursors to earthquake and volcanism with the help of Department of Atomic Energy and Department of Science and Technology, Government of India. The volatile entities, namely radon, gamma and helium concentrations, are considered as geochemical signals for the purpose. Data are taken round the clock (24x7) and with the help of VSAT facility transferred to VECC/SINP campus at Kolkata for analysis. In the recent past precursory signals obtained have been successfully correlated with the subsequent occurrence of seismic disturbances especially around the eastern and south-eastern regions. Typical anomalous geochemical signals of radon and gamma observed are shown in Figure 11. Though these observations are clearly predict the earthquake well in advance, a lot of R&D is still necessary to find out the exact location with these observations.
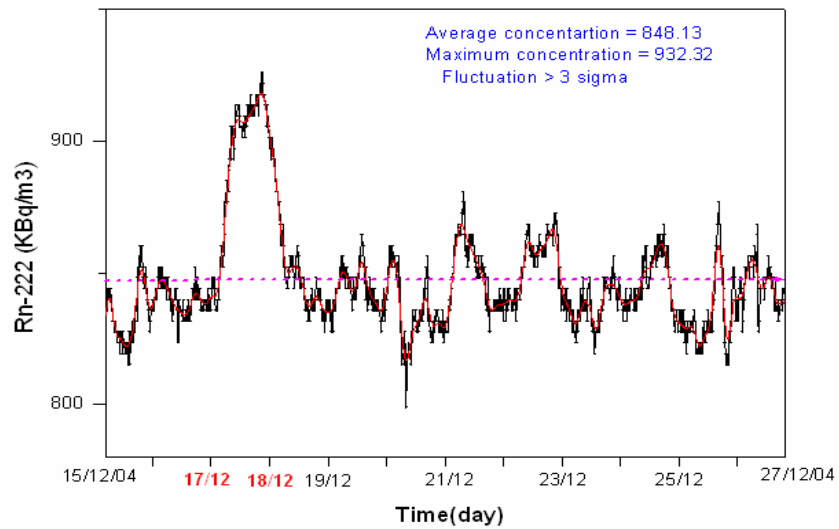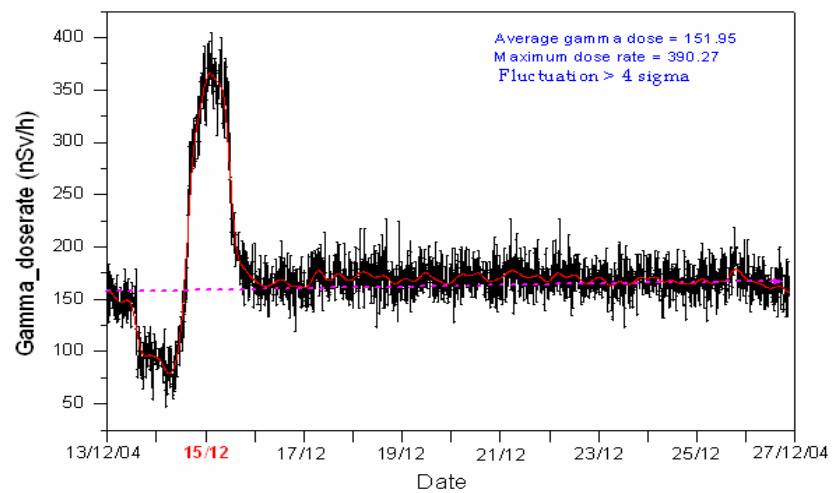
**Figure 11:** Typical anomalous geochemical signals of radon and gamma observed during the earthquake.

5.3.8 References

1. A. S. Devatia, Santimay Chatterjee, S. S. Ramamurthy and N. K. Ganguly; Proc. 10th Int. Conf. On Cyclotrons and their Applications, East Lansing, Machigan (1984),445.
2. C. Mallik for VECC staff; Proc. 16th Int. Conf. On Cyclotrons and their Applications, East Lansing, Machigan (2001),114.

3. R.K. Bhandari, 16th Intl. Conf. on Cyclotrons and their Applications, May 13 – May 17 2001, edited by F. Marti, p. 84.
4. H.G. Blosser, IEEE Trans. on Nuclear Science, Vol. NS-26, No.2, April 1979, p.2024.
5. D.P. May et. al., Proc. 10th Int. Conf. on Cyclotrons and their Applications, April 30-May 3, 1984, ed. F. Marti, p. 195.
6. Alok Chakrabarti ,Journ. Phys. G : Nucl. Part. Phys., 24 (1998) 1361.
7. V. Banerjee et. al., Nucl. Instrum. Method A447 (2000) 345.
8. A. Chakrabarti et. al., Nucl. Instrum. Method A535 (2004) 599.
9. N. Fieuer and P. Mandrillon, Proc. of the 14th Int. Conf. on Cyclotrons and their Applications, Cape Town, (1995) 598.
10. V. S. Pandit and P. S. Babu, Nucl. Instr. and Methods **A** 523 (2004) 19.
11. V. S. Pandit, InPAC 2003, Indore, Feb 2003, p. 69.

5.4 Ion Optics for the Superconducting Heavy Ion Linac at New Delhi

P.N. Prakash & Amit Roy
Inter University Accelerator Centre,
P.O.Box 10502, Aruna Asaf Ali Marg, New Delhi - 110067, India
mail to: prakash@iuac.ernet.in

5.4.1 Introduction

A superconducting heavy ion linear accelerator as booster to the existing 15UD Pelletron accelerator is presently under construction at the Inter University Accelerator Centre (IUAC), New Delhi [1]. The linac would accelerate beams up to mass 100 above the Coulomb barrier. One cryostat module, out of the eventual three such modules, is installed in the beam line and is presently being tested. The accelerating structure in the linac is a niobium quarter wave resonator (QWR) operating at 97 MHz [2]. Eight resonators along with a superconducting solenoid magnet (SSM) are installed in a module. A pre-linac superbuncher and a post-linac rebuncher are also part of the linear accelerator system.

5.4.2 Linac Ion Optics

5.4.2.1 *Design Goals and Constraints*

The design goal was to work out a lattice and an arrangement of the linac modules that could deliver either very short time spread ($\Delta t < 150$ ps) or narrow energy spread ($\Delta E < \pm 250$ keV) ion beams on the target with minimum distortion in the longitudinal phase space, while preserving the spatial magnification. The design also aimed at easy variability of energy and studying the steering caused by misaligned elements, particularly the superconducting solenoid magnets. There were constraints in terms of civil construction (for the building expansion), existence of a corridor between the present experimental beam hall and linac vault, engineering constraints such as erection of EOT crane, laying of the cryogenic transfer lines, etc., and the optics design had to be worked out with all of them in mind.

5.4.2.2 *Theory*

The basic idea of the theory is the concept of matching of the phase acceptance of different beam transport elements with that of the beam. A particle near the synchronous phase ϕs undergoes an elliptical orbit in phase space oscillating in phase and energy as given by the following equation:

$$\Delta E^2 / \{2Ek/\omega\sqrt{(2E/A)}\}^2 + \Delta\phi^2 / \Delta\phi_o^2 = 1, \tag{1}$$

where E is the energy and A the mass of the ion, $\omega = 2\pi f$ is the angular frequency, $\Delta\phi$o is the phase angle difference at time t = 0, and k2 is given by:

$$k^2 = \omega/(2E)\sqrt{\{A/(2E)\}} \; q \; E_a \; \sin\phi_s , \tag{2}$$

where q is the charge state of the ion, Ea the accelerating electric field and ϕs the phase angle of the synchronous particle.

If the boundaries of the phase space ellipse are within the acceptance limits of the linac, the beam is said to be matched. In such a case, although the matched beam rotates in the phase space, it is not distorted. The condition for matching is that in all parts of the linac the energy spread must be related to the time spread by:

$$\Delta E/\Delta t = 1.32 \times 10^4 \, [q/A \, E_a \, f \, \sin\phi_s]^{1/2} \, A^{1/4} \, E^{3/4} \tag{3}$$

where f if the rf frequency in Hz, E_a the accelerating electric field in MV/m, A the ion mass in amu, and the energies are in MeV.

The angular rate of rotation dψ/dz of a matched ellipse is given by:

$$d\psi/dz = 4.74 \times 10^{-6} \, [\, q/A \, f/\beta^3 \, E_a \, \sin\phi_s \,]^{1/2} , \tag{4}$$

where dψ/dz is in radians per meter and β is the relative velocity v/c.

For the beam to be properly matched within the phase acceptance of the linac (typically 5° of the rf), it must be compressed to less than 150 ps width pulses. This is done in two stages; a pre-tandem buncher (located in the low energy section of the Pelletron) compresses the beam to about 1.5 ns FWHM pulse. A second buncher, located in the high energy section of the Pelletron, compresses the beam to about 150 ps FWHM pulses for injection into the linac. The modulation energy required to bunch a beam of mass m, energy E and time width Δt, at a distance L is given by:

$$\Delta E_m = 0.014 \, E^{3/2} \, \Delta t/(L\sqrt{m}), \tag{5}$$

where ΔE_m and E are in MeV, Δt is the full width of the injected beam in ns, L is in meter and m in amu. This modulation energy produces a bunch width at the point of time focus given by:

$$\Delta t_f = 35.7 \, L \, \sqrt{m} \, \Delta E_i/E^{3/2} , \tag{6}$$

where Δt_f is in ns and ΔE_i is the energy spread in the beam in MeV.

As can be seen from the above equation the modulation energy required for the pre-tandem buncher, where the singly charged negative ion beam energy is typically hundreds of keV only, is considerably lower than the post tandem buncher where the energies are typically hundreds of MeV. For this reason a superconducting resonator is used as buncher for injection into the linac and is often referred to as a *superbuncher*.

In the post linac section a rebuncher is used to either re-bunch or de-bunch the beam to deliver a short time spread or a narrow energy spread beam on target. The working principle of the rebuncher is same as that of the superbuncher.

5.4.2.3 *Computer Modeling*

In order to study the beam dynamics through the linear accelerator a computer program was developed [3]. The program traces trajectories of one hundred fifty particles, generated randomly, through the resonators. The program treats the accelerating quarter wave structure as a series of three coaxial tubes (two gaps) at the appropriate potentials. The on-axis dc potential for a pair of tubes is well known [4]. The concept is extended to several tubes using the principle of superimposition. For example, four coaxial tubes would represent three gap structures such as half wave or split ring resonators, and five coaxial tubes would represent four gap structures such as the inter-digital resonators. For a three tube arrangement the potential along the z axis is given by:

$$\phi(z) = (V_2 - V_1)/(2\omega s/R)$$
$$\times \ln[\{\cosh(2\omega z/R) + \cosh(2\omega(a+s)/R)\}/\{\cosh(2\omega z/R) + \cosh(2\omega a/R)\}], \quad (7)$$

where V_2 and V_1 are the voltages on the central and outer tubes, 2a is the length of the central tube, R is the radius of the tubes, s is the gap between the outer and central tube and $\omega = 1.31835$ is a constant. For this cylindrically symmetric system the off axis potential can be calculated using the power series expansion:

$$\phi(r,z) = \phi(z) - r^2/4.\phi''(z) + r^4/64.\phi^{iv}(z) - \ldots \quad (8)$$

where $\phi(z) = \phi(r=0,z)$ and $\phi''(z)$ and $\phi^{iv}(z)$ represent the 2nd and 4th derivatives of $\phi(z)$ respectively. The on and off-axis electric fields are calculated from the potentials. The computed on-axis electric field has been found to be in good agreement with measured values from the standard bead pull technique [5]. The above equations are for dc fields; the time varying rf field can be written as: $E(r,z,t) = E(r,z).\cos(\omega t)$.

The program traces the trajectories using z, rather than time, as the independent variable. This way the potentials and their derivatives, which are calculated at the mesh points (typically 1 mm size), can be used without further interpolation. In each iteration the new position x and velocity v_x of the particle is calculated at the mesh point using the following equations (with similar equations for y), and the process is repeated till the particle has reached the end of the resonator.

$$x = x_0 + (dx/dt)_0.\Delta z/v_0 - \tfrac{1}{2}.q/m.(d\phi/dr)_0.\cos\theta.(\Delta z/v_0)^2 - 1/6.q/m$$
$$\times [(d^2\phi/drdz)_0.(dz/dt)_0 + (d^2\phi/dr^2)_0.(dr/dt)_0].\cos\theta.(\Delta z/v_0)^3 \quad (9)$$

$$v_x = dx/dt = (dx/dt)_0 - q/m.(d\phi/dr)_0.\cos\theta.\Delta z/v_0 - \tfrac{1}{2}.q/m$$
$$\times [(d^2\phi/drdz)_0.(dz/dt)_0 + (d^2\phi/dr^2)_0.(dr/dt)_0].\cos\theta.(\Delta z/v_0)^2 \quad (10)$$

where $r^2 = x^2 + y^2$ & $\tan\theta = y/x$, m, q and $v_0 = \Delta z/\Delta t$ are the mass, charge and velocity of the ion. The program can run up to 120 elements. An element pointer keeps track of the current element and can be reset to start the calculation from that point onwards. The phase space ellipse at any element position, radial & longitudinal beam envelops, sequence of the linac elements and beam statistics can be displayed. For the quadrupole and solenoid magnets the trajectories are computed using their transfer matrices.

5.4.2.4   *Ion Optics Calculations*

Several options for the lattice design of the linac modules and their arrangement were studied. The constraints outlined in section 2.1 along with other aspects of the beam dynamics dictated the final choice of the lattice design and arrangement. It is beyond the scope of this report to discuss all of them. One of the major aspects which was evaluated for each option was the packing of the resonators, which must be kept tight in order to avoid degradation in the longitudinal emittance of the beam. In actual running conditions the operator is often forced to switch off some resonators due to hardware problems or simply because it cannot be kept phase locked. It is therefore not wise to have a loosely packed configuration to begin with. Loosely packed design would also require insertion of several transverse focussing elements, which can push the cost up. In the final choice a lattice consisting of eight quarter wave resonators and one superconducting solenoid magnet in a module arranged in the sequence 4 QWRs + 1 SSM + 4 QWRs was selected. The overall length of the linac module is about 2.7 m. Besides being symmetric, this configuration has the advantage of having a solenoid magnet every three meters to take care of the transverse focussing needs. Outside the linac modules the focussing elements in the beam line are quadrupole magnets.

(a)   (b)
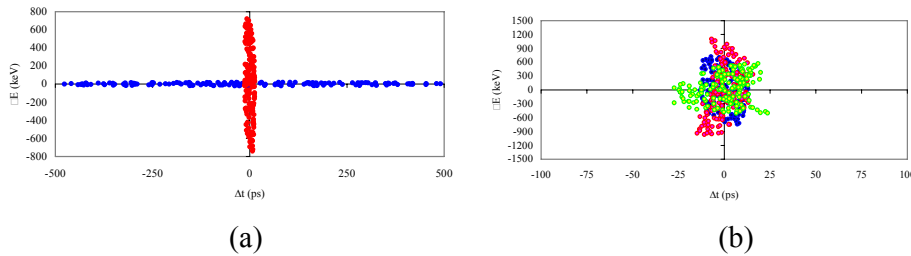
Figure 1: (a) the longitudinal emittance plots before and after the superbuncher in blue and red colours respectively; (b) the longitudinal emittance at the entrance, exit of the linac and on the target in blue, red and green colours respectively.

Detailed calculations were performed using four representative beams between S32 and I127 to cover the broad velocity range [6]. A separate numerical study was conducted to work out the expected charge states and intensities of the ion beams from the Pelletron accelerator [7] and the results were verified from the operational experience of the machine. Although the Pelletron accelerator produces a low emittance (transverse and longitudinal) near monochromatic beam, a relatively large longitudinal emittance of 20π keV-ns for light ions and 50π keV-ns for heavy ions was used in the calculations to take care of other sources of time jitter. Figure 1(a) shows the computed phase space plot for Ni58 beam before and after the superbuncher. Figure 1(b) shows the beam at the entrance and exit of the linac (with all three modules) and on the target. The injection and final beam energies are 235 MeV and 484 MeV respectively. Figure 2 shows the

spatial and time envelops of the beam (half width) through the linear accelerator starting from the superbuncher up to the target. As can be seen in figure 2(b) the phase ellipse undergoes π degrees of rotation through the accelerator.

(a)   (b)
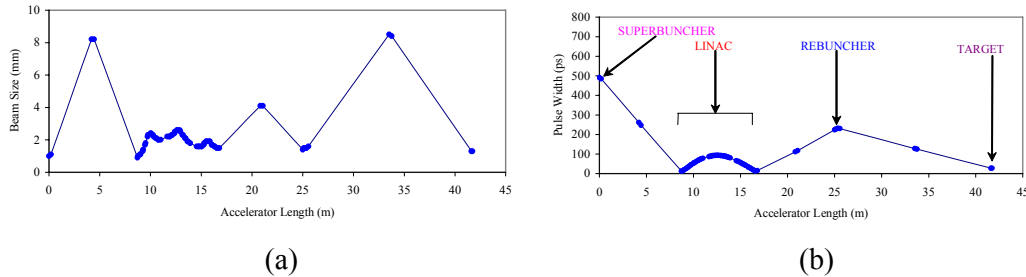
Figure 2: Through the length of the accelerator: (a) the beam size; and (b) the time envelop.

For covering the total energy range from the linac, calculations were performed at one half and one quarter of the full energy gain by switching off resonators in the high energy section of the linac. This way the velocity profile in the low energy section of the linac could remain unchanged. The effect of element misalignment was also studied. It was observed that if an individual resonator was misaligned by up to 2 mm, there was no appreciable steering of the beam on target. However, if an entire cryostat was misaligned by 2 mm (but not the solenoid magnet) the beam is steered about 3 mm on the target. The effect of solenoid magnet misalignment is, however, more severe. The effect of a misaligned solenoid magnet by 2 mm causes a S^{32} beam to steer 3 mm on the target. Steering magnets have been incorporated in the beam line to correct this. In order to simulate realistic running conditions in a linac some resonators were switched off to see the effect on the ion optics. No significant degradation of the beam ellipse was seen even when 10% of the resonators were randomly turned off in the linac.

5.4.3   Acknowledgements

5.4.4   References

1.   P.N. Prakash et al., PRAMANA, Journal of Physics, Vol. 59, No. 5, Nov. 2002, p849
2.   P.N. Prakash, A.Roy & K.W. Shepard, Proceedings of 8th Workshop on RF Superconductivity, Abano Terme (Padova), Italy, October 6-10, 1997, p633
3.   P.N. Prakash, A.P. Patro and A. Roy, IUAC Technical Report, Ref. NSC/TR/PNP/95/110, June 1995
4.   Electron beam lenses and optics, Vol. 1, A.B. El-Kareh & J.C.J. El-Kareh, Academic Press, 1976
5.   L.C. Maier and J.C. Slater, Journal of Applied Physics, Vol. 23, No. 1, Jan. 1952, p68
6.   P.N. Prakash and Amit Roy, IUAC Technical Report, Ref. NSC/TR/PNP/96/132, January 1996
7.   R. Mehta, Linac Group, IUAC, private communication

6 Workshop and Conference Reports

6.1 Report on the 37th ICFA Beam Dynamics Workshop on Future Light Sources

Kwang-Je Kim, Argonne National Laboratory
mail to: kwangie@aps.anl.gov

The 37th ICFA Beam Dynamics Workshop on Future Light Sources was held 15 – 19 May 2006 at DESY in Hamburg, Germany. It succeeded in bringing together 150 experts working on the development and design of the various types of accelerator based light sources.

The 5 day workshop program consisted of 2 half days devoted to 11 plenary talks which covered the scientific challenges in synchrotron radiation research and selected accelerator physics issues. Two full days were reserved for discussions in five working groups, leading to about 120 presentations. A poster session (15 contributions) was dedicated to laboratory reports and new projects.

The workshop contributions (presentation material and papers) are published within the JACOW system (http://www.jacow.org) and on the workshop webpage (http://fls2006.desy.de).

6.1.1 Plenary Talks

– First Experimental Experience at FLASH, W. Wurth, University Hamburg
– Energy Recovery Linac Experimental Challenges, D. Bilderback , Cornell University
– Trends in X-ray Synchrotron Radiation Research , J. Schneider, DESY
– Trends in XUV Synchrotron Radiation Research on Atoms, Molecules and Clusters, S. Svensson, Upsalla U
– Design Considerations for Table-Top FELs , F. Gruener, Ludwig Maximilian University München
– Inverse Compton Scattering: A Small Revolution in X-Ray Sources and Applications, D. Moncton, MIT
– CW Superconducting RF for Future Linac-Based Light Sources, J. Knobloch, BESSY
– Synchronization and Timing Challenges for Future Light Sources, G. Hirst, CCLRC
– Short Radiation Pulses in Storage Rings, S. Khan, Universiy Hamburg
– Attosecond Pulses in XFELs, E. Saldin, DESY
– Seeding and Harmonic Generation in Free Electron Lasers, L. Gianessi, ENEA

6.1.2 Working Groups

WG1: Storage ring based synchrotron radiation sources
Chair: K. Harkay (APS), A. Ropert (ESRF)

The discussions on storage ring light sources started with an evaluation of the future source parameter needs. Possibilities and difficulties of exceeding the performance of present day 3rd generation sources with new designs were discussed, leading to a review of the status and needs for further accelerator technology development. Upgrade possibilities for existing sources were presented and evaluated. Finally the question of low-cost sources, multipurpose or specialized sources was raised.

WG2: Energy Recovery Linac based synchrotron radiation sources
   Chair: G. Hoffstätter (Cornell), S. Smith (CCSRC)

Issues and challenges common to all ERL based radiation sources were reviewed, starting from short project overviews and continuing with discussion on optimal schemes to minimize bunch length and energy spread, optimal injector-to-linac merger design, start to end simulations, beam abort strategies and beam loss tolerances, beam stabilization strategies, diagnostic, vacuum and aperture needs, undulator issues, advantages and limits of multi-turn ERLs, bandwidth limits for ERLs and optimal parameters for superconducting cavities of an ERL.

WG3: Free Electron Lasers
   Chair: Z. Huang (SLAC), L. Serafini (INFN)

The biggest working group of the workshop discussed new results from FEL experiments and operating facilities and the prospects of the short wavelength X-ray FELs on the horizon. Further topics have been start-to-end simulations, which are invaluable tools to understand the performance and tolerance of FELs, the theoretical progress is still made in many areas, and seeding as a promising route to improve the temporal coherence of the SASE radiation. Novel source ideas based on FEL-like mechanism were presented, which may provide compact sources for coherent radiation from THz to X-rays.

WG4: Low emittance electron guns
   Chair: W. Graves (MIT), M. Krasilnikov (DESY), F. Stephan (DESY)

A benchmarking problem, based on a complete set of beam parameter measurements from PITZ, was discussed and used for comparison of different simulation codes before and during the workshop. In addition, several talks dealt with gun developments and tests at various laboratories. New ideas for small emittance generation, like longitudinal/transverse phase space manipulation, were also presented.

WG5: Beam diagnostics and stability
   Chair: J. Byrd (LBNL), D. Nölle (DESY)

The working group devoted a complete day on developments in measuring and stabilising the longitudinal phase space. The main topics were synchronisation and timing issues and longitudinal phase space characterization for the fs regimes present in FELs. The second day dealt with measurements in transverse phase space like synchrotron radiation diagnostics in storage ring or high precision single-pass BPMs. Machine protection issues were also presented.

6.2 Mini-workshop on CSNS Accelerator Engineering Design

Jie Wei and Shinian Fu
Institute of High Energy Physics, China/Brookhaven National Laboratory, USA
mail to: weijie@ihep.ac.cn or jwei@bnl.gov

The Mini-workshop on China Spallation Neutron Source (CSNS) Accelerator Engineering Design was held at the Institute of High Energy Physics, Beijing, from April 25 to 27, 2006. Seven accelerator physicists and engineers from the Brookhaven National Laboratory and the Lawrence Berkeley Nation Laboratory attended the workshop, extensively exchanged experiences on the construction and operations of high intensity proton accelerators, and reviewed the engineering design of the CSNS accelerator systems. Related information may be found on the project web site at:

http://bsns.ihep.ac.cn/

There are 40 talks presented in the three-day workshop. Upon completion, a workshop CD was produced to document the talks and discussions (see following). The CD is available upon request.

Main Session

1. Accelerator Projects in China, S. –X. Fang
2. Project Management, D. Lowenstein/presenter J. Tuozzolo
3. BSNS Project Overview and Status, J. Zhang
4. BSNS Accelerator Design and R&D, J. Wei/S. Fu
5. Mechanical Engineering Challenges at AGS Booster and SNS, J. Tuozzolo
6. BSNS Magnet Protoptype Status & Issues, C.-D. Deng
7. BSNS Injection and Extraction Issues, J.-Y. Tang
8. Magnet Measurement Techniques, A. Jain
9. Electrical engineering challenges at AGS Booster and SNS, J. Sandberg / presenter J. Tuozzolo
10. BSNS Resonance Power Supply R&D Issues, J. Zhang
11. BSNS Injection & Extraction Pulsed Power R&D Issues, Y.-L. Chi
12. BSNS Controls R&D Activity, C.-H. Wang
13. SNS Ring High Power and Low Level RF System Design, Test and Fabrication, A. Zaltsman
14. BSNS RF System R&D Activity and Issues, H. Sun
15. BSNS Linac RF System & Power Supply, J. Li
16. BSNS Diagnostics Plan, J.-S. Cao
17. SNS Ring Vacuum Design and Experience, H. Hseuh
18. BSNS vacuum system prototyping status & issues, H.-Y. Dong
19. Why I Designed the SNS Front End the Way I Did, and What I Would Change? J. Staples
20. SNS RFQ Engineering and Tests, S. Virostek
21. SNS Front End Systems, Diagnostics, Commissioning and Operating Experience, J. Staples

21. BSNS Linac Conventional Facility Plan, T.-G. Xu
22. BSNS RCS Conventional Facility Plan, S. Wang
23. BSNS Radiation & Shielding Considerations, Q.-B. Wang

Linac Session
1. BSNS Ion Source Design & Plan, J.-H. Li
2. ADS RFQ Status, S.-N. Fu
3. BSNS RFQ & Front End Design, H.-F. Ouyang
4. BSNS DTL Design and R&D, S.-N. Fu

Ring Mechanical Systems Session
1. Injection & Extraction Magnet Design, W. Kang
2. BSNS Collimator and Beam Dumps, T.-G. Xu
3. Survey & Alignment Plan, L. Dong
4. 3D Magnet Modeling, Y. Chen

Magnet Measurement Session
1. BSNS Magnet Measurements Plan, W. Chen

Workshop Summary
1. Summary on Ring Mechanical Session, J. Tuozzolo
2. Summary on Ring Electrical Session, Z.-X. Xu
3. Summary on Ring RF, Zaltsman
4. Summary on Ring Vacuum, H. Hseuh
5. Summary on Front End & Linac, S.-N. Fu/J. staples
6. Summary on Magnetic Measurements, A. Jain
7. Comments to BSNS Accelerator, H. Hseuch, J. Tuozzolo, A. Zaltsman
8. Workshop Summary, J. Wei/S.-N. Fu

Appendix
I. Workshop Agenda
II. BSNS Parameters List
III. BSNS WBS

6.3   The Fourth Overseas Chinese Physics Association Accelerator School

Alex Chao
Stanford Linear Accelerator Center, Stanford University, CA 94309, USA
mail to: achao@slac.stanford.edu

An OCPA Accelerator School was held July 27 – August 5, 2006, Yangzhou, China. It was the fourth in the series. The previous three were held in Hsinchu (1998), Yellow Mountain (2000), and Singapore (2002).

In the past two decades, there has been a rapid growth in the science and technology of accelerators. The prospect looks especially encouraging in the Chinese community including Mainland China and Taiwan, as several significant accelerator projects are currently being constructed or approved for construction. The progress however also

comes with it a demanding need for trained accelerator scientists. The OCPA Accelerator Schools are our attempt to help addressing this need, particularly for Chinese-speaking students. The spoken language at the 2006 school is Chinese.

Since its start in 1998, the OCPA School has received strong support from the Chinese, Taiwanese, and Singaporean accelerator laboratories and funding agencies. Demand of participation has been very strong. In this 2006 school, the number of student applications far exceeded our anticipation so that we finally decided to implement quotas to each participating laboratories. The final number of students, with the school capacity stretched to the limit, was 83 (72 from Mainland, 10 from Taiwan, 1 from Japan). There were 28 lecturers.

The school's organization and its sponsors are shown in Appendix I. The curriculum is shown in Appendix II. Other detailed information of the school can be found on the web site www.ssrf.ac.cn/ocpaschools06/. The Curriculum Committee was co-chaired by Professors Zhiyuan Guo from IHEP, Beijing, and June-rong Chen from NSRRC, Taiwan. The Local Committee was chaired by Professor Zhentang Zhao from SSRF, Shanghai.

Yangzhou is a small city about 300 km northwest of Shanghai. It was chosen as the school site because of its proximity to the local host SSRF, the Shanghai Synchrotron Radiation Facility. The SSRF has a 3.5-GeV facility currently under construction. It has a sizable young staff that could benefit greatly from such a school. In turn, the very strong support from SSRF was what made this school possible.

The course duration was 10 days. As can be seen from Appendix II, the curriculum was quite demanding. The courses are divided into three categories: basics, advanced, and seminars. Students are required to familiarize themselves with the basic courses, learn as much as possible with the advanced courses, and be informed of the seminar lectures. The emphasis of the 2006 school is synchrotron radiation and free electron lasers, although high-energy and neutron applications are also lectured in seminars.

One memorable special session was that dedicated to Professor Lee Teng honoring his 80-th birthday. There were an unexpectedly large number of participants who wanted to speak, so that the keynote lecture (on the topic of Advanced Acceleration) by Teng was squeezed into a short (and moving) speech.

With the help from Yangzhou University, another exciting session was a special laboratory course on computer controls. Students were given a hands-on opportunity to simulate the on-line control of an accelerator, not unlike a flight simulator.

Students were assigned homework problems each day. After 8 hours of lectures, the students gathered in the evenings to work through their homework assignments. In addition, there was an exam held at the end of the school. The exam was taken seriously by students and lecturers alike. Lecturers worked overnight to grade the exam papers so that the results could be announced next morning. The students generally did well on the exam. The best 10 students were awarded small prizes in a simple ceremony at the conclusion of the school.

Yangzhou offers a beautiful combination of culture, scenery, and exquisite food. The school site is at a local hotel. At the beginning of the school, we suggested that students not to leave the site during the school days except for the excursion day, and students obliged. It turned out however that this suggestion was not necessary as the students were in any case very occupied by the workload. Most students studied after mid-night every day after long hours of lectures during the day. Bravo for the students!

This school was clearly a success. It was touching to see how much effort the lecturers put into their lectures, and the students into their studies. The quality of lecture materials has been first rate judged by any standard. In fact, the best indicator of this school being a success is the fact that all participants made their very best efforts, by the lecturers, by the students, as well as by the organizers. One additional most memorable feature to many of us has been the time together with many old and new friends.

There has been a decision of holding a fifth OCPA School in 2008. No decision has been made on its location, but likely locations being mentioned included Beijing and Taiwan.

Appendix I.   The Fourth OCPA Accelerator School Organization

Organized by
Division of Beam Physics, Overseas Chinese Physics Association
Shanghai Synchrotron Radiation Facility, Institute of Applied Physics, CAS

Sponsored by
Overseas Chinese Physics Association
National Natural Science Foundation of China
National Synchrotron Radiation Research Center, Hsinchu
Institute of Applied Physics, Shanghai
Institute of Modern Physics, Lanzhou
Institute of High Energy Physics, Beijing
University of Science and Technology of China, Hefei
Tsinghua University, Beijing
EDMI, Ltd., Singapore
AMAC Int'l Inc. USA
Wuhu Cowemv Electronics Co. Ltd, Anhui
World Scientific Pub. Co., Singapore

Organizing Committee
Alex Chao, SLAC, Chair
Chien-Te Chen, NSRRC
Hesheng Chen, IHEP
Jiaer Chen, Peking University
Shouxian Fang, IHEP
Duohui He, USTC
Keng Liang, NSRRC
Yuzheng Lin, Tsinghua University, Beijing
K.K. Phua, SEATPA
Lee Teng, ANL
Hongjie Xu, SINAP
Wenlong Zhan, IMP

Curriculum Committee
Zhiyuan Guo, IHEP, Co-Chair
June-Rong Chen, NSRRC, Co-Chair
Kuo-Tung Hsu, NSRRC
Guimin Liu, SINAP
Zuping Liu, USTC

Chuanxiang Tang, Tsinghua University, Beijing
Wu-Tsung Weng, BNL

Local Committee
 Zhentang Zhao, SINAP, Chair
 Ying Fan, SINAP
 Zhanjun He, SINAP
 Weicheng Hu, SINAP
 Jie Tang, SINAP
 Chunxiang Wang, SINAP
 Xiaohong Wang, SINAP
 Heping Yan, SINAP
 Wei Zhou, SINAP

Appendix II.   Program of the Fourth OCPA Accelerator School

TIME	Thursday 27 July	Friday 28 July	Saturday 29 July	Sunday 30 July	Monday 31 July
08:00 – 09:00	Welcome Accelerator history 1	Dynamic aperture 1	Effects of mechanical stability 1	Introduction to synchrotron radiation 1	Introduction to synchrotron radiation 3
09:00 – 10:00	Accelerator history 2	Dynamic aperture 2	Effects of mechanical stability 2	Introduction to synchrotron radiation 2	RF 1
	Break				
10:15 – 11:15	Transverse dynamics 1	Insertion devices 1	Instability and beam quality 1	Beam Control 1	RF 2
11:15 – 12:15	Transverse dynamics 2	Insertion devices 2	Instability and beam quality 2	Beam Control 2	RF 3
12:15	**Lunch**				
14:00 – 15:00	Transverse dynamics 3	Lattice design 1	Instability and beam quality 3	Beam control software 1	Electron linac 1
15:00 – 16:00	Transverse dynamics 4	Lattice design 2	Instability and beam quality 4	Beam control software 2	Electron linac 2
	Break				
16:15 – 17:15	Longitudinal dynamics 1	Colliders ILC 1	Beam diagnostics 1	Beam control software 3	Electron linac 3
17:15 – 18:15	Longitudinal dynamics 2	Colliders ILC 2	Beam diagnostics 2	Heavy ions accelerators	Inductive linac
18:30	**Dinner**				
20:00 – 21:00	Office hours and discussion	Office hours and discussion	Office hours and discussion	On-site computer simulation1	Banquet
21:00 – 22:00	Assignment and discussion	Assignment and discussion	Assignment and discussion	On-site computer simulation2	Assignment and discussion

TIME	Tuesday 1 August	Wednesday 2 August	Thursday 3 August	Friday 4 August	Saturday 5 August
08:00 – 09:00	E X C U R S I O N	Frequency map analysis 1	Low emittance electron gun 1	Superconducting cavities 1	FEL and advanced proposals 1
09:00 – 10:00		Frequency map analysis 2	Low emittance electron gun 2	Superconducting cavities 2	FEL and advanced proposals 2
		Break			
10:15 – 11:15		Vacuum 1	Injection and pulse magnets 1	Cryogenics 1	Closing
11:15 – 12:15		Vacuum 2	Injection and pulse magnets 2	Cryogenics 2	
12:15		**Lunch**			
14:00 – 15:00		Magnets 1	Spallation neutron source 1	Exam	D E P A R T U R E
15:00 – 16:00		Magnets 2	Spallation neutron source 2		
		Break			
16:15 – 17:15		Magnets 3	Accelerator application 1		
17:15 – 18:15		Memorial talk Advanced acceleration	Accelerator application 2		
18:30		**Dinner**			
20:00 – 21:00		Free discussion	Office hours and discussion	RFQ design and performance 1	
21:00 – 22:00		Assignment and discussion	Assignment and discussion	RFQ design and performance 2	

7   Announcements of the Beam Dynamics Panel

7.1   ICFA Beam Dynamics Newsletter

7.1.1   Aim of the Newsletter

The ICFA Beam Dynamics Newsletter is intended as a channel for describing unsolved problems and highlighting important ongoing works, and not as a substitute for journal articles and conference proceedings that usually describe completed work. It

is published by the ICFA Beam Dynamics Panel, one of whose missions is to encourage international collaboration in beam dynamics.

Normally it is published every April, August and December. The deadlines are 15 March, 15 July and 15 November, respectively.

7.1.2 Categories of Articles

The categories of articles in the newsletter are the following:
1. Announcements from the panel.
2. Reports of beam dynamics activity of a group.
3. Reports on workshops, meetings and other events related to beam dynamics.
4. Announcements of future beam dynamics-related international workshops and meetings.
5. Those who want to use newsletter to announce their workshops are welcome to do so. Articles should typically fit within half a page and include descriptions of the subject, date, place, Web site and other contact information.
6. Review of beam dynamics problems: This is a place to bring attention to unsolved problems and should not be used to report completed work. Clear and short highlights on the problem are encouraged.
7. Letters to the editor: a forum open to everyone. Anybody can express his/her opinion on the beam dynamics and related activities, by sending it to one of the editors. The editors reserve the right to reject contributions they judge to be inappropriate, although they have rarely had cause to do so.
8. Editorial.

The editors may request an article following a recommendation by panel members. However anyone who wishes to submit an article is strongly encouraged to contact any Beam Dynamics Panel member before starting to write.

7.1.3 How to Prepare a Manuscript

Before starting to write, authors should download the template in Microsoft Word format from the Beam Dynamics Panel web site:

http://www-bd.fnal.gov/icfabd/news.html

It will be much easier to guarantee acceptance of the article if the template is used and the instructions included in it are respected. The template and instructions are expected to evolve with time so please make sure always to use the latest versions.

The final Microsoft Word file should be sent to one of the editors, preferably the issue editor, by email.

The editors regret that LaTeX files can no longer be accepted: a majority of contributors now prefer Word and we simply do not have the resources to make the conversions that would be needed. Contributions received in LaTeX will now be returned to the authors for re-formatting.

In cases where an article is composed entirely of straightforward prose (no equations, figures, tables, special symbols, etc.) contributions received in the form of plain text files may be accepted at the discretion of the issue editor.

Each article should include the title, authors' names, affiliations and e-mail addresses.

7.1.4   Distribution

A complete archive of issues of this newsletter from 1995 to the latest issue is available at

http://icfa-usa.jlab.org/archive/newsletter.shtml

This is now intended as the primary method of distribution of the newsletter.

Readers are encouraged to sign-up for electronic mailing list to ensure that they will hear immediately when a new issue is published.

The Panel's Web site provides access to the Newsletters, information about future and past workshops, and other information useful to accelerator physicists. There are links to pages of information of local interest for each of the three ICFA areas.

Printed copies of the ICFA Beam Dynamics Newsletters are also distributed (generally some time after the Web edition appears) through the following distributors:

Weiren Chou	chou@fnal.gov	North and South Americas
Rainer Wanzenberg	rainer.wanzenberg@desy.de	Europe* and Africa
Susumu Kamada	Susumu.Kamada@kek.jp	Asia** and Pacific

*   Including former Soviet Union.

**   For Mainland China, Jiuqing Wang (wangjq@mail.ihep.ac.cn) takes care of the distribution with Ms. Su Ping, Secretariat of PASC, P.O. Box 918, Beijing 100049, China.

To keep costs down (remember that the Panel has no budget of its own) readers are encouraged to use the Web as much as possible. In particular, if you receive a paper copy that you no longer require, please inform the appropriate distributor.

7.1.5   Regular Correspondents

The Beam Dynamics Newsletter particularly encourages contributions from smaller institutions and countries where the accelerator physics community is small. Since it is impossible for the editors and panel members to survey all beam dynamics activity worldwide, we have some Regular Correspondents. They are expected to find interesting activities and appropriate persons to report them and/or report them by themselves. We hope that we will have a "compact and complete" list covering all over the world eventually. The present Regular Correspondents are as follows:

Liu Lin	liu@ns.lnls.br	LNLS, Brazil
S. Krishnagopal	skrishna@cat.ernet.in	RRCAT, India
Sameen Ahmed Khan	rohelakhan@yahoo.com	SCOT, Middle East and Africa

We are calling for more volunteers as *Regular Correspondents*.

7.2 ICFA Beam Dynamics Panel Members

Caterina Biscari	caterina.biscari@lnf.infn.it	LNF-INFN, Via E. Fermi 40, C.P. 13, Frascati, Italy
Yunhai Cai	yunhai@slac.stanford.edu	SLAC, 2575 Sand Hill Road, MS 26 Menlo Park, CA 94025, U.S.A.
Swapan Chattopadhyay	swapan@jlab.org	Jefferson Lab, 12000 Jefferson Avenue, Newport News, VA 23606, U.S.A.
Weiren Chou (Chair)	chou@fnal.gov	Fermilab, MS 220, P.O. Box 500, Batavia, IL 60510, U.S.A.
Yoshihiro Funakoshi	yoshihiro.funakoshi@kek.jp	KEK, 1-1 Oho, Tsukuba-shi, Ibaraki-ken, 305-0801, Japan
Miguel Furman	mafurman@lbl.gov	LBL, Building 71, R0259, 1 Cyclotron Road, Berkeley, CA 94720-8211, U.S.A.
Jie Gao	gaoj@ihep.ac.cn.	Institute for High Energy Physics, P.O. Box 918, Beijing 100039, China
Ajay Ghodke	ghodke@cat.ernet.in	RRCAT, ADL Bldg, Indore, Madhya Pradesh, India 452 013
Ingo Hofmann	i.hofmann@gsi.de	GSI, Darmstadt, Planckstr. 1, 64291 Darmstadt, Germany
Sergei Ivanov	ivanov_s@mx.ihep.su	IHEP, Protvino, Moscow Region, 142281 Russia
Kwang-Je Kim	kwangje@aps.anl.gov	Argonne Nat'l Lab, 9700 S. Cass Ave,, Bldg 401, Argonne, IL 60439, U.S.A.
In Soo Ko	isko@postech.ac.kr	Pohang Accelerator Lab, San 31, Hyoja- Dong, Pohang 790-784, South Korea
Alessandra Lombardi	Alessandra.Lombardi@cern.ch	CERN, CH-1211, Geneva 23, Switzerland
Yoshiharu Mori	mori@kl.rri.kyoto-u.ac.jp	Research Reactor Inst., Kyoto Univ. Kumatori, Osaka, 590-0494, Japan
Chris Prior	c.r.prior@rl.ac.uk	ASTeC, Rutherford Appleton Lab, Chilton, Didcot, Oxon OX11 0QX, U.K.
David Rice	dhr1@cornell.edu	Cornell Univ., 271 Wilson Laboratory, Ithaca, NY 14853-8001, U.S.A.
Yuri Shatunov	Yu.M.Shatunov@inp.nsk.su	Acad. Lavrentiev, prospect 11, 630090 Novosibirsk, Russia
Junji Urakawa	junji.urakawa@kek.jp	KEK, 1-1 Oho, Tsukuba-shi, Ibaraki-ken, 305-0801, Japan
Jiuqing Wang	wangjq@mail.ihep.ac.cn	Institute for High Energy Physics, P.O. Box 918, 9-1, Beijing 100039, China
Rainer Wanzenberg	Rainer.wanzenberg@desy.de	DESY, Notkestrasse 85, 22603 Hamburg, Germany
Jie Wei	wei1@bnl.gov	BNL, Bldg. 911, Upton, NY 11973- 5000, U.S.A.

The views expressed in this newsletter do not necessarily coincide with those of the editors. The individual authors are responsible for their text.